1st Faculty of Medicine, Charles University, Kateřinská 32, Prague 2, 121 08

Institute of Hematology and Blood Transfusion, U Nemocnice 1, Prague 2, 128 20

- The Biochemistry of Zinc and Iron -

Proteomic Studies

THESIS

Mgr. Marek Babušiak, 2007

„*My brain says I'm recieving pain*

A lack of oxygen From my life support

My iron lung“ Radiohead

Table of contents

Introduction

Biochemistry of iron

Iron – general properties

Iron is the fourth most abundant element in the earth's crust (5.6%). Geophysical theories generally fall in proposal that the earth's core is actually a giant – moon sized rotating iron globe. In living systems, iron is essential for virtually all organisms.

In periodic table iron belongs to d-block elements. Its electron configuration [Ar] $3d^6 4s^2$ (has four uncoupled valence electrons) makes iron a reactive element which can readily form coordination covalent bonds in complex ions. Cubic and hexagonal crystalline structures are characteristic for complex iron compounds. Iron has two common oxidation states: the bivalent ferrous ion Fe(II) and trivalent ferric ion Fe(III). Less common is iron in the form of very unstable ferrate ion Fe(VI). Other oxidation species are probably present transitionally. For instance, in the function of methane monooxygenase or ribonucleotide reductase, the presence of iron Fe(IV) containing complexes has been proposed to carry out oxidative processes [1, 2].

Iron forms compounds as oxides, hydroxides, acetates, carbonates, sulfides, nitrates, sulfates and great number of organometallic complexes. Importantly, iron plays a crucial role in the stucture and function of many biomolecules acting as a cofactor and electron transporting agent.

The importance of iron in miscellaneous biochemical pathways has a common feature - the shift of electrons between iron and donor or acceptor molecules. This is the basal mechanism of cellular respiration and energy production by controlled oxidation of carbohydrates, proteins, and lipids. In *vivo*, the iron atom is usually ligated by the

chemical functional groups present on metalloproteins or low molecular weight organic molecules. The ligand environment around the iron ion is of crucial importance regarding its physiological function. The roles of iron metalloproteins are diverse. Whereas some are involved in iron transport and/or storage, others, generally referred to as metalloenzymes, catalyze a wide spectrum of biologically important reactions. Here is a brief summary of basic functions of iron containing metalloenzymes:

- **Transport of oxygen:** In the lungs, oxygen diffuses across the alveolar membrane and the red cell membrane in lung capillaries. Oxygen molecule encounters a molecule of hemoglobin and binds itself between the iron atom and a histidine residue of the globin chain located adjacent to the heme group. One molecule of hemoglobin with its four heme groups is capable of binding four molecules of diatomic oxygen [3]. Other examples of mammalian oxygen transporting iron containing metalloproteins include very well described muscular oxygen storage protein myoglobin [4, 5] or recently discovered hemoproteins cytoglobin and tissue specific neuroglobin [6, 7]. Marine invertebrates can utilize oxygen using oligomeric non-heme iron containig protein hemerythrin [8, 9].

- **Electron transfer:** Molecular basis of cellular respiration is supplied by membrane proteins like iron-sulfur clusters and heme containing cytochromes. Two hydrogen ions, two electrons, and an oxygen molecule react to form water as a product with energy released in an exothermic reaction. This simple reaction requires several precisely controled steps. Iron atoms present in Fe-S clusters and heme groups of mitochondrial respiratory Complexes 1-4 serve as a redox centers which let the electrones to transfer their energy along the membrane employing ubichinione and cytochrome c as soluble mobile electron cargo (Fig.1). The respiratory enzyme complexes couple the energetically favorable transport of electrons to the pumping of H^+ out of the matrix. The

resulting electrochemical proton gradient is crucial for energy metabolism. The energy released is coupled with the formation of three ATP molecules per every cycle of the electron transport chain [10].

Fig.1 Schematic ilustration of electron transport by Complexes 1-4 in mitochondria

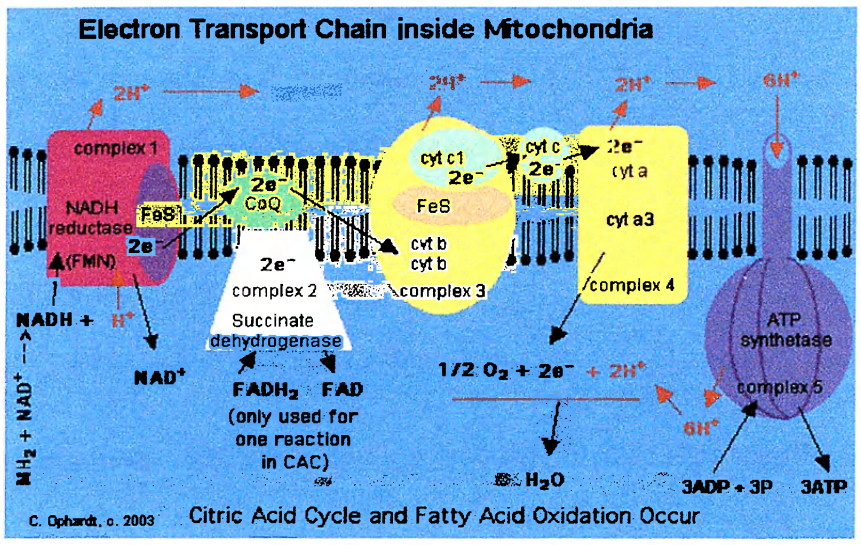

Image source: http://courses.ed.asu.edu/clark/teams/marathon/paul%20and%20grant/Lesson.htm

- **Oxidative and reductive transformations:** The most important catalytic function of iron atoms in nature is the mediation of redox transformations. Many iron containing metalloenzymes catalyze reactions involving reduction or oxidation of a substrate. Example of this subclass include enzymes of cytochrome P-450 oxidases family (CYP) [11], which metabolise vast variety of substrates (drugs and toxic compounds as well as metabolic products such as bilirubin) using heme group at the active side.

Other example of iron metalloenzyme with oxidative function is soluble methane monooxygenase (sMMO) found in methanotropic bacteria. The active site in sMMO contains a di-iron center bridged by an oxygen atom [12].

Redox properties of iron also qualify the activity of several protective enzymes, which are involved in the detoxification of reactive oxygen species like superoxide and hydrogen peroxide.

Catalases and peroxidases are heme containing proteins that are involved in H2O2 metabolism [13, 14]. Catalase reaction occurs in two stages [15].

H_2O_2 + Fe(III)-E H_2O + O=Fe(IV)-E

H_2O_2 + O=Fe(IV)-E H_2O + Fe(III)-E + O_2

Although copper/zinc superoxide dismutases (SOD's) [16, 17] are the most studied, also some iron and manganese containing SOD's are known [18, 19].

Here is an example of a typical reaction of an SOD protein containing copper and zinc:

Cu^{2+} SOD + O_2 Cu^{1+} SOD + O_2

Cu^{1+} SOD + O_2 + $2H^+$ Cu^{2+} SOD + H_2O_2.

Hydrolysis reactions are catalyzed by a class of metalloenzymes that in most cases is zinc dependent [20]. A few systems do not use zinc but another metals including iron. Examples of such hydrolytic enzymes are the serine-threonine phosphatases, which are involved in the hydrolysis of phosphate esters [21].

Iron absorption, storage and toxicity in human

Iron stores in human adults usually balance between 2 and 4 grams, (50 mg/kg in men and 40 mg/kg in women). There are actually no effective regulated mechanisms for iron excretion in human body, the regulation of dietary iron absorption is therefore a critical process for iron homeostasis [22]. Any excess iron is stored in body tissues primarily in the liver, heart and pancreas. Macrophages, cells of reticulo-endothelial system or Kupffer cell are capable of processing and releasing iron acquired by phagocytosis of immunosensitized red blood cells [23]. As such, the liver is the part of the body that is most susceptible to the toxicity of iron (see paragraph below). An exquisite balance between dietary uptake and loss maintains the iron stores in equilibrium. Daily

absorption of 1–2 mg of dietary iron is compensated with iron losses. About 1 mg of iron is lost each day through sloughing of cells from skin and intestinal mucosal surfaces [24]. Menstruation increases the average daily iron loss to about 2 mg per day in premenopausal female adults [25].

Absorption of iron occurs mainly in small intestine, particularly in the duodenum and upper jejunum [26]. Iron can be basically absorbed in two forms as non-heme and heme iron. Bioaviability of iron for absorption decreases in succession heme iron > non-heme Fe(II) > non-heme Fe(III). Absorption of **non-heme iron** is significantly influenced by its oxidation state and dietary factors. At physiological pH, inorganic ferrous iron is readily oxidized to water insoluble ferric hydroxide form. Low pH enviroment in the proximal duodenum enhances the solubility and uptake of ferric iron (which originates from non-heme bound iron in metalloproteins present in food). Iron is internalized into cells by the duodenal import transporter DMT1 (also reffered as DCT1 or Nramp2) [27]. Expression of DMT1 responses to actual iron availability and body needs – increases during iron deficiency and decreases in conditions of iron excess [28, 29].

Factors that have an infuence on intestinal no-heme iron absorption:

Inhibitors: phytates, polyphenols, calcium, starch, antacids, iron overload

Enhancers: ascorbate, citrate, amino acids, muscle tissue, iron deficiency

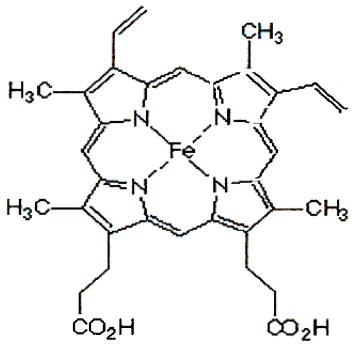

Heme

Heme is a remarkable iron containing biomolecule which consists of one iron atom bound in the center of a heterocyclic ring - porphyrin. Not all porphyrins contain iron, but a substantial fraction of porphyrin-containing metalloproteins use heme as their prosthetic group; these are known as

hemoproteins. Hemoproteins possess diverse biological functions including the transport of diatomic gases, chemical catalysis, diatomic gas detection, and electron transfer. There are several biologically important types of heme which mutually differ in their side chain groups. The most common type is heme B (see figure above) that is present in hemoglobin, myoglobin and peroxidases. Other important types include heme which differs from heme B in that a methyl at ring position 8 is oxidized into a formyl group, and one of the vinyl side chains, at ring position 2, is replaced by an isoprenoid chain (present in cytochrome c oxidase). Heme C differs from heme B in that the two vinyl side chains are covalently bound to the apoprotein itself through thioether linkages. Iron present in heme C is usually coordinated to two side chains, making the iron hexacoordinate.

In humans heme is absorbed by mechanism completely different to that of inorganic iron. The process is more efficient and is independent of duodenal pH. As in case of inorganic iron, detailed description of heme absorption was missing. Only the last year Shayeghi M et al. characterized a novel putative heme carrier protein 1 (HCP1) using a subtractive hybridization approach. HCP1 is thought to mediate heme uptake by the cells in a temperature-dependent and saturable manner. This protein is highly expressed in duodenum and regulated by hypoxia. Moreover, HCP1 protein is iron regulated and localized to the brush-border membrane of duodenal enterocytes in iron deficiency [30]. These data indicate that HCP1 could represent the long-sought intestinal heme transporter.

The fate of absorbed heme is not known in details. Some heme fraction could be also recycled and used for intact incorporation into hemoglobin as described on erythroid cells [31, 32]. Enterocyte heme pool may be degraded by hemoxygenase – an

enzyme which is known to be able to release iron from heme. In fact, inhibition of heme oxygenase activity in the intestine can produce iron deficiency [33]. The best nutrition sources of heme iron are meats.

Iron is essential for life, however there is also permanent risk of metabolic iron-induced toxicity. In the body enviroment, the cells continuously produce reactive oxygen intermediates (ROI) as a side products of electron transfer. The most common ROI species include peroxides, superoxides and hydroxyl radicals. Another examples of cellular ROI production are the free radicals originating from peroxisomes, microsomes and miscellaneous enzymatic reactions catalyzed by oxygenases and reductases. The most reactive and dangerous among reactive oxygen intermediates is hydroxyl radical. It is produced by the reaction between superoxide and hydrogen peroxide.

The reaction called Fenton reaction is catalysed by Fe(II) [34].

$$Fe(II) / Fe(III)$$

$$O_2^{-\cdot} + H_2O_2 \text{ ---------- } > OH^{\cdot} + OH^{-} + O_2$$

Products of iron catalyzed Fenton-like reactions, particularly the hydroxyl radical may cause site specific accumulation (mitochondia, biomembranes) of free radicals and initiate biomolecules damage, particularly on lipids, proteins and DNA [35]. The initial reaction with each of these molecules is the formation of peroxides (*e.g.*, lipid peroxides) that can interact with other molecules to form cross links. These cross-linked molecules perform their normal functions either poorly or not at all. Peroxidaiton promotes cross links in membrane lipids, creating islands or domains of dysfunctional molecules. Cell membranes, which consist primarily of lipids, stiffen and acquire odd shapes. Protein cross linking create protein clusters, particularly in membranes of red cells which lack membrane repair mechanisms [36, 37, 38]. Iron accumulation is known to occur under

pathological conditions in many inflammatory skin diseases or in human skin chronically exposed to UV light [39]. Abnormalities in iron and ferritin expression have been observed in many types of cancer. An interest in characterizing iron compounds in human brain has increased due to advances in determining a relationship between excess of iron accumulation and neurodegenerative diseases. [40, 41, 42]. Other cells which are sensitive to iron mediated toxicity are hepatocytes. Hepatocytes, the primary component cells of the liver, are the major storage site for body iron. With iron overload, these cells are relentlessly attacked by ROI and eventually die [43]. They are replaced by fibroblast cells. The collagen laid down by fibroblasts produces liver fibrosis and, eventually, cirrhosis.

Besides iron, other transition metals like copper, manganese or cobalt are also able to catalyze Fenton reaction, however high iron deposits present in the body make iron a prominent metal trigger of free radical production. When iron is bound to a chelator molecule such as small oranic chelating agent or a protein, its reactivity and potencial toxicity is generally greatly diminished. For such purpose organisms developed specialized iron storage proteins.

One of the best studied metalloproteins is the key iron storage protein in the body called **Ferritin.** Ferritin is a very large spherical shaped cytosolic protein of molecular weight 474,000 kDa. Twenty four subunits are folded into ellipsoids and they make up a hollow protein cavity which can store up to 4500 Fe(III) ions [49]. Ferritin subunits are either of the light (L) or the heavy (H) type with a molecular weight of 19 kDA or 21 kDa respectively. Inside of the ferritin shell, iron ions form crystallites together with phosphate and hydroxide ions. Iron is deposited as semi-crystalline deposits inside these protein cavities and is metabolically inactive. The intersections of ferritin subunits form two types

of channels present on the protein wall. Different roles are suggested for both ferritin channels. Hydrophobic 4-fold channel is coated with leucine residues and 3-fold channel is lined with hydrophilic glutamate and aspartate residues [44].

H type ferritin chain contains a dinuclear ferroxidase site that is located within the four-helix bundle of the subunit; it catalyzes the oxidation of ferrous iron by O_2, producing H_2O_2. L subunit of ferritin lacks this site but contains additional glutamate residues on the interior surface of the protein shell which produce a microenvironment that facilitates mineralization and turnover of Fe(III) at the ferroxidase site. Recent spectroscopic studies have shown that a di-Fe(III) peroxo intermediate is produced at the ferroxidase site followed by formation of a oxobridged dimer, which then fragments and migrates to the nucleation sites to form incipient mineral core species [45]. Once a sufficiently sized core has developed, the processes of iron oxidation and mineralization take place primarily on the surface of the growing crystallite, thus minimizing the production of potentially harmful H_2O_2 [45].

Mitochondrial ferritin (MtFt) is a unique H-type ferritin homopolymer expressed in mitochondria. MtFt contains a ferroxidase centre formed by ferritin shells that binds iron [46, 47]. The expression of this molecule is correlated with tissues that have high numbers of mitochondria (e.g., testis), rather than with tissues involved in Fe storage (e.g., the liver). Interestingly, MtFt was highly expressed in sideroblasts of patients with X-linked sideroblastic anemia (XLSA) but not in normal erythroblasts [48].

The overexpression of MtFt results in increase of TfR1 level, and a decrease in cytoplasmic ferritin synthesis. Moreover, the enzymatic activities of iron-sulphur cluster-containing enzymes, such as mitochondrial and cytosolic aconitase, were decreased. The induction of MtFt causes a shift of iron from cytosolic ferritin to MtFt and iron once

stored in MtFt appears to be less accessible to chelation than iron that was stored in cytoplasmic ferritin [49].

Hemosiderin is another iron-storage protein complex. Its molecular nature is poorly defined, but it is thought to contain Fe(III) oxyhydroxide in an insoluble form (Fig.2). Hemosiderin was reported to be redox active molecule [50] and majority of evidence suggests that it might plays a significant role in the pathogenesis of Fe-overload disease [51]. Hemosiderin is most commonly found in macrophages, lysosomes and siderosomes and is especially abundant in situations following hemorrhage into tissues. Hemoglobin from the disrupted red blood cells is released into the intracellular space where it is engulfed by macrophages that produce hemosiderin and porphyrin [52].

Fig.2 Kupffer cells with iron (hemosiderin), haematoxylin and eosin stain

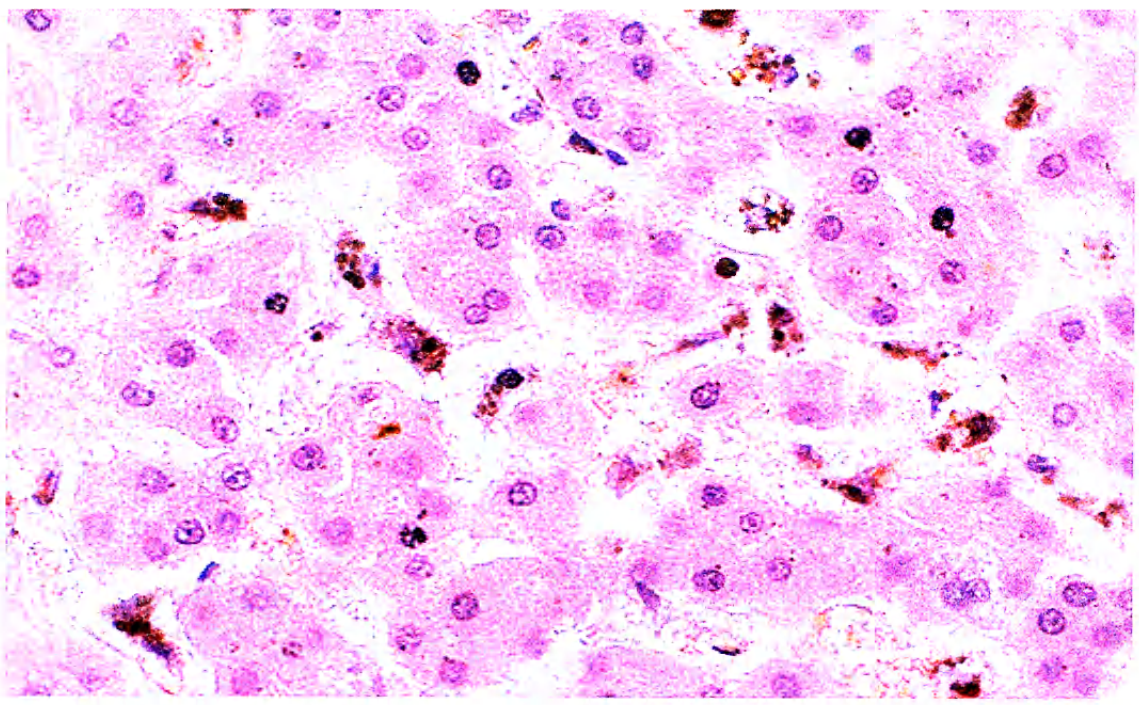

Image source: http://www.md.huji.ac.il/mirror/webpath/LIVER060.jpg

Iron transport and homeostasis

The detailed mechanism of iron absorption in the intestinal tract and its transport into the blood stream remained elusive for a long time despite extensive research. Only the recent discoveries of several novel key molecules (DMT1, Dctyb, Ireg1, hephaestin and hepcidin) involved in the regulation of iron homeostasis brought in some fresh significant insights (Fig.3). The first identified mammalian iron transporter was divalent metal transporter 1 (DMT1), a brush border ferrous iron transport protein [53, 54]. So far, four **DMT1** isoforms have been identified that differ in both the N- and the C- terminus. Two of the isoforms have a 3' iron responsive element (IRE) in their mRNA (IRE is disscused bellow) [55, 56]. Higher expression levels of IRE containing DMT1 splice variant in duodeum suggest a potential role of IRE in the regulation of intestinal DMT1 expression [56, 57]. A rapid decrease in DMT1 mRNA and protein levels have been observed following an oral dose of iron in rats [58, 59]. Because most of dietary non-heme iron is present in the form of ferric iron complexes, these must be reduced to ferrous ions before iron can be successfully transported by DMT1. After brush-border surface ferric reductase enzymic activity has been demonstrated [60, 61], McKie et al. used a subtractive cloning strategy designed to identify intestinal genes involved in iron absorption, to isolate a previously unidentified gene encoding a cytochrome b-like molecule, which was named **Dcytb** (for duodenal cytochrome b). Dcytb appears to lack any conventional NADH, NADPH, or flavin binding motifs that would allow these cofactors to act as intracellular electron donors. The lack of sequence homology with yeast and plant sequences indicates that Dcytb evolved independently as a mammalian ferric reductase. For iron reduction, cytochrome b561 receives an electron from ascorbate [62] and does not appear to require other components [63].

Another recently discovered molecule involved in intestinal iron transport is the basolateral iron exporter **IREG1** also reffered as ferroportin or MTP1 [64, 65]. The expression of IREG1 seems to be cell-specific. In enterocytes IREG1 is upregulated by iron deficiency, since in macrophages and neuronal cells the same effect is produced by cellular iron accumulation [66]. IREG1 is responsible for iron efflux in the process of intestinal iron absorption, while in Kupffer cells IREG1 mediates iron export for reutilization by the bone marrow [67]. Increase of neuronal IREG1 expression in response to cell iron accumulation opens up the hypothesis that neurons and astrocytes may be able to down-regulate the concentration of potentially toxic intracellular iron through IREG1 expression [66, 68]. Results of Jeong and Davis suggest that iron efflux from neural cells through IREG1 may be dependent on a presence of glycosylphosphatidylinositol-anchored ceruloplasmin [68].

Fig.3 Schematic ilustration of iron absorption (DMT1) and export (ferroportin, IREG1) in enterocyte.

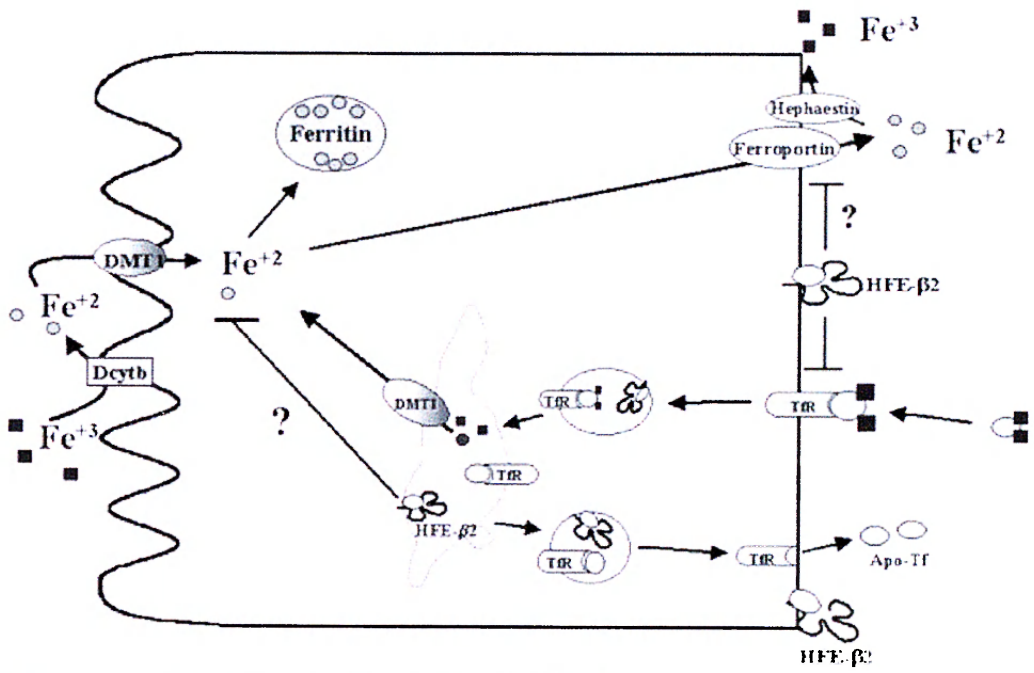

Image source: http://www.scielo.cl/fbpe/img/bres/v39n1/fig32.gif

Extracellular iron is transported within the serum bound to a Fe-binding glycoprotein, transferrin (Tf) [69, 70]. **Transferrin** (80 kDa) is a protein with extraordinarily high binding affinity for ferric iron. One molecule of iron free apo-transferrin is capable to bind two Fe(III) ions. Two iron ions carrying tranferrin (holotransferrin) binds to the surface of cells through a specific receptor, the **transferrin receptor** (TfR, 85 kDa) [71].

Virtually all cells express transferrin receptors and utilize the endocytic transferrin cycle for iron uptake [72]. The level of transferrin receptor expression reflects the needs of the cellular iron uptake, which is influenced by the rate of cell divisions as well as by special metabolic needs, such as the production of hemoglobin. Total iron binding capacity (**TIBC**) is typically measured along with serum iron to suspected of having either iron deficiency or iron overload. The serum iron divided by TIBC multiplied by 100 gives the **transferrin saturation**, which is a useful indicator of body iron status (normal saturation 30-40 %). The uptake of differic-Tf via the transferrin receptor 1 (TfR1) results in receptor-mediated endocytosis of the Tf-TfR1 complex (Fig.4), [73].

Fig.4 Schematic ilustration of extracellular iron internalization by endosomal Tf-TfR complex.

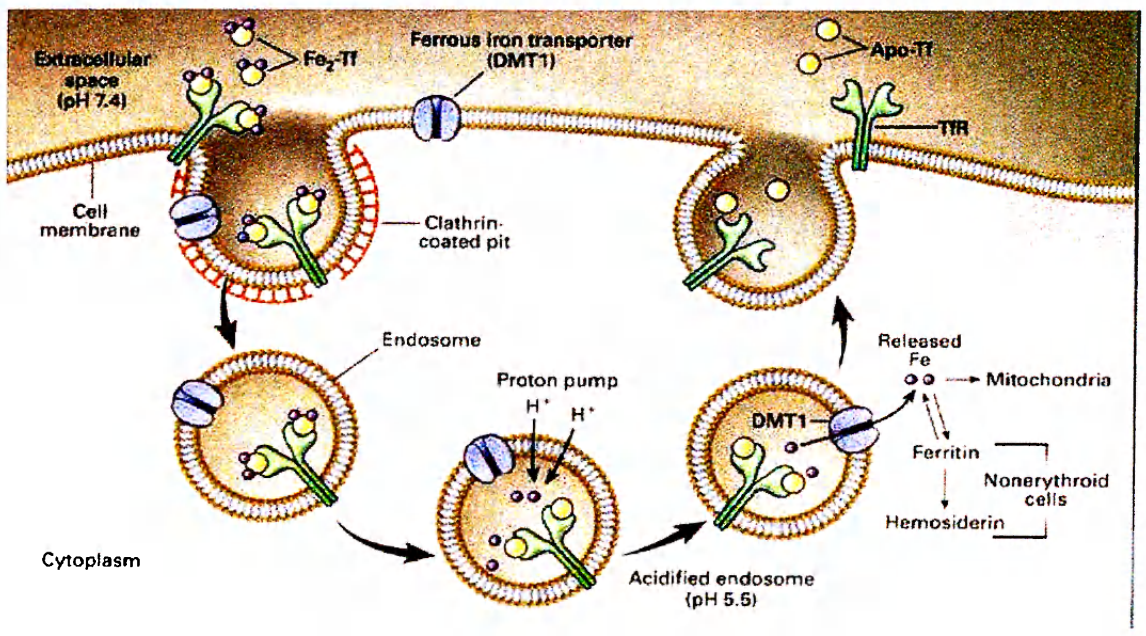

Image source: http://www.chem.duke.edu/~alc/labgroup/tf_files/image002.jpg

Besides TfR1, which is ubiquitously expressed, there is also TfR2, that is restricted to hepatocytes, duodenal crypt cells, and erythroid cells. Its function is unknown, though levels of TfR2 was recently proved to be regulated by diferric transferrin, but not by apotransferrin, specifically in hepatocytes [74, 75] which makes TfR2 an attractive candidate for the sensor of iron levels in the circulation [76].

A reduction in endosomal pH by a proton pump promotes the conformational changes in both Tf and TfR1 to release Fe [77]. An essential step in the delivery of iron from transferrin into the cytosol is the active acidification of the endosome, which aids in the release of iron from transferrin. An unidentified ferrireductase subsequently reduces Fe(III) to Fe(II), allowing DMT1, a protein also known as the natural resistance-associated macrophage protein 2 (Nramp2), to transfer Fe2+ across the endosomal membrane into the cytoplasm [78]. Apo-Tf and TfR1 are then recycled to the cell surface, where each can be used for further cycles of iron binding and uptake. An alternative iron uptake mechanisms may exist, particularly in pathological conditions, but these have not yet been fully characterized [79].

Iron regulatory proteins – IRP/IRE system

The best characterized homeostatic control mechanism of iron metabolism is the post-transcriptional regulation largely interlocked by RNA-binding proteins known as iron-regulatory proteins 1 and 2 (IRP1 and IRP2). IRPs are sensitive to cytosolic iron levels and post-transcriptionally regulate the expression of iron metabolism genes to optimize cellular iron requirements. In iron deficient cells IRPs associate with iron-responsive elements (IREs), which are conserved hairpin structures found in untranslated regions of mRNAs encoding iron-related proteins [80, 81]. The formation of **IRE/IRP complexes** on

the 5` UTR of some iron-related mRNAs serves to inhibit early steps of the translation process [82], while the IRE/IRP interaction in the 3` UTR serves to stabilize the mRNA [81]. IRP1 registers cytosolic iron status mainly through an iron-sulfur switch mechanism, alternating between an active cytosolic aconitase form and apoprotein form that binds IREs. High cellular iron levels leads to the formation of an [4Fe-4S] cluster in IRP1 that prevents binding to the 3`-IRE in transferrin receptor 1 mRNA, leading to decrease in its stability and translation. In contrast, the inability of IRPs to bind to the 5`-IRE of ferritin mRNA allows its translation. Conversely, under Fe deficiency, the [4Fe-4S] cluster in IRP1 does not form and the opposite process occurs (Fig.5), [81].

IRP2 is homologous to IRP1, but its activity is regulated primarily by iron-dependent degradation through the ubiquitin-proteasomal system in iron-replete cells. Targeted deletions of IRP1 and IRP2 in animals have demonstrated that IRP2 is the chief physiologic iron sensor. The early death of mouse embryos that lack both IRP1 and IRP2 suggests a central role for IRP-mediated regulation in cellular viability [82]. Transcriptional regulation of iron uptake occurs in the Tf and TfR genes and it is due to the interaction between the hypoxia iducible factor (HIF-1) and the hypoxia responsive element (HRE) [83].

Fig.5 Scheme of post-transcriptional regulatory actions of IRP/IRE system.

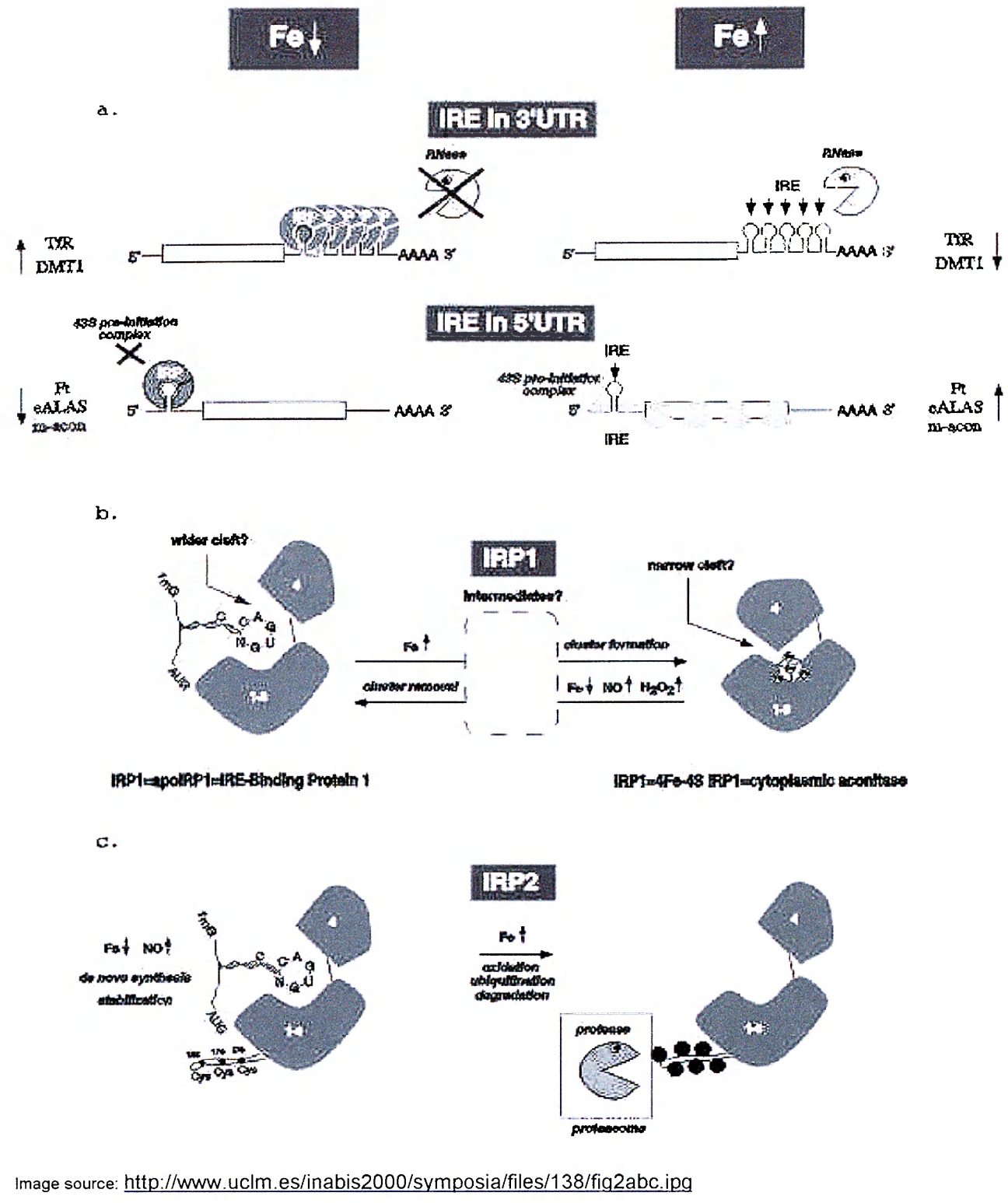

Image source: http://www.uclm.es/inabis2000/symposia/files/138/fig2abc.jpg

Mitochondrial iron metabolism

In all cell types, significant part of intracellular iron traffic is directed toward mitochondria, where substantial amounts of iron are needed for **heme biosynthesis** [85] and **biogenesis of [Fe-S] clusters** [86]. No conclusive evidence is available in what form iron must be presented to mitochondria to be competent for import. Erythroid cells have by far the greatest need for iron, which is used for hemoglobin synthesis. Therefore, in hemoglobin synthesizing erythroid cells, nearly all Fe is needed for heme synthesis, hence iron uptake from Tf is directed mainly to mitochondria [85, 87]. Mitochondria is an actual place for iron transit and utilization. Heme synthetized in mitochondria is transported back to cytosol and respiration cycle utilizes iron in cytochromes and [Fe-S] clusters. In non-erythroid cells, far less Fe is directed to the mitochondrion with a larger proportion being incorporated into cytosolic Fe-containing molecules in excess of metabolic needs.

In yeast, import of Fe into mitochondria is partially mediated by 2 transporters identified as mitochondrial solute carrier protein 3 (MRS3) and MRS4 [88]. No iron transporters have been identified in mammals, however, the export of „free" Fe from mammalian mitochondria may involve a promising candidate from the ABC half-type transporter family - MTABC3 (mammalian mitochondrial ABC protein 3 or ABCB6) [89]. Latest data published by Shaw et al. point to another mitochondrial solute carrier protein (MRS25) as a principal mitochondrial iron importer essential for heme biosynthesis. This protein which was named **mitoferrin** (mfrn) was found to be highly expressed in haematopoietic tissues of zebrafish and mouse [90].

For years, it has been suggested that Fe transported from the endosome to the cytosol enters a poorly characterized "**labile iron pool**" (LIP) which is presumably composed of

iron low Mr chelating agents [91, 92] or iron loosely bound by molecules with larger Mr (>5000) [93, 94]. The real chemical nature of this metabolically active pool has not been defined. To account for the targeting of Fe to the mitochondrion, a direct and transient physical contact between the mitochondrion and the iron-loaded endosome has been proposed in a 'kiss and run' hypothesis [87]. This model proposes that iron is released from Tf in endosome, it is passed from endosomal to mitochondrial proteins and is protein-bound until it reaches ferrochelatase in the mitochondrion. Such a transfer could be mediated by the direct interaction of the endosome with the mitochondrion.

Recent research focused on phenomenon of pathological accumulation of Fe in mitochondria of Friedrich Atatxia patients and XLSA patients (sideroblasts) opened up the disscusion about the existence of putative mitochondrial hemosiderin – degradation product of m-Ferritin, which may be critical in determining the pathology of Friedrich Atatxia and somehow linked to expression of another iron binding protein frataxin [95, 96]. **Frataxin** is a conserved mitochondrial protein of unknown function. Its deficiency is known to cause Friedreich ataxia (FRDA) - an autosomal recessive neuro degenerative disease [97]. Cavadini et al. proposed iron binding properties for human frataxin under native conditions, which assembles into a stable homopolymer that can bind approximately 10 atoms of iron per molecule of frataxin [98]. One of the hallmarks of Friedreich ataxia is also the decreased activity of iron/sulfur-containing enzymes including respiratory complexes I, II and III [99] and energy metabolism enzymes of likes aconitase, glutamate synthase or succinate dehydrogenase [100]. Recently yeast frataxin (Yfh1), the homolog of the human frataxin is thought to be directly involved in the process of Fe-S cluster biogenesis [101, 102].

Mitochondrial [Fe-S] clusters

Assembly of the [Fe-S] clusters is dedicated to mitochondria. It is mediated by a highly conserved iron-sulphate cluster assembly (ISC) machinery. This apparatus consists of some ten proteins including a cysteine desulfurase producing elemental sulfur for biogenesis, a ferredoxin involved in reduction, and two chaperones. [Fe-S] cluster assembly complex is composed of the scaffold protein Isu1 and the cysteine desulphurase Nfs1. It was reported that yeast frataxin Yfh1 binds specifically to the central [Fe-S] cluster assembly complex in iron dependent manner which suggests a role of frataxin/Yfh1 in iron loading of the Isu scaffold proteins [103, 104]. The mitochondrial Fe-S cluster synthesis apparatus not only assembles mitochondrial [Fe-S] proteins, but also initiates the formation of extra-mitochondrial [Fe-S] proteins [105]. [Fe-S] cluster-containing proteins perform important tasks in catalysis, electron transfer and regulation of gene expression. The mitochondrion contains crucial [Fe-S] cluster proteins such as the enzymes of the respiratory chain (Complexes I, II, and III), ferrochelatase (heme synthesis), and enzymes of the citric acid cycle such as aconitase and succinate dehydrogenase.

Mitochondrial aconitase (m-Acon) mRNA is a very interesting molecule in terms of iron metabolism. Iron-sulfur cluster in the active side of aconitase is a very sensitive redox sensor of reactive oxygen and nitrogen species [106]. Cubane-type $[4Fe\text{-}4S]^{2+}$ cluster contains three iron atoms bound to cysteinyl groups and inorganic sulfur atoms and a fourth labile iron atom (Fe-α). This Fe-α is uniquely bound to a hydroxyl group of substrate and water instead of cystein group [107]. Fe is released upon oxidation of the $[4Fe\text{-}4S]^{2+}$ cluster with the concomitant formation of inactive $[3Fe\text{-}4S]^{1+}$ enzyme [108]. Moreover, m-Acon is a potential target for the regulation by iron regulatory proteins (IRPs), suggesting a link between dietary iron intake, m-Acon synthesis, and energy

metabolism [109, 110]. Aconitase is also linked to controversial protein frataxin, since specific interaction of m-Acon with frataxin has been described [111]. Other important [Fe-S] cluster-containing proteins are for example already mentioned human aconitase homolog - cytosolic iron response protein 1 (IRP1), which is involved in the regulation of cellular Fe uptake and storage and the nuclear endonuclease Nth1, that is functional in base excision repair [112].

Mitochondrial heme synthesis

Heme biosynthesis occurs virtually in all cells, but the greatest amount of heme is synthetized in erythroid cells and hepatocytes [85]. The biosynthesis of heme involves eight steps, four of which occur within the cytosol, while the remaining four steps occur within the mitochondrion.

In the mitochondrial matrix, δ-aminolevulinic acid synthase (ALAS) catalyzes the first step of the heme synthesis pathway, namely a condensation reaction between glycine and succinyl CoA resulting in δ-aminolevulinic acid (ALA) [113]. ALA is transported to the cytosol where the next four steps take place. ALA dehydratase converts 2 molecules of ALA to porphobilinogen (PBG). Two subsequent enzymatic steps convert 4 molecules of PBG into uroporphyrinogen III. It is then decarboxylated to form coproporphyrinogen III that is transported into mitochondria and subsequently decarboxylated to protoporphyrinogen IX [85]. The mechanism of the transport of porphyrins into mitochondria is not fully understood. Latest results point at mitochondrial ATP-binding cassette transporter ABCB6 that is uniquely located in the outer mitochondrial membrane and is required for mitochondrial porphyrin uptake [114]. The final step of heme biosynthesis pathway involves the insertion of one atom of Fe(II) into PIX by the inner mitochondria membrane-associated enzyme ferrochelatase. Only

ferrous iron can be used by ferrochelatase [115], but neither the site where iron reduction occurs and nor the source of electrons are known.

In non-erythroid cells, the rate of heme synthesis is dependent on the formation of ALA. The rate-limiting step of heme biosynthesis by erythroid cells has been suggested to be the acquisition of Fe from Tf. Non-erythroid and erythroid cells posses the different regulatory systems for the biosynthesis of heme [85]. A functional iron-responsive element (IRE) motif has been identified in the 5'-untranslated region of the human erythroid ALAS mRNA implying that translation of ALAS mRNA is controlled by cellular iron availability during erythropoiesis [116].

Liver and iron

The liver is a very important organ in iron homeostasis. It is the major site of iron storage and it is suggested to regulate iron uptake and body traffic through its production of the iron related peptide hepcidin [117]. Liver is also the site where major proteins of iron metabolism such as transferrin and ceruloplasmin are synthetized.

Ceruloplasmin is also known as ferroxidase or iron(II):oxygen oxidoreductase. It contains 8 atoms of copper in its structure. Although it is often considered to be a copper transport protein, it is not its primary function. Ceruloplasmin catalyzes the oxidation of ferrous iron Fe(II) to ferric iron Fe(III), therefore assisting in its transport in the plasma in association with transferrin, which can only carry iron in the ferric state. Most of the iron that enters the liver is derived from plasma in form of Tf-TfR complex. In pathological situations, non-transferrin-bound iron, ferritin, and hemoglobin/haptoglobin and heme/hemopexin complexes assume greater importance in iron delivery to the organ. The liver can divest itself of iron through the plasma membrane iron exporter IREG1, a

process that also requires ceruloplasmin [118]. The last results indicate that brush border iron uptake is most strongly regulated by intracellular iron levels and support the proposal that basolateral transfer is regulated by systemic factors which reflect body iron requirements. The nature of these body signals is unclear but it is proposed that circulating hepcidin signals the body's iron requirements to the cells of the intestine. There is appearent inverse relationship between hepcidin expression in the liver and iron transporter expression in the duodenum, suggesting that a primary target of hepcidin may be IREG1 [29].

Hepcidin (HAMP, LEAP 1) is a 25 amino acid cysteine rich peptide with antimicrobial properties that has recently been identified as an important regulator of iron homeostasis (Fig.6). It is almost exclusively synthesised by hepatocytes. Mouse unable to express hepcidin was found to have iron overload resembling hemochromatosis where iron deposition was significant in the liver, pancreas, heart and kidneys but not in the spleen [119]. Conversely, transgenic mice constitutively expressing hepcidin have profound iron deficiency [120]. Hepcidin expression is increased with iron loading of animals suggesting it is a compensatory response to limit iron absorption from the intestine and when injected into mice it inhibits iron absorption. It also inhibits macrophage iron release [121]. Hepcidin has antimicrobial properties and its expression is increased in mice and humans with inflammation, suggesting that it may also play an important part in the causation of anaemia of chronic disease [122]. Hepcidin expression is increased during the acute phase response and is mediated by the inflammatory cytokine IL-6 [123]. Recently, IREG1 has been identified as a putative hepcidin receptor; binding of hepcidin to IREG1 results in internalisation of IREG1 and loss of its function [124, 125]. Thus it is hypothesised that when hepcidin levels are increased in iron overload or inflammation, iron release from intestinal crypt cells and macrophages is

reduced. In contrast, in iron deficiency when hepcidin levels are reduced, it is likely that IREG1 expression and iron release from intestinal cells and macrophages is increased [126, 127].

Fig.6 Regulatory actions of hepcidin on iron efflux from enterocytes, hepatocytes and macrophages.

(A) Iron in intestinal content is reduced by Dcyt B protein and transported across the enterocyte brush border membrane via divalent metal transporter DMT1. Iron is transported from the enterocyte via protein Ferroportin/IREG1 and binds to circulating transferrin. In macrophages and hepatocytes, iron is released from storage protein ferritin and transported across cellular membrane via Ferroportin/IREG1 to circulating transferrin. (B) Hepcidin binds to Ferroportin/IREG1 on the cell surface causing the internalization and lysosomal degradation of the hepcidin/IREG1 complex. Iron efflux from enterocytes, hepatocytes and macrophages is blocked causing a decrease in serum iron concentration.

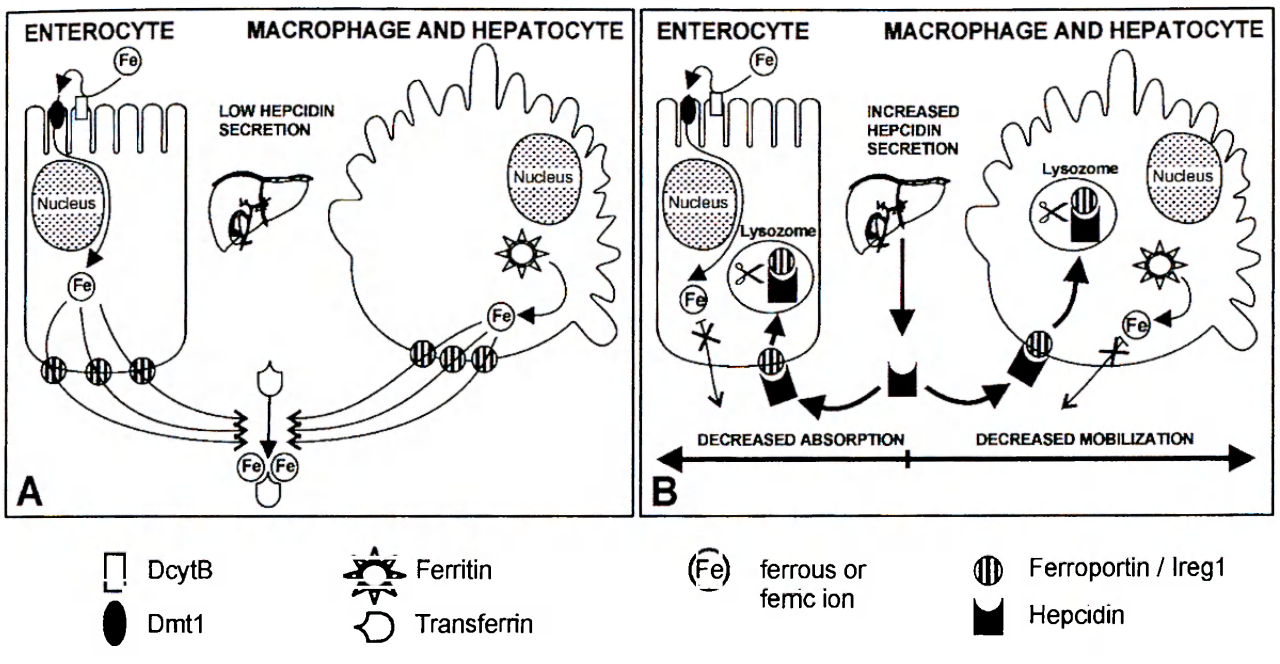

Image source: Vyoral D, Petrak J, Int J Biochem Cell Biol. 2005 Sep;37(9):1768-73.

Iron disorders

Because iron plays such a crucial role in the body, it is important for us to maintain an adequate supply of iron to form hemoglobin and the other molecules in the body that depend on iron to function properly. When the body's supply of available iron is too low, a condition known as **iron deficiency** results. People with iron deficiency cannot produce an adequate amount of hemoglobin to meet their body's oxygen-transport needs. When the deficiency becomes severe (so that there are too few circulating red blood cells or the hemoglobin content of these cells is very low), the condition is diagnosed as **iron-deficiency anemia**. The most common symptoms of iron-deficiency anemia are tiredness and weakness (due to the inadequate oxygen supply to the body's cells) and paleness in the hands and eyelids (due to the decreased levels of oxygenated hemoglobin, which is red-colored). Iron-deficiency anemia can be treated with iron supplements, and by adopting strategies to improve the body's absorption of the iron in the supplements .

It is also possible to have too much iron deposited in the body tissues. This condition is known as **iron overload.** If the iron overload becomes severe (usually when the total amount of iron in the body exceeds 15 g), the condition is diagnosed as **hemochromatosis.** Hemochromatosis can result in serious damage to the body's tissues, including cirrhosis of the liver, heart failure, diabetes, abdominal pain, and arthritis. A recessive genetic mutation can put some people (e.g., those of Irish or Celtic descent) at a higher risk for developing hemochromatosis. The haemochromatosis protein (HFE) is also expressed by hepatocytes and is likely to regulate TfR1-mediated uptake of trensferrin bound iron. TfR2 is highly expressed in human liver and is likely to play an important role in liver iron loading in iron overload states. Unlike TfR1, TfR2

lacks an iron response element and thus is not reciprocally regulated in response to the level of plasma iron. Instead, TfR2 protein expression is regulated by transferrin saturation. TfR1 and HFE play key roles in enterocyte iron absorption. TfR1 is ubiquitously expressed and transferrin mediated iron uptake is thought to occur in most cell types. HFE however is highly expressed in crypt cells. HFE is a MHC class 1-like molecule which interacts with alpha 2-microglobulin and forms a complex with TfR1. Its role in the regulation of TfR1 mediated transferrin-bound iron (TBI) uptake still remains unclear. It has been shown that HFE competitively inhibits the binding of TBI to TfR1, reduces the cycling time of the HFE/TfR1- TBI complex through the cell and reduces the rate of iron release from transferrin inside of the cell. Treatment for hemochromatosis consists of removing blood from the patient to decrease the amount of iron in the body, and treating the symptoms (e.g., liver disease and diabetes).

High iron concentrations in the brains of patients and the discovery of mutations in the genes associated with iron metabolism suggest that iron misregulation in the brain plays a part in neuronal death in some **neurodegenerative disorders**, such as Alzheimer's, Parkinson's, Huntington's diseases and Hallervorden-Spatz syndrome [41].

Biochemistry of zinc

Zinc – general properties

Zinc (Zn) is an essential trace element required by all organisms because it is an important catalytic and/or structural cofactor for hundreds of zinc-dependent enzymes and other proteins such as transcription factors. A significant portion of cellular zinc is found in the nucleus where it appears to be critically involved in maintaining genetic stability and in the process of gene expression. The zinc finger, one of the major structural motifs used for sequence specific binding of proteins to DNA, has been identified in many regulatory proteins which control cell proliferation, differentiation and apoptosis. Two families of cellular zinc transporters are known: the ZIP family that imports zinc and ZnT family that functions in releasing zinc or sequestering zinc internally.

Zinc ion plays critical roles in a wide variety of biochemical processes including growth, development and reproduction. In humans, the significance of zinc is illustrated by the devastating effects of zinc deficiency, which include dermatitis, diminished immune response, decreased healing and neurological changes [128]. Nutritional zinc deficiency in a newborn or growing animal can be fatal. It is most probably a consequence of enzyme defects, as it is known that over 300 mammalian enzymes are zinc dependent [129, 130]. Zn enzymes encompass all known classes of enzymes, i.e. oxidoreductases, transferases, hydrolases, lyases, isomerases, and ligases, which participate in a wide variety of metabolic processes such as synthesis and/or degradation of carbohydrates, lipids, proteins, and nucleic acids. In zinc-containing enzymes or proteins, zinc has two major functions, i.e. catalytic and structural. The

catalytic role specifies that zinc participates directly in enzyme catalysis. Structural zinc atoms are required for stabilization of proteins by supporting their folding and oligomerization. Zinc is therefore not simply the cofactor for enzyme catalytic functions but also the structural factor for folding of domains involved in protein-protein and protein-DNA interactions.

Although zinc is essential, excess zinc can be toxic to cells [131]. The mechanism of zinc toxicity is not known but the metal may bind to inappropriate intracellular ligands or compete with other metal ions for enzyme active sites, transporter proteins, etc. Therefore, while maintaining adequate levels of zinc, cells must also control intracellular levels when exposed to excessive zinc concentrations. Several mechanisms exist to detoxify excess zinc including the binding of the metal to cytoplasmic macromolecules.

Metallothionein proteins may play such a detoxification role [132]. Zinc transporters can also aid in detoxification by facilitating intracellular sequestration within organelle or efflux of zinc across the plasma membrane. The association of excessive zinc intake with resultant sideroblastic anemia has been rarely reported [133, 134]. Zinc promotes the synthesis of metallothionein, that binds copper, causing impaired absorption and hypocupremia. Copper´s major carrier proteins, ceruloplasmin and α_2-macroglobulin, have ferroxidase activity. Copper deficiency inhibits iron mobilization from storage depots, decreases the formation of an iron-transferrin complex required for heme synthesis and inhibits transport of iron from cell cytoplasm to mitochondria in the process of heme synthesis [135 ,136].

Although most metal cations facilitate the formation of oxidative stress, zinc appears to prevent it. The most likely mechanism for the ability of this redox inactive metal ion to reduce oxidative stress seems to be the displacement of redox active metal ions from site-specific loci where damage occurs [137].

Zinc transporters

The total body Zn content of human subjects is 2-4 g. However, Zn is referred to as a trace element, as its plasma concentration is only 12-16 μM. In the serum, Zn is predominantly bound [138] to albumin (60%, low-affinity), α_2-macroglobulin (30%, high-affinity) and transferrin (10%). The recommended dietary allowance (RDA) for zinc in humans is set at 8 mg for women and 11 mg for men [139]. The daily intake must be adjusted according to health status, since Zn steady state is regulated not only by uptake, but also by fluctuations in Zn excretion. Acute infections lead to redistribution of Zn to the liver, decreasing immunologically-important serum pool [140].

Early studies generally focused on transport proteins in the blood (albumin and transferrin) that brought zinc to the transport sites in the membrane [141-143]. Exogenous Zn enters the cell within minutes. However, it is not clearly known how Zn enters the cell. As of now, the **ZIP family of Zn transporters** and **DCT1 transporter** are the best candidates for transporters that bring zinc into cells. ZIP transporters (Zrt, Irt-like Proteins) were identified initially by their structural and functional analogy to the Zrt family in yeast Saccharomyces cerevisiae [144] and Irt transporters in Arabidopsis thaliana [145]. Zrt1 is a zinc transporter in yeast and Irt1 is an iron transporter in plants. ZIP family transporters transport also other divalent cations into cells. Human ZIP transporters (ZIP 1-3) (Fig.7a, Fig.8) appear to play roles in zinc uptake the plasma membrane. Human ZIP-2 mRNA expression has only been detected in prostate and uterine tissue indicating restricted tissue-specificity. Functional assays indicated that the human ZIP-2 protein is a functional zinc transporter [146]. When human ZIP-2 was overexpressed in K562 erythroleukemia cells grown in culture, these cells were capable of a twofold greater uptake of the zinc than control cells. A fluorescent antibody revealed

that the human ZIP-2 was localized to the plasma membrane but no intracellular location was seen. These results indicated that human ZIP-2 may serve in zinc uptake in the few tissues where it is expressed. Zinc uptake mediated by human ZIP-2 transporter was stimulated by HCO_3 in the medium. This discovery is important because a zinc transport defect in infants, Acrodermatitis enteropathica, has been characterized by a lack of a bicarbonate-stimulated zinc transport mechanism [147].

Fig.7 Schematic ilustration of zinc binding domains in ZIP and ZnT proteins

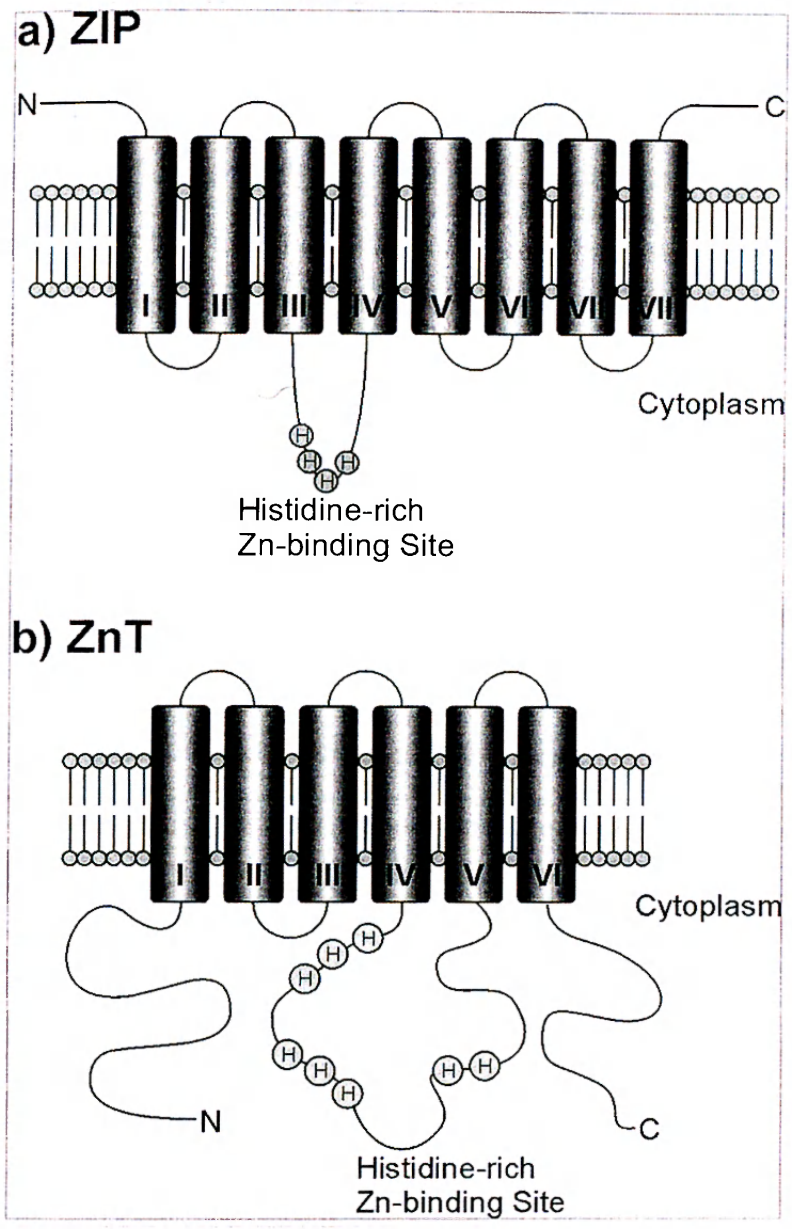

Another human ZIP transporter (ZIP-1) is the endogenous zinc uptake system in K562 cells [148]. K562 cells express ZIP-1 mRNA and the functional ZIP-1 protein is localized to the plasma membrane of these cells. Overexpression of human ZIP-1 mRNA by approximately twofold increased zinc uptake activity by twofold as well. This increased uptake activity in human ZIP-1 overexpressing cells was in contrast to human ZIP-2 overexpressing cells biochemically indistinguishable from the endogenous system in K562 cells. Finally, antisense oligonucleotides targeted to inhibit human ZIP-1 expression also inhibited the endogenous zinc uptake activity. These results strongly suggest that human ZIP-1 is the endogenous transporter in K562 cells. The antisense human ZIP-1 oligonucleotide treatment reduced zinc uptake to 10-20% of control levels suggesting that human ZIP-1 is the major pathway of zinc uptake in these cells. In contrast to the human ZIP-2 gene, ZIP-1 gene is expressed in a wide variety of different cell types. Thus, human ZIP-1 may be primary component of zinc uptake in many human tissues. This conclusion was supported by a correlation between human ZIP-1 expression levels and zinc uptake in human malignant cell lines derived from the prostate [149]. Expression of human ZIP-1 was repressed by adding zinc to the medium suggesting some regulation of zinc uptake occurs in response to cellular zinc status. A closely related ortholog of human ZIP-1 from the mouse was reported [150]. This protein was named Zirtl (zinc-iron regulated transporter-like protein). Like human ZIP-1, The ZIRTL gene is expressed in a wide variety of tissues. Both human ZIP-1 and ZIP-2 transporters have a surprisingly low affinity for zinc. K_m values are approximately 3 μM for free Zn^{2+} ions. Similar K_m values were reported for zinc transporters in a large number of mammalian cell types [151]. Because of the high chelation capacity of serum (binding to albumin, transferrin and to aminoacids such as histidine and cysteine), the free Zn^{2+} concentration in serum is calculated to be in the nM range. The capacity of

ZIP transporters for Zn uptake is relativelz high to the cellular demand for yinc. Sufficient levels of Zn can be obtained despite the apparent low affinitz of these transporters.

Some metal transporters exhibit transport capability for a spectrum of metals. This is characteristic for Fe^{2+} transporter known as DCT1 (divalent cation transporter 1)/ DMT1 (divalent metal transporter1)/ Nramp2 (natural resistance-associated macrophage protein 2) that is also involved in zinc transport [152]. This protein is a member of the Nramp family of transporters which is unrelated to ZIP transporters. Nramp family are membrane proteins conserved from yeast to man. Gunshin et al. [153] provided evidence that DCT1 was capable of Zn^{2+} uptake but these results have been recently questioned [154].

The other family of mammalian zinc transporters designated **ZnT** are five integral membrane proteins with specific groups for attaching and moving zinc (Fig.1b, Fig.2). The first zinc transporter (ZnT-1) was described by Palmiter and Findley [155]. ZnT-1 gene transfected into zinc sensitive baby hamster kidney (BHK) cells conferred the ability to resist high levels of extracellular zinc [155]. Most ZnT has six transmembrane-spanning domains to anchor the protein to the membrane and a histidine-rich loop extending into the cytosol to engage Zn destined for transport. ZnT proteins transport zinc in the direction opposite to that of the ZIP proteins, promoting zinc efflux or compartmentalization by pumping zinc from the cytoplasm out of the cell or into the lumen of an organelle. ZnT family control free zinc buildup and eliminate potential toxic effects to the cell. Five members of the ZnT family have been characterized, i.e., ZnT-1, ZnT-2, ZnT-3, ZnT-4 and ZnT-5 [155-161]. Liuzzi et al. [159] analysed 15 rat tissues to determine the relative expression of the ZnT-1, ZnT-2 and ZnT-4 mRNAs and their responses to zinc. ZnT-1 mRNA and ZnT-4 mRNA were present in all 15 rat tissues, but not to the same extent. The highest expression of ZnT-1 was in placenta, kidney,

adipose and upper intestine, i.e. in mostly excretory tissue involved in transmural movement of zinc. ZnT-2 also favored intestine and kidney but was less dominant than ZnT-1 in placenta and absent from adipose tissue. ZnT-4 mRNA was found mainly in intestine and mammary gland and in very low concentration in all other tissues. Liver seemed to express only ZnT-1 and muscle showed very low expression of all analysed ZnT. ZnT-1 and ZnT-2 were detected in two sizes whereas ZnT-4 was processed as a single transcript. ZnT-1 and ZnT-2 respond to zinc level in the diet in contrast to ZnT-4. ZnT-1 is expressed in the enterocytes of the duodenum and the jejunum, i.e. the primary sites of zinc absorption [162].

Fig.8 Schematic ilustration of cellular zinc uptake and export

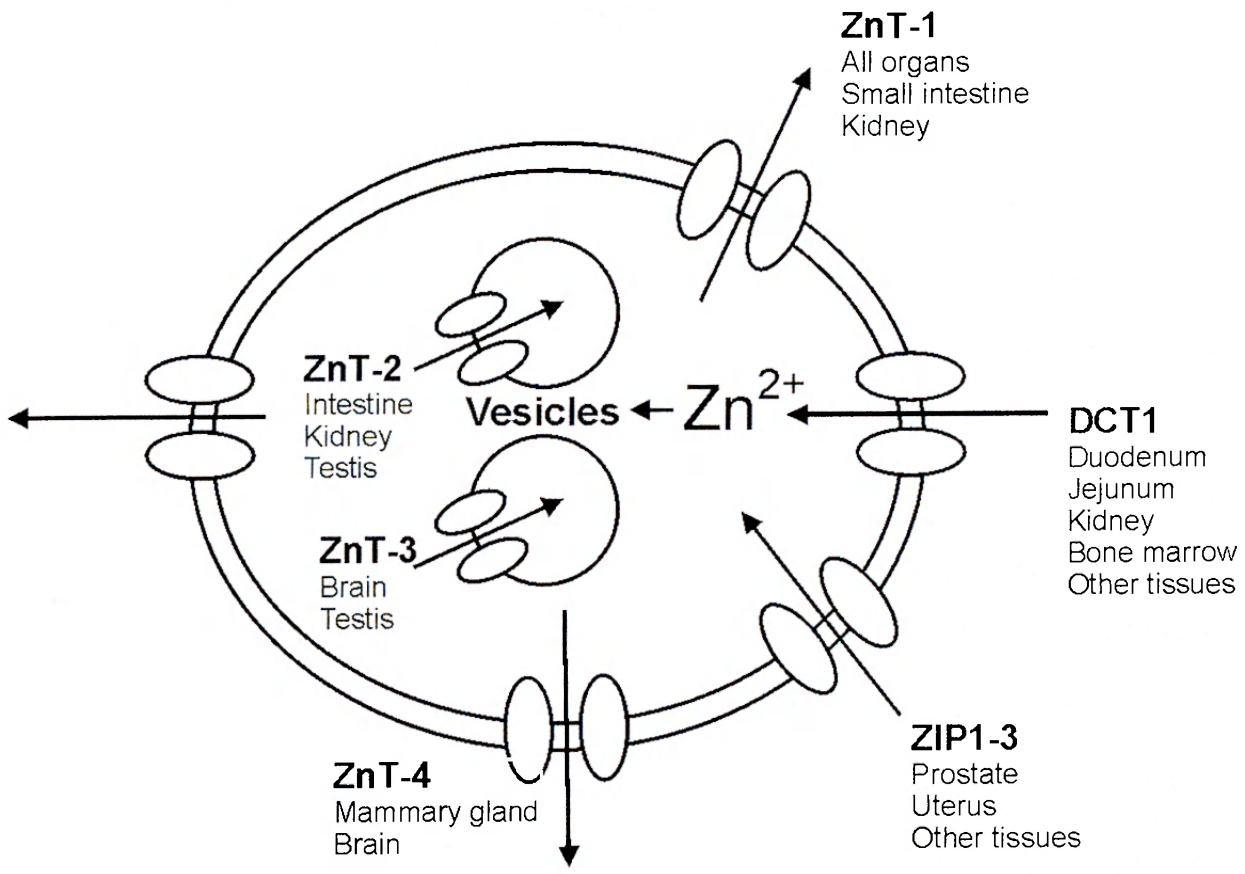

The expression of ZnT-3 is restricted to the brain and testis (Fig.8), implying some specific role in these two tissues [163, 164]. ZnT-3 was shown to be targeted to vesicles in the synaptic termini of glutamatergic neurons, implicating a role in Zn packaging for triggered release from synaptic vesicles [158]. Human ZnT-4 gene is expressed in both resting and lactating breast epithelial cells and its expression is not increased as a result of lactation [160]. Recently identified human ZnT-5 has 15 predicted membrane-spanning domains and is ubiquitously expressed in all tested human tissues and abundantly expressed in the pancreas [161]. In the human pancreas, ZnT-5 was expressed abundantly in insulin-containing beta cells that contain zinc at the highest level in the body. ZnT-5 plays an important role fortransporting Zn into secretary granules in pancreatic beta cells [161].

Zinc finger proteins

Zinc finger proteins are among the most abundant proteins in eukaryotic genomes. Their functions are extraordinarily diverse and include DNA recognition, RNA packaging, transcriptional activation, regulation of apoptosis, protein folding and assembly, and lipid binding. Zinc finger structures are as diverse as their functions. The zinc finger was first recognized by Miller et al. [165] as a repeated zinc-binding motif, containing conserved cysteine and histidine ligands, in Xenopus transcription factor IIIA (TFIIIA) (Fig.9). The consensus sequence for TFIIIA-type zinc finger domains is Tyr/Phe-X-Cys-X_{2-4}-Cys-X_3-Phe –X_5-Leu-X_2-His-X_{3-5}-His (where X is any amino acid). This sequence is present in from 2 upto 37 copies per protein, usually arranged in tandem and connected by linkers. Since 1985, numerous other zinc-binding motifs have been identified and designated as zinc fingers. Many of these proteins containing zinc fingers are transcription factors that

function by recognition of specific DNA sequences [166]. Many proteins containing the classical Cys_2His_2 zinc finger have a highly conserved linker of sequence TGEKP that connects adjacent fingers [166]. Early mutagenesis studies suggested that the linkers do play a role in DNA binding [167].

Fig.9 Scheme of binding motif in zinc finger protein.

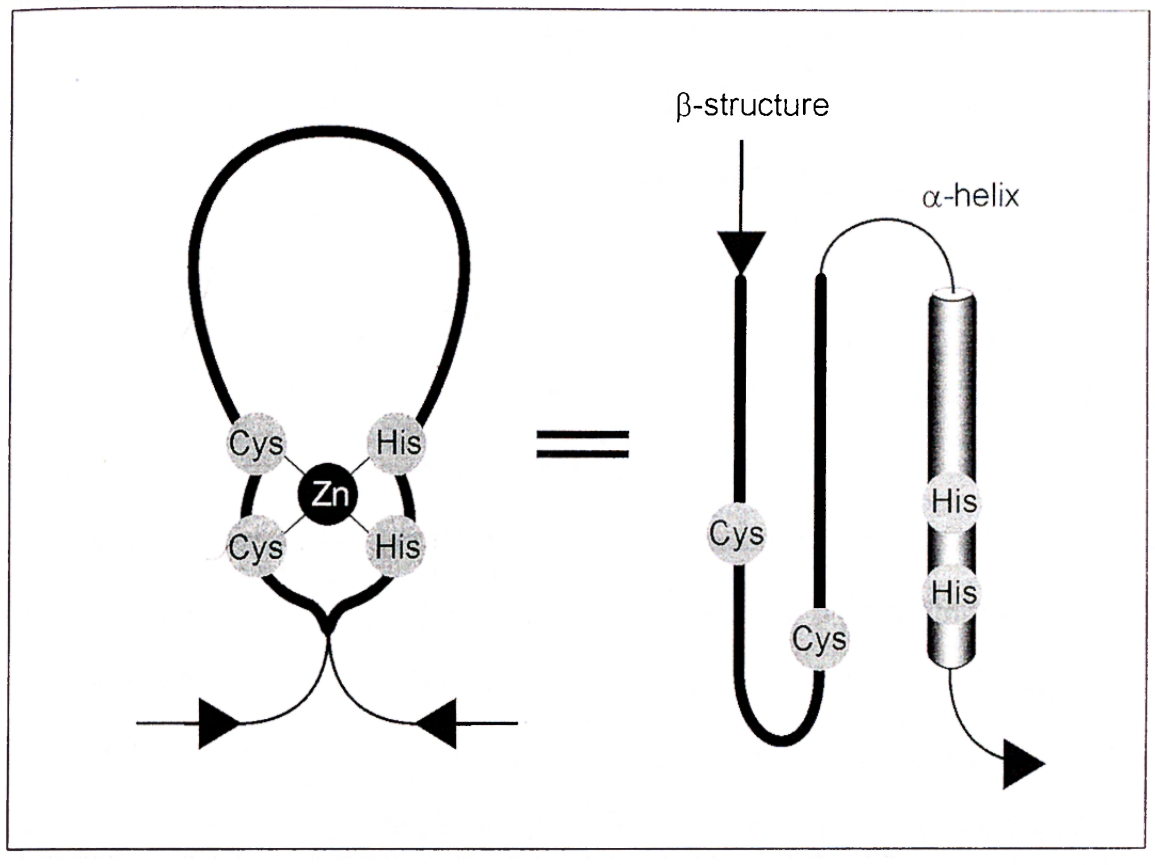

Although originally recognized in an RNA polymerase III transcription factor (TFIIIA), further analysis revealed potential zinc fingers in transcription factors influencing transcription by RNA polymerase II. The erythroid Krűppel-like factor (EKLF) is a transcription factor for the transcription of erythroid-specific genes including β-globin genes in erythroid cells. EKLF is a protein containing three TFIIIA-like zinc fingers in DNA-binding domain that binds to the β-globin CACCC element [168]. EKLF zinc fingers

share homology with the Krüppel family of Drosophila transcription factors. CACCC motifs were found also in the promoters of a number of erythroid-specific genes including GATA-1, erythropoietin receptor, porphobilinogen deaminase, carbonic anhydrase I, glycophorin B and the erythroid isoform of pyruvate kinase. The transcription factor SP1 which is broadly expressed in mammalian tissues also contains three Krüppel-like zinc fingers in DNA-binding domain. SP1 is best known for binding to GC-rich elements that are often present as multiple copies in unmethylated CpG islands in promoters of various housekeeping and tissue-specific genes [169].

The synthesis of metallothionein proteins [132] which acts to chelate and sequester the excess metal (also zinc) from the cellular environment is induced by zinc excess . Metallothionein synthesis is regulated through the metal-response element (MRE) by the transcription factor MTF-1 (MRE-binding transcription factor 1), which contains six Cys_2His_2 zinc fingers [170]. Fingers two to four of MTF-1 are involved in DNA binding, whereas finger one appears to function as a unique metal-sensing domain that prevents MTF-1 from binding to the MRE in the absence of exogenous zinc [170].

Although the majority of the Cys_2His_2 zinc finger proteins identified to date are implicated in nucleic acid binding, it is becoming increasingly clear that some members of this superfamily function by mediating protein-protein interactions. For example, the zinc finger protein Ikaros, which plays a crucial role in lymphoid differentiation, forms homodimers through the association of the two C-terminal Cys_2 His_2 zinc finger motifs [171]. The Ikaros-related protein Aiolos both homodimerizes and forms heterodimers with Ikaros through a two-zinc finger domain [172]. Zinc fingers also mediate functional interactions [173] between an important hematopoietic transcription factor GATA-1 which contains two CCCC zinc fingers (Cys-X_2-Cys-X_{17}-Cys-X_2-Cys) and the protein FOG (friend of GATA). The FOG family of proteins includes the erythroid FOG-1 and

the widely expressed FOG-2, asd well as the Drosophila U-shaped protein, all of which contain eight or nine zinc fingers homologous to the classical TFIIIA-type Cys_2His_2 zinc fingers. In five of the zinc fingers in each protein, however, the last histidine ligand is replaced by cysteine [174]. The interactions between GATA-1 and FOG involve the N-terminal zinc finger of GATA-1 and three to four of the CCHC zinc fingers of FOG [174]. The Cys_2His_2 zinc fingers of FOG play no part in binding GATA-1 and are presently of unknown function. The residues involved in DNA binding and FOG binding are located on different faces of the N-terminal zinc finger of GATA-1, suggesting that it might simultaneously participate in recognition of GATA promoter sites and binding to the FOG cofactors [175]. The FOG CCHC zinc fingers are the first example of naturally occurring proteins containing substitutions of ligands within the Cys_2His_2 motif. Very recently Nichols et al. [176] described for the first time a mutation in the GATA-1 gene in a family with X-linked dyserythropoietic anemia and macrothrombocytopenia. This missense mutation (V205M) leads to a reduced interaction of the N-terminal zinc finger of GATA-1 with its essential cofactor FOG-1. Another mutation (D218G) in the same zinc finger of GATA-1, showing pronounced X-linked macrothrombocytopenia and some features of dyserythropoiesis but with no marked anemia has been recently reported [177]. The interaction of GATA-1 and FOG-1 is clearly very important in both megakaryocyte and erythroid development. FOG-2 interaction with GATA-4 results in either synergistic activation or repression of GATA-dependent cardiac promoters, depending on the specific promoter and the cell type in which they are tested [178]. FOG-2 gene is expressed predominantly in developing and adult heart, brain and testis and is involved in the control of cardiac and neuronal gene expression by GATA transcription factors [178].

The role of zinc fingers in leukemogenesis

Promyelocytic leukemia zinc finger (PLZF) gene encodes a transcription factor with nine Krüppel - like zinc fingers, seven of which are retained in the t (11;17) (q23;q21) fusion proteins RARα (retinoic acid receptor α)-PLZF and PLZF-RARα [179, 180]. Acute promyelocytic leukemia (APL, AML-M3 as it was classified by the French-American-British /FAB/ group) is characterized cytogenetically by a consistent translocation t (15;17) (q21;q11.2-12) between chromosomes 15 and 17. Both products of the reciprocal translocation are found in these cells. RARα gene on chromosome 17 and PML (promyelocytic leukemia) gene on chromosome 15 are involved in this translocation. Fusion protein PML-RARα is an aberrant retinoid receptor with altered DNA binding and transcriptional activities that can act to block the action of wild-type RARα in a dominant negative manner. PML belongs to a family of proteins characterized by the presence of the RING-B-box-coiled-coil (RBCC) motif, which consists of a C_3HC_4 zinc finger (RING finger) and one or two additional Cys-rich regions (B-boxes) followed by a predicted leucine coiled –coil region [181]. The PML RING finger is thought to mediate protein-protein interactions. The RING finger domain is present in several proteins associated with cellular transformations, including the human tumor suppressor, BRCA-1, in which an identified cancer predisposing mutation results in the deletion of the RING finger. PML can act as a growth and tumor suppressive protein. Recent data have provided new insights into the function of PML in modulating two important cellular processes in response to DNA damage and oncogenic stimuli, apoptosis and cellular senescence. Both PML-RARα and PLZF- RARα oncoproteins seem to exert their functions through recruitment of transcriptional co-repressors and histone deacetylases (HDAC). Treatment with pharmacologic doses of all-trans retinoic acid (ATRA) results in

release of the transcription repression only in the case of PML-RARα oncoprotein [179, 182]. PLZF in the fusion protein PLZF-RARα contributes to independent, strong interaction with SMRT (silencing mediator for retinoid and thyroid receptors) co-repressor and is able to restore effective repression also in the presence of ATRA [179].

The ecotropic virus integration site-1 (EVI-1) gene, located at chromosome band 3q26, encodes a nuclear DNA-binding protein with zinc finger domains [183, 184]. EVI-1 protein has two zinc finger DNA binding domains and an acidic domain at its carboxyl terminal. The first zinc finger domain contains seven zinc fingers and binds to a consensus sequence GA(T/C)AAGATAAGATAA, whereas the second domain contains three zinc fingers and binds to the sequence GAAGATGAG. EVI-1 expression was not detected in normal marrow or peripheral blood, but is expressed in a subset of acute myelogenous leukemias (AML) and patients with myelodysplasia (MDS). The chromosome translocation t (3;21) generates a fusion genes AML1/EVI-1 and AML1/MDS1/EVI-1. Resultant fusion proteins which cause leukemic transformation of hematopoietic cells blocks AML1-induced transactivation by interaction of EVI-1 protein with C-terminal binding protein (CtBP) to repress transforming growth factor beta (TGF-β)-induced transactivation [185]. CtBP mediates transcriptional repression by its interaction with HDAC1 [185]. The reciprocal chromosome translocation t (8;21) is frequently found in M2-type (FAB classification) acute myeloid leukemia [186-188].

The transcription factor AML1 is juxtaposed to the zinc finger nuclear protein ETO (Eight-Twenty-One), resulting in transcriptional repression of AML1 target genes. ETO has been shown to interact with co-repressors, such as N-CoR (nuclear receptor co-repressor) and SMRT to form complexes containing HDAC. Consistent with this mechanism, ETO and AML1-ETO are both associated with cellular HDAC activity. PLZF also has recently been implicated in the pathogenesis of M2 leukemias harboring the

AML1-ETO fusion protein. It has been shown that AML1-ETO and PLZF can physically interact and that in transient transfection assays AML1-ETO can block transcriptional repression by PLZF. This effect by AML1-ETO is dependent of the presence of the ETO zinc finger moiety. Conversely, ETO interacts with PLZF-RARα and enhances its ability to repress RARα transcription through the retinoic acid responsive element [189].

Functions of zinc in cellular signalling

Zinc is involved in extracellular signal recognition, second messenger metabolism, protein phosphorylation and dephosphorylation and activity of transcription factors. Zinc might function as a local hormone that is secreted with insulin from pancreatic β-cells and participates in the regulation of liver metabolism [190]. The cellular contents of the second messengers, cyclic adenosine monophosphate (cAMP) and cyclic guanosine monophosphate (cGMP), are regulated via their synthesis by cyclases and their degradation by **cyclic nucleotide phosphodiesterases** (PDEs). PDEs are zinc hydrolases and their catalytic activity is dependent on zinc [191]. This activity is stimulated by zinc concentrations up to 1μM whereas zinc concentrations above 1μM had inhibitory effects [191]. Zinc chelation abolished the stimulation of mitogen-activated protein kinases (MAPK) by insulin-like growth factor –1 (IGF-1) in rat fibroblasts, and this inhibition was reversed by addition of equimolar concentrations of zinc sulfate [192]. Treatment of human bronchial epithelial cells with subtoxic concentrations of Zn^{2+} activated the MAP kinases ERK (extracellular signal-regulated kinases), JNK (c-Jun NH_2-terminal kinase) and p38 and evoked increased phosphorylation of the transcription factors Jun and ATF-2, which are substrates of MAP kinases [193]. The stimulating effect of zinc on tyrosine phosphorylation may be caused at least partially by

interference with tyrosine dephosphorylation, because zinc inhibited various protein tyrosine phosphatases in human airway epithelial cells [194]. A regulatory function of zinc for protein kinase C (PKC) is inferred from the observation that nanomolar concentrations of zinc can activate PKC and cause a translocation to the plasma membrane, a cental event in the activation of PKC [195].

Regulatogy functions of zinc in cell proliferation

The requirement for zinc for growth and cell division is well established and several studies have suggested that DNA synthesis and cell division are more susceptible to lack of zinc than is protein synthesis [196]. Indeed several studies have reported reduced activity of DNA polymerase and thymidine kinase in various tissues following zinc depletion. Further studies have indicated that both **DNA and RNA polymerase are zinc metalloenzymes**, but this does not seem to apply to thymidine kinase [196]. Loss of DNA polymerase activity does not appear to be reversible by the addition of zinc *in vitro* which, together with other evidence suggests reduced induction of several enzymes in zinc-deficient tissue [197]. Furthermore, in several models inhibition of thymidine incorporation by zinc deficiency was proportional to the reduction in the number of cells which incorporated thymidine, which suggests that individual cells either incorporate thymidine normally or not at all. In turn this is indicative of a role for zinc in the induction of enzymes needed for DNA synthesis in the S phase of the cell cycle [198]. In several studies with mammalian cells *in vitro* in which zinc deficiency was induced by addition of EDTA (ethylenediaminetetraacetic acid) to the culture medium, the reduction in DNA synthesis was greater than that of RNA or protein, and required the EDTA to be present for some time before DNA synthesis was affected. All effects of EDTA were reversible

specifically by added zinc, which again points to an involvement of zinc in metabolic events preceding DNA synthesis rather than DNA synthesis per se [196].

The cellular homeostasis of zinc is at least partially controlled by metallothionein (MT), which has been shown to play a role in the regulation of cell proliferation. Not only the total cellular level but also the subcellular location of this protein is remarkably variable in the course of the cell cycle. Whereas MT is normally found in the cytoplasm, a translocation of MT into the nucleus was observed during the early S-phase of growth factor-stimulated primary rat hepatocytes [199]. The nuclear translocation of MT probably is a vehicle for the achievement of a high nuclear zinc level in the S-phase of the cell cycle.

Role for zinc in cell differentiation and apoptosis

The differentiation of myoblasts to myotubes was inhibited by the lack of zinc [200]. A novel role for zinc mediated by MT was found in the process of differentiation of 3T3L1 preadipocytes [201]. After stimulation of differentiation by insulin and dexamethasone, these cells enter into a phase of rapid proliferation with a concomitant rise in cellular zinc and MT contents. Simultaneously MT is translocated from the cytoplasm into the cell nucleus. Upon entry of the cells into the subsequent actual differentiation, the elevated levels of zinc and MT return to the initial amounts and a redistribution of MT to the cytoplasm occurs. Similar changes in subcellular localization pf zinc and MT were also observed in the course of differentiation of two myoblast cell lines to myotubes [202]. Apoptosis or programmed cell death is a major form of cell death. Zinc is involved to some extent in DNA damage and activation of p53 gene, but in addition inorganic zinc has been reported to protect against UV-induced apoptosis by reducing the extent of the

primary DNA damage possibly by acting as an antioxidant [203]. A number of other studies with animals and with cells in culture have demonstrated that zinc-deficiency induced by dietary deprivation or by membrane-permeable zinc chelators induces apoptosis, whereas zinc supplementation can protect against apoptotic death [204, 205]. Transcription factor and tumor suppressor p53 plays an important role in regulating the cellular response to DNA damage, including the cell cycle arrest and the induction of apoptosis. The specific DNA-binding domain of p53 has a complex tertiary structure that is stabilised by a zinc and is disrupted and unfolds in cells exposed to a membrane-permeable zinc chelator but refolds on removal of the chelator [206].

Zinc - remarks and perspectives

Research over past years has produced major advances in our knowledge of zinc transporters and their regulation in eukaryotic organisms. Study of these transporters has identified their various roles in zinc uptake, rfflux, compartmentalization, storage, and detoxification. Moreover, the regulatory mechanisms that control the activity of these transporters in response to zinc status are becoming increasingly clear. Despite this progress, however, we are still very far from a complete picture of these processes in zinc homeostasis and metabolism. Functional analysis of these transporters will identify their substrates and determine their biochemical mechanisms of action. Localization studies will determine the tissue and cell-specific expression patterns of these proteins and define their subcellular locations. Genetic studies, e.g., targeted gene disruption in mice, will assist in determining transporter function through the phenotypic analysis of the resulting mutants.

With growing awareness of entire genomes and the resources available to investigate this information, there are increased opportunities to examine the impact of zinc on gene expression. The tools of genomics, including cDNA arrays have been recently used for this purpose in the study of the modulation of intestinal gene expression by dietary zinc status in rats [207]. Messenger RNA differential display method allowed to identify intestinal uroguanylin precursor as an upregulated gene in zinc deficiency [208] and this was confirmed by both Western blot analysis and immunohistochemistry [209]. Uroguanylin has a role in the etiology of diarrhea observed in human zinc deficiency. Diarrheal disease has long been recognized as a major international health problem and is one of the major causes of infant mortality, especially in developing countries [209].

The advent of genomic sequencing and the availability of the complete sequences of several genomes provide new opportunities to study biology and to develop therapeutic strategies through specific modulation of the transcription of target genes. Therefore, regulation of the transcription level by "artificial repressors" is of special importance. Zinc finger motifs offer an attractive framework for the design of novel tailored DNA binding proteins [210-212]. Such DNA binding proteins would be expected to possess a unique binding sequence with high specificity and affinity. The example of this "artificial reppressor" are three or four zinc- finger proteins targeted against $p190^{BcrAbl}$ fusion oncogene cDNA. Corresponding fusion oncoprotein is involved in leukemogenesis [213, 214].

Proteomics, metalloproteins and native separation methods.

The goal of proteomics is the fundamental understanding of complex biological processes mediated by proteins. It has become one of the most important and growing research fields after the so-called post-genomic era. Proteome is a dynamic expression of the entire set of proteins from a cell or a tissue [215].

The variations of proteomes generally involve the coordinated expressions and interactions of multiple genes and proteins in synergistic efforts. Protein-protein interactions are important and operative at almost every functional level of the cell. Aberrant protein-protein interactions are implicated in a number of diseases, therefore detection, identification, and quantification of the multiple proteins, determination of their interactions and localizations within the cell as well as characterization of their post-translational modifications are essential toward understanding the regulation of biological systems.

By estimations, over 30% of known proteins require metal cofactors for proper functionality. Metalloproteins are hot topic in biology and medicine because of their various functions in connection with protein folding, neurodegenerative diseases, metalloenzyme activity, and detoxification through transport and storage mechanisms. The isolation, determination and chemical structural determination of a metalloprotein, are challenging proteomics tasks that require the use of numerous complementary biological processing and instrumental components. Because the metal cofactor is often bound to the protein by loose non-covalent interactions it is important to isolate and analyze the metalloprotein in its native conformation preferably. This prerequisite is significant for detection methods that are based on tracing the metal ions present in proteins (radio labeling, inductively coupled plasma mass spectrometry (ICP-MS)). Such

biochemical task requires the development of multidisciplinary methodologies that contribute to solving the larger analytical problem.

Biological tissues are often pre-purified using various types of chromatography ranging from classical methods such as size exclusion and ion exchange to different types of affinity chromatography [216]. The immunoaffinity approach is frequently used to determine whether two proteins associate *in vivo* and to identify interaction partners within a complex [217, 218]. In a typical experiment, protein complexes are captured from a cell lysate by an immobilized antibody that recognizes an epitope on one of the known components of the complex. After extensive washing to remove unspecifically bound proteins and contaminants, the complexes are eluted and the individual components identified by mass spectrometry. The use of this method is limited by the availability of proper antibodies and is not practicable when analyzing yet unknown protein targets. The use of metal-affinity beads is another method for tracking down the metalloproteins, altough it can comprise a significant unspecific binding of proteins to the matrix beads. In this case the use of proper controls and blank samples is very necessary [219].

Other approach includes the separation of pre-purified metabolically metal radio-labeled tissues using native gel electrophoresis. Blue Native electrophoresis (BN PAGE) enables a native separation of multi-protein complexes. It is a charge shift method in which the electrophoretic mobility of a protein complex is determined by the negative charge of bound CBB G dye and the size and shape of the complex [227]. BN-PAGE combined with MS has the potential to resolve and identify intact metalloprotein complexes of both, water soluble and membrane proteins.

Our proteomics group at Institute of Hematology was focused on the development of the effective methods for native electrophoretic separation, visualisation and

identification of iron and zinc binding proteins for quite a long time. Pioneer experiments were done on modifications of Laemli electrophoresis technique adopting it for native separations of metalloproteins and their identification by storage phosphorimaging [93, 94, 220, 221, 222].

Experimental work presented in this thesis is a logical follow up to these efforts, as it brings in several fresh enhancements and new discoveries in the field of zinc- and iron-binding multi-protein complexes.

Aims of the thesis

Aim A: To investigate [^{59}Fe] heme uptake and its subsequent intracellular utilization in heme binding protein complexes by developing erythroid cells.

Aim B: To investigate protein-protein interactions in purified brush border membranes (BBM) by blue native electrophoresis (BN PAGE) and to test the suitability of the method for the separation and characterization of BBM zinc binding protein complexes.

Materials and methods

Materials and methods A

[^{59}Fe] hemin synthesis

[^{59}Fe] Hemin was synthesized by the non-enzymatic incorporation of ^{59}Fe (^{59}FeCl3, HCl solution, specific activities 20– 40 mCi/mg; New England Nuclear, PerkinElmer, Boston, MA, USA) into protoporhyrin IX (PPIX) (Calbiochem, San Diego, CA, USA) under anaerobic conditions. Fifty microliters of PPIX in a pyridine (Sigma-Aldrich, St. Louis, MO, USA) stock solution (6 mg/mL) was added to 450 mL of glacial acetic acid (Lachema, Neratovice, Czech Republic) at 60°C under a nitrogen atmosphere. Thioglycolic acid (0.25 mL; Sigma-Aldrich) was added into the HCl solution containing 30 mg of ^{59}Fe and the resulting mixture was immediately injected into the prepared PPIX solution and held at 60 C for 30 min under a nitrogen atmosphere. Air was bubbled through the reaction mixture for 1.5 h at room temperature. The mixture was then transferred into 20 mL of ether and washed 6 times with 30 mL of 1 M HCl in order to remove the remaining protoporphyrin and iron. The ether fraction was dried overnight under a stream of gaseous nitrogen. Dried [^{59}Fe] hemin was dissolved in 200 mL of DMSO (Sigma-Aldrich) and the solution was stored at 4 C.

The purity of the product was verified by thin layer chromatography on silica gel plates using ether:acetic acid:- methanol (20:3:2) mobile phase at room temperature. Labeling and extraction efficiency ranged from 92–95%.

Cell culture and [^{59}Fe] hemin cell labeling

MEL cells (line 707) were grown in RPMI 1640 medium (Gibco, Invitrogen, Carlsbad, CA, USA), supplemented with 10% fetal bovine serum (GIBCO, Invitrogen) under a 5%CO2 atmosphere. Erythroid differentiation of the cell culture was induced by adding hexamethylene-bis acetamide (Sigma- Aldrich) to the final concentration of 5 mM [223]. Cells were harvested after 4 d of induction. Induced cells were washed 3 times with 50 mL of PBS (pH 7.4) and collected by centrifugation (10 min, 18006*g*, 4 C). Cells were resuspended in 1mL of PBS (pH 7.4) at room temperature, adjusting the cell density to 16108/mL. Forty microliters of [^{59}Fe] hemin stock solution in DMSO (100 pmol of hemin) was then added and cells were incubated for 30 min at 37 C without agitation. After centrifugation (5 min, 30006*g*, 4 C), the labeling solution was discarded. The cells were washed twice in 10 mL of PBS and consecutively lysed in 1 mL of buffer composed of 1.5% Triton X-100, 10 mM HEPES and 0.14 M NaCl supplemented with EDTA-free protease inhibitor cocktail (Roche, Penzberg, Germany) according to the manufacturer's instructions. The lysis was performed at 15 C, to increase the solubility of membrane proteins and to disrupt the detergent resistant membrane areas (lipid rafts) [224]. The lysate was cleared by centrifugation (15 min, 16 0006*g*, 15 C) and the resulting supernatant was diluted with 0.1% Triton X-100, 20mM HEPES, pH 8.0 buffer to the final volume of 5 mL.

Flow protein liquid chromatography

Anion exchange liquid chromatographic separation was performed at room temperature using the medium-pressure BioLogic HR system (Bio-Rad, Hercules, CA, USA). In these studies, 5 mL of labeled cellular lysate was loaded onto the Mono Q HR 5/5 column (Pharmacia Biotech, New Jersey, USA) equilibrated with 0.1% Triton X-100 and 20 mM

HEPES, pH 8.0. Proteins and protein complexes trapped on the column were eluted with a linear gradient of sodium chloride from 0–1 M NaCl (flow rate 1 mL/min). The elution of ^{59}Fe-labeled proteins was monitored by a radioactivity flow detector for gamma emitters (Gabi Star, Raytest, Straubenhardt, Germany). A total nine radioactive fractions were collected, concentrated and desalted using Microcon microfilter units with a 5000 nominal molecular weight (NMWL) cut-off (Millipore, Billerica, MA, USA). The final protein concentration was measured by the Bio-Rad protein assay reagent using a Pye Unicam PU 8600 spectrophotometer (Bio-Rad) at 595 nm.

Native electrophoresis and gel processing

Concentrated radioactive fractions were separated on a linear gradient (3–12%) polyacrylamide gel in the presence of the nonionic detergent Triton X-100, in Tris-glycine buffer as previously described [93, 220]. External cooling was set to 15 C. The separation on Hoefer SE600 glass plates proceeded for 4 h at a constant current of 55 mA. After electrophoresis, the gel was sandwiched between two cellophane foils (soaked and washed four times in 200 mL of double distilled water) and vacuum dried for 3 h at 40 C. The dried gels were exposed to the storage phosphorimaging screen (Fuji imaging plate BAS-IP-MS 2025) for 24 h and then scanned on a Fuji phosphorimager FLA 2000 (Fuji, Cypress, CA, USA). The resulting digital radiogram was analyzed using Aida software (Raytest).

Tryptic digestion and MS analysis

Detected radioactive protein bands were excised from the dry gel. The gel slices were rehydrated, cellophane removed, cut into small cubes and sonicated for 10 min with 20 mM DTT, 50 mM Tris-Cl, pH 8.5 in 50% acetonitrile (ACN) to achieve reduction of

cysteine residues. Proteins were alkylated with 15% acrylamide in 50mMTris-HCl,pH8.5 for 40 min at room temperature. The gel pieces were successively sonicated for 10 min in ACN, water, 50% ACN and dried in a Savant SpeedVac© concentrator (TeleChem, Sunnyvale, CA, USA). Dry gel pieces were reconstituted in cleavage buffer containing 0.01% 2-mercaptoethanol, 0.1 M 4-ethylmorpholine acetate, 1 mM $CaCl_2$, 10% ACN and sequencing grade trypsin (50 ng/mL; Promega, Madison, WI, USA). Digestion was carried out overnight at 37 C. Resulting peptides were extracted by the addition of 40%ACN and 0.5% TFA. Extracted peptides were dried in a SpeedVac©, solubilized in 20 mL of 5% ACN/ 2% acetic acid and desalted using ZipTip C18 (Millipore). Desalted and concentrated peptides were loaded onto a capillary column (id 100 mm) packed with 10 cm of MAGIC C18 reversed-phase resin (Michrom BioResources, Auburn, CA, USA). After 10 min of equilibration in solvent A (5% ACN, 0.5% acetic acid in water) the peptides were separated and eluted with a linear gradient of solution B (95% ACN, 0.5% acetic acid.) ranging from 0%–35% B for 100 min and from 35%–100% B for 20 min. The column was connected with an ion trap mass spectrometer LCQ DECA (Thermo-Finnigan, San Jose, CA, USA). Positive full scan spectra were collected over the mass range of 350–2000 Da. Each full scan was followed by the MS/MS scan from the top three ions. Dynamic exclusion was enabled with two repeat counts and repeat duration lasting 3 min. Tandem mass spectra were interpreted with SEQUEST software (ThermoFinnigan) and the data were finally compiled with the DTA Select and Contrast software [225]. Spectra were searched against a database created by extracting rat, mouse, swine and human entries from the non-redundant database downloaded from the NCBI ftp site. All hits were validated manually. The criteria taken into account were: continuity of b- or y-ion series, good signal-to-noise ratio, y-ions corresponding to proline should be intense, unassigned intense fragments should correspond either to loss of

one of two amino acids from one end of the peptides or to doubly- and triply-charged ions with neutral loss. Other features taken into consideration were specific cleavage at aspartic acid as well as losses of water (form S, T, D, E), ammonia (from N, Q, K, R), and of CH_3SOH from the oxidized methionine.

Materials and methods B

Cells and BBM preparation

Mouse intestines were obtained from three male BALB/c mice of 3 months age, fed on a standard diet. Animals were fasted for 24 h and euthanized. The duodenum and proximal 10 cm of jejunum were dissected, flushed with ice-cold PBS and placed inside out on wooden sticks. Surface enterocytes were scraped down gently into ice-cold PBS and sedimented at 1000 g for 10 min (Hettich Universal 16R). Intestinal BBM were prepared by calcium precipitation and differential centrifugation as previously described [226]. Enterocytes (85% pure and 80% viable as estimated by trypan blue exclusion test) were homogenized with Dounce homogenizer (15 strokes with a tight fitting pestle) in BBM buffer (20 mL/g of tissue, 50 mM mannitol, 2 mM Tris-HCl, pH 7.5) supplemented by protease inhibitors (Complete mini, Roche, 1 tabl/10 mL of the buffer). Solid $CaCl_2$ was added to a final concentration of 10 mM to the homogenate; the homogenate was stirred for 2 min and allowed to settle down for 30 min at 4 C. Suspension was spun down at 30006*g* (Hettich Universal 16R) for 15 min. Supernatant was finally spun down at 27 0006*g* for 30 min (Heraus Suprafuge 22) to collect the BBM fraction.

Radiolabeling of BBM with ^{65}Zn

BBM were radiolabeled with ^{65}Zn to visualize zinc-containing protein complexes. $^{65}ZnCl_2$ was purchased from DuPont NEN (Lacomed s.r.o., Czech Republic). Specific activity of $^{65}ZnCl_2$ solution in 0.5 M HCl was 132.744 mCi/mg, concentration was 53.09 ng Zn/mL. Isolated BBM (20 mg total protein) were resuspended in 1 mL of PBS and incubated with 2 mCi of $^{65}ZnCl_2$ for 10 min at 37 C, followed by the removal of nonspecifically bound ^{65}Zn by double wash with 50 mL of ice-cold PBS.

Blue native electrophoresis and native Western blotting

BBM (20 mg total protein) were solubilized in a lysis buffer containing 300 mL of 750 mM aminocaproic acid, 50 mM Bis-Tris, pH 7, and 60 mL of 10% dodecylmaltoside at 4 C. The buffer was supplemented with protease inhibitors cocktail (Complete mini, Roche 1 tabl/5 mL). After 10 min on ice, the suspension was centrifuged for 15 min at 14 000 rpm (Eppendorf centrifuge 5402), 4 C. Shortly before loading the samples on the gel, 30 mL of 5% Coomassie brilliant G (Sigma) stock solution in 50 mM aminocaproic acid (Sigma) was added into the supernatant to produce a detergent/Coomassie ratio of 4:1 (g/g). BBMs were separated on a linear gradient (4–20%) polyacrylamide gel (29:1 acrylamide/*bis*-acrylamide stock solution) in 15 mM Bis-Tris, 50 mM Tricin (pH = 7.0) as previously described [227]. Gels were 16 cm x 18 cm sized, with thickness of 1.5 mm. Blue native electrophoresis was run at 100 V, after 1 h the voltage was increased to 500 V, with current limited to 15 mA. External cooling was set to 5 C. The separation on Hoefer SE600 (Amersham) proceeded for 8 h. Gels were then stained with Coomassie brilliant G (Sigma) [228]. For purposes of native blotting, the amount of Coomassie brilliant G in cathode buffer was lowered from 0.02 to 0.002% (g/g) and after 1 h it was replaced with Coomassie free cathode buffer. Proteins were transferred onto Hybond-P

membranes (Amersham, YA0490) using semidry Western blotting system SEMI-PHOR TE77 (Hoeffer) at a constant voltage of 20 V for 1 h. Coomassie free cathode buffer was used as a transfer solution. Membranes were blocked in blocking solution containing PBS, 5% low fat milk (Friesland, Czech Republic), 0.05% Tween-20 (Sigma). For the detection of aminopeptidase N we used goat polyclonal anti-aminopeptidase N (dilution 1:500, Santa Cruz, sc-6995). Membranes were incubated with antibodies for 1 h in incubating and washing solution (IWS) containing PBS, 0.05% Tween-20 (Sigma), then washed four times for 10 min with IWS. Membranes were then probed for 1 h with donkey anti-goat IgG-HRP (dilution 1:35 000, Santa Cruz, sc-2020) in IWS, and then washed four times for 10 min with IWS. Aminopeptidase N blots were visualized as described in following section.

Immunoprecipitation and immunodetection

Preparation of Protein G beads with covalently linked antibody

Fifty microliters of Protein G beads (Sigma, P-4691) were mixed with 100 mL of rabbit polyclonal aminopeptidase N antibody (Santa Cruz, sc-15360, 200 mg IgG/mL) in a loose slurry and incubated at room temperature for 1 h with gentle rocking. Beads were washed twice with 0.2 M sodium borate (pH 9.0). After second wash, beads were resuspended in 0.5 mL of 0.2 M sodium borate (pH 9.0) and solid dimethyl pimelimidate (Sigma, D-8388) was added to bring the final concentration to 20 mM. The mixture was incubated for 30 min. Coupling reaction was stopped by washing the beads in 0.2 Methanolamine (pH 8.0) and 2 h incubation in 0.2 M ethanolamine with gentle mixing. Beads were then washed with PBS and equilibrated with BBM lysis buffer containing 600 mL of 750 mM aminocaproic acid, 50 mM Bis-Tris HCl (pH 7.0), and 100 mL of 10%

dodecylmaltoside (Sigma, D-4641). Less than 5% of the covalently linked antibody was released by boiling in SDS loading buffer as seen on SDS gels analyzing dimethylpimelimidate - crosslinked and non-crosslinked Protein G / aminopeptidase N antibody beads.

Analysis of anti-aminopeptidase N immunoprecipitate

BBM pellet was solubilized in 600 mL of 750 mM aminocaproic acid, 50 mM Bis-Tris HCl (pH 7.0) and 100 mL of 10% dodecylmaltoside (Sigma, D-4641) at 4 C. Suspension was cleared by 15 min centrifugation at 4 C at 14 000 rpm (Eppendorf centrifuge 5402). The supernatant was mixed with previously prepared anti-aminopeptidase N-coupled Protein G beads and incubated for 1 h at room temperature with gentle mixing. Beads were washed four times with excess of BBM lysis buffer and PBS. After final wash the immunoprecipitated proteins were stripped from the beads by the addition of 50 mL of 2 x SDS loading buffer (0.5 M Tris-HCl (pH 6.8), 4.4% w/v SDS, 20% v/v glycerol, 2% v/v 2-mercaptoethanol, and Bromophenol blue) at 85 C. Extraction step was repeated three times. Extracts were pooled and loaded on 4–20% Tris-Glycine gel (Invitrogen, EC60252BOX) with total protein concentration ranging 8–20 mg. SDS electrophoresis was run on Novex Mini Cell (Invitrogen) at the constant voltage of 110 V for 2 h. Proteins separated by SDS electrophoresis were transferred onto Hybond-P membranes (Amersham, YA0490) using semidry Western blotting system SEMI-PHOR TE77 (Hoeffer) at a constant current of 90 mA/gel for 1 h. Membranes were blocked in a blocking solution containing PBS, 5% low fat milk (Friesland), 0.05% Tween-20 (Sigma). For the detection of aminopeptidase A, membrane was incubated with goat polyclonal anti-aminopeptidase A (dilution 1:500, Santa Cruz, sc-18065) for 1 h in IWS containing

PBS, 0.05% Tween-20 (Sigma), then washed four times for 10 min with IWS. Membranes were then probed for 1 h with donkey anti-goat IgG-HRP (dilution 1:35 000, Santa Cruz, sc-2020) in IWS, and then washed four times for 10 min with IWS. For the detection of sucrase isomaltase, we used rabbit anti-rat sucrase isomaltase IgG (dilution 1:3000) kindly provided by Dr. Kwo-yih Yeh (Louisiana State University Health Sciences Center, New Orleans, USA). Membrane was incubated and washed in the same way as in the case of aminopeptidase A membrane. As a secondary antibody for the chemiluminiscence detection of sucrase-isomaltase, we used mouse anti-rabbit IgG-HRP (dilution 1:5000, Santa Cruz, sc- 2357). Chemiluminiscent substrate system LumiGLO (KPL, 54-61-01) was used for detection of all probed proteins. Chemiluminiscence signal was detected using Amersham Hyperfilm™ ECL™ (AP Czech).

Proteolytic digestion and sample preparation

Stained protein bands were cut from the gel and washed several times with 10 mM DTT, 0.1 M 4-ethylmorpholine acetate (pH 8.1) in 50% ACN. After complete destaining, the gel was washed with water, shrunk by dehydration with 50% ACN and reswollen again in water. Next, the gel was partly dried using a SpeedVac© concentrator, and then reconstituted with cleavage buffer containing 0.01 M 2-mercaptoethanol, 0.1 M 4-ethylmorpholine acetate, 10 M ACN, 1 mM $CaCl_2$, and sequencing grade trypsin (Promega, 50 ng/mL). Digestion was carried out overnight at 37 C, the resulting peptides were extracted by the addition of 40% ACN and 1% TFA (Sigma). Extracted peptides were dried in a SpeedVac, solubilized in 20 mL of 5% ACN/2% acetic acid, desalted using ZipTip C18 (Millipore), and subjected to mass spectrometric analysis.

Mass spectrometric analysis

Tryptic peptide mixture was applied on the PepMap™ – C18 column, 0.3 mm x 250 mm, 300A (LC packings, NL) and separated using gradient elution: 35 min from 5% ACN/0.5% acetic acid to 20% ACN/0.4% acetic acid, 90 min from 20% ACN/0.5% acetic acid to 40% ACN/0.4% acetic, acid and 15 min from 40% ACN/0.5% acetic acid to 95% ACN/0.4% acetic acid at flow rate 4 mL/min. The column was connected to an LCQ DECA IT mass spectrometer (ThermoQuest, San Jose, CA, USA) equipped with a nanoelectrospray ion source. Spray voltage was held at 1.2 kV, tube lens voltage was 10 V. The heated capillary was kept at 1507C with a voltage 32 V. Collisions energy was kept at 42 U and the activation time was 30 ms. Collisions were done from the first intense ion in each chromatographic peak, every two scans were accumulated. Positive-ion full scan and CID mass spectra were recorded. Full scan spectra were acquired over *m/z* range 350–1600. Spectra were searched with the SEQUEST software against the database created by extracting rat, mouse, swine, and human entries from the non-redundant database (nr.fasta, February 2006) downloaded from the NCBI ftp site. For spectra from a multiply charged peptide, an independent search was performed on both the 21 and 31 mass of the parent ion. The search parameters were as follows: no enzyme specificity; mass errors 2 Da for precursor and 0.8 Da for fragment ions; possible modifications: 116 Da for Met and Trp and 157 Da for Cys. SEQUEST results were automatically processed with the DTASelect and Contrast software [225] using the following criteria: *X*Corr values were 1.6 for singly charged, 1.8 and 2.7 for doubly and triply charged peptides, respectively; lowest DCn was set to 0.05; maximum Sp ranking was 450, minimum sequence length was five amino acids, and maximum sequence length was 30 amino acids. This filtering is not stringent enough to automatically remove all false-positive hits but it retains true hits albeit with lower scores. Such cases include

cleavages at proline and formation of doubly and triply charged ions with neutral loss. All hits were finally validated manually. The criteria taken into account were: continuity of *b*- or *y*-ion series, good S/N, *y*-ions corresponding to proline should be intense, unassigned intense fragments should correspond either to loss of one of two amino acids from one of the end of the peptides or to doubly and triply charged ions with neutral loss. Other features taken into consideration were specific cleavage at aspartic acid as well as losses of water (from S, T, D, E), ammonia (from N, Q, K, R), and of CH_3SOH from the oxidized methionine. For identifications based on the single peptide (this includes also cases where 21 and 31 of the same mass, oxidized Met or in-source fragments were found) only the fully tryptic peptides with continuous series of *b*- or *y*-ions and with higher scores (over 2.6 and 3.5 for doubly and triply charged peptides, respectively) were retained. Single peptide identifications based on the MS/MS from a singly charged peptide were excluded. The number of transmembrane helixes was predicted using SOSUI software application (http://sosui.proteome.bio.tuat.ac.jp/sosuiframe0.html) [229].

Results

Results A

Here we present a new native 2-D separation technique combining native chromatography with native electrophoresis and its application for separation and identification of intact protein complexes. We have demonstrated the potential of this method through identification of heme protein complexes in red blood cells. The aim of this study was to investigate [^{59}Fe] heme uptake and its subsequent intracellular utilization by developing erythroid cells. We focused our attention on the distribution and binding of radioactive heme by various cellular proteins and protein complexes. Murine erythroleukemia cells (MEL) were metabolically labeled with [^{59}Fe] hemin and cellular lysates were separated by ion-exchange chromatography. Eluted chromatographic fractions containing radioactivity were collected and further separated by native electrophoresis in presence of a non-denaturing detergent (Triton X-100).

Composition of protein complexes labeled with [^{59}Fe] heme was analyzed by LC-MS/MS. Using this 2-D separation, we identified several novel heme-containing multi-protein complexes.

We initially attempted to apply the technique of blue native electrophoresis [227] for the native and non-denaturing separation of [^{59}Fe] heme labeled proteins. However, we found that radiolabeled heme was displaced from hemoproteins by the relatively hydrophobic Coomassie blue R250 dye during electrophoresis. Displaced [^{59}Fe] heme caused vertical smearing of the radioactive signal (results not shown). Blue page native electrophoresis was therefore not suitable for our purposes and alternative procedures were needed to achieve efficient native complex separations.

We developed a novel combination of liquid chromatography with native electrophoresis for separation of protein complexes. Ion exchange chromatography was performed in the presence of the nonionic detergent Triton X-100 to enable separation of detergent-soluble membrane proteins and protein complexes. In addition to a conventional UV detector, a chromatographic column was coupled to a gamma radiochemical detector enabling the selection of protein fractions containing radiolabeled proteins (see elution profile on Fig.10).

Figure 10. Chromatogram of MEL cellular lysates

(4.16 mg protein) separated on MONO Q anion-exchange column, eluted in presence of detergent Triton X-100 (0.1%) by linear gradient of NaCl concentration (0–1 M , flow rate 1 mL/min). The radioactive signal of ^{59}Fe in eluate was monitored by a gamma detector. Radioactive fractions (18–26) were collected (shaded area).

Proteomics 2005, *5,* 340–350

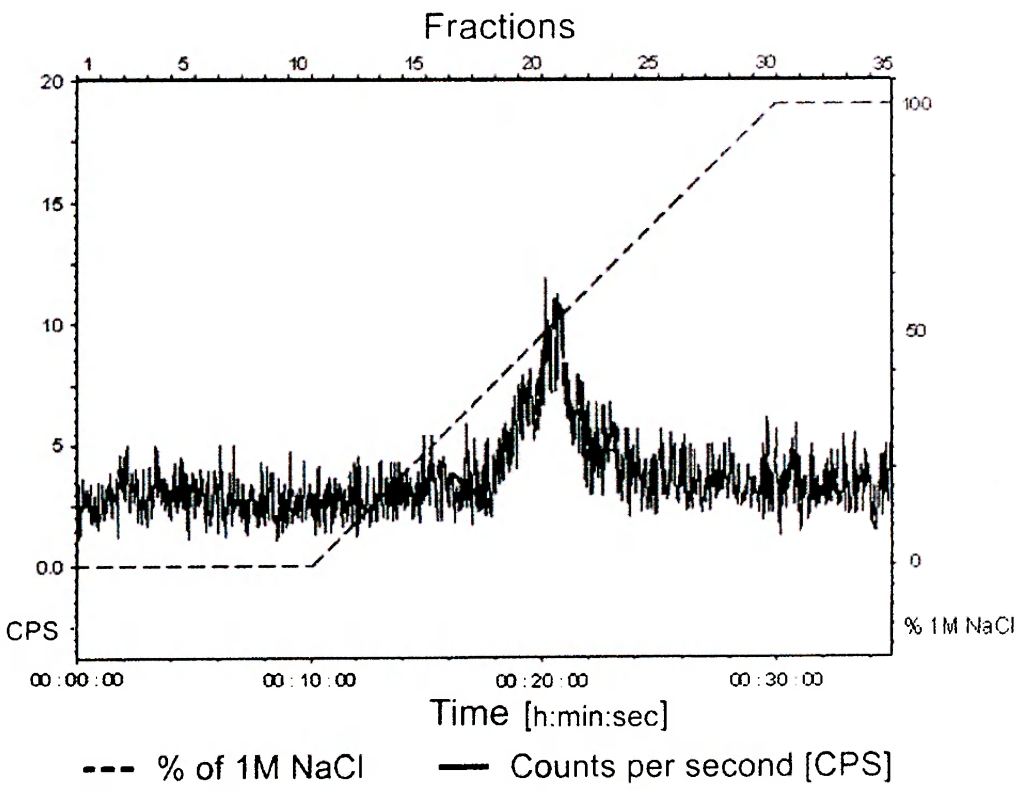

The radioactive signal could originate either from intact [^{59}Fe] heme incorporated into hemoproteins or from ^{59}Fe released from the heme by intracellular heme oxygenase and subsequently transferred into metalloproteins [31]. Each of the nine collected radioactive fractions contained only between 0.5–2.8% of the initial protein amount (4.16 mg) applied on the chromatographic column.

As the second separation step, we employed native polyacrylamide gradient electrophoresis in the presence of the detergent Triton X-100. This method offers efficient separation of water- and Triton X-100-soluble proteins and multi-protein complexes [93, 220]. Furthermore, its combination with sensitive autoradiography, enables detection and quantification of femtogram amounts of ^{59}Fe [230]. To visualize radioactive bands and to identify the composition of multiple protein components by LC-MS/MS we dried the gels between sheets of cellophane foil under mild temperature conditions. Autoradiography revealed 13 distinct bands representing [^{59}Fe] heme containing protein complexes marked A to M (Fig.11A). All bands detected on radiograms were excised from the dried original gels and subjected to a tryptic digestion. Resulting peptide mixtures were extracted and analyzed by LC-MS/MS (Fig.12). In total we identified 33 proteins (Table 1). Autoradiographs and images of Coomasie blue stained native gels of identical samples were aligned and showed the presence of a highly consistent and corresponding band pattern (Fig.11B). After analysis the proteins were assigned to four individual novel heme-binding protein complexes (Complex I–IV). Detailed composition and possible physiological function of the complexes is discussed below in the Discussion A section.

Fig.11 Native electrophoretic separation of radioactive fractions 18–26.

Concentrated chromatographic fractions containing radioactivity (50–110 mg protein *per* lane), were separated by native gel electrophoresis using gradient (3–12%) polyacrylamide gels and detergent Triton X-100. (A) Dried gels were exposed to the storage phosphorimaging screen (Fuji imaging plate BAS-IP-MS 2025) for 24 h and then scanned on a Fuji phosphorimager FLA 2000. All 13 radioactive bands (A–M) were cut from the gels and proteins present were identified by LC-MS/MS. Identified proteins were assigned to four individual heme-binding protein complexes (complex I–IV). (B) To visualize all migrating proteins gels were stained with colloidal Coomassie blue. Comparison of the stained gels with radiograms confirmed that bands A–M represent distinctly migrating bands with protein content high above the background.

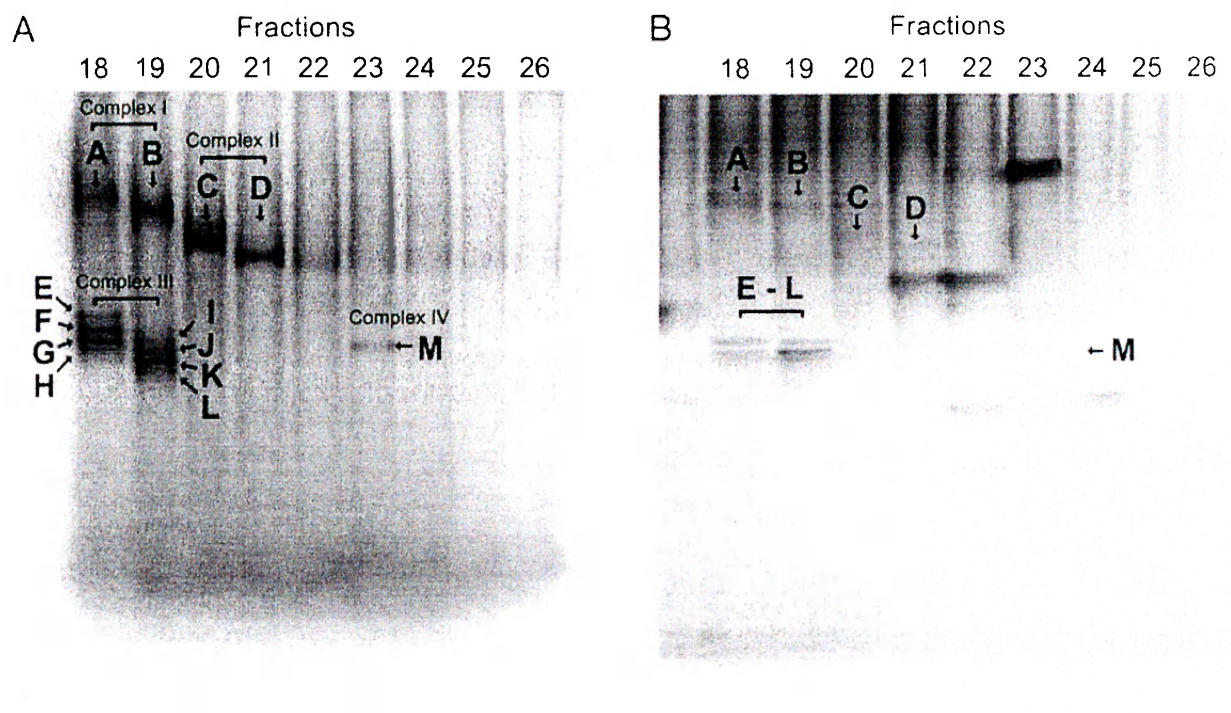

Fig 12. Representative examples of MS/MS spectra of tryptic peptides originating from (A) carbonic anhydrase, (B) alpha hemoglobin and (C) heme-binding protein, p22 HBP.

Ions of y- and b-ion series which can be found in the individual spectrum are marked in the inserted sequences.

Proteomics 2005, *5*, 340–350

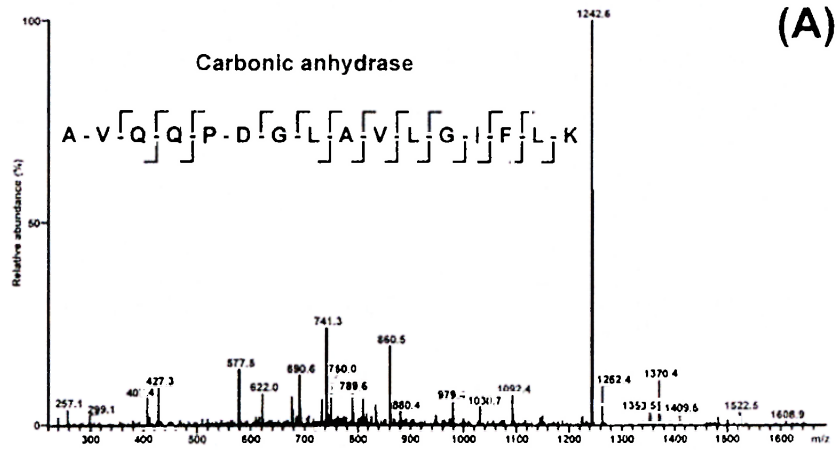

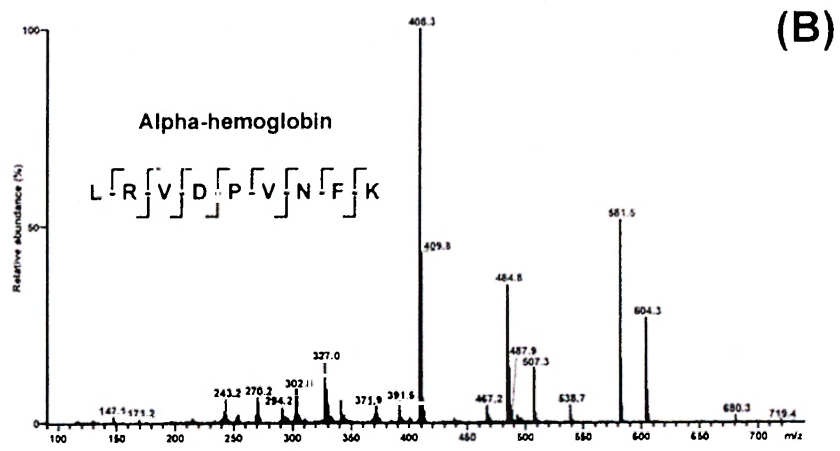

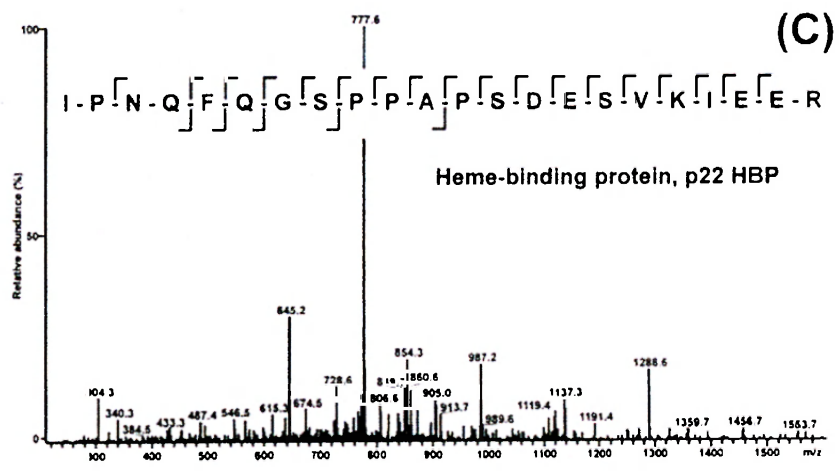

Table 1 Summary of proteins identified by LC-MS/MS

Band	Protein name [a]	Peptide sequence [b]	No. of identified peptides	NCBI no.
	Complex I			
	Alpha-hemoglobin	IGGHGAEYGAEALER	3	8481284
	Hemoglobin beta-1 chain (B1) (Major)	K.VNSDEVGGEALGR.L	11	4504349
	Hemoglobin beta-2 chain (B2) (Minor)	R.YFDSFGDLSSASAIMGNPK.V	7	21595521
	Human Hemoglobin delta chain	R.LLVVYPWTQR.F	3	4504351
A	G protein beta subunit like	R.LWDLTTGTTTR.R	4	475012
	Aldolase A protein	K.GILAADESTGSIAK.R	2	28595
	Peroxiredoxin 1 (HBP 23)	R.QITINDLPVGR.S	3	16923958
	Transketolase	R.SVPMSTVFYPSDGVATEK.A	2	11066098
	Peptidylprolyl isomerase B (cyclophilin B)	K.TVDNFVALATGEK.G	2	4758950
	Integrin-associated protein	K.ISVSDLINGIASLK.M	1	6754382
	Ubiquilin 1 isoform 2	R.NPEISHMLNNPDIMR.Q	1	22726191
	Peroxiredoxin 2 (Thioredoxin peroxidase 1)	EGGLGPLNIPLLADVTK	3	12846252
	Alpha-hemoglobin	MFASFPTTK	2	8481284
	Hemoglobin beta-1 chain (B1) (Major)	K.VNSDEVGGEALGR.L	7	4760590
	Hemoglobin beta-2 chain (B2) (Minor)	R.YFDSFGDLSSASAIMGNPK.V	2	21595521
B	**Peroxiredoxin 1 (HBP 23)**	R.LVQAFQFTDK.H	2	16923958
	Peroxiredoxin 2 (Thioredoxin peroxidase 1)	SAPDFTATAVVDGAFK	3	12846252
	Complex II			
	ATP synthase, beta polypeptide	K.VLDSGAPIKIPVGPETLGR.I	13	4502295
C	**Peroxiredoxin 1 (HBP 23)**	R.KEGGLGPLNIPLLADVTK.S	3	12837636
	Peroxiredoxin 2 (Thioredoxin peroxidase 1)	R.GLFIIDAK.G	3	12846252
	Rho GDP-dissociation inhibitor 1	R.VAVSADPNVPNVIVTR.L	2	21759130
	Ferritin light chain 1	K.NLNQALLDLHALGSAR.T	1	6753914
	Stress-induced phosphoprotein 1	R.LAYINPDLALEEK.N	1	13277819
	ATP synthase, beta polypeptide	R.DQEGQDVLLFIDNIFR.F	9	4502295
	Peroxiredoxin 1 (HBP 23)	R.KEGGLGPLNIPLLADVTK.S	3	12837636
D	**Ferritin light chain 1**	K.NLNQALLDLHALGSAR.T	1	6753914
	Peroxiredoxin 2 (Thioredoxin peroxidase 1)	R.GLFIIDAK.G	3	12846252
	Complex III			
	Alpha-hemoglobin	K.LRVDPVNFK.-	1	8481284
	Hemoglobin beta-1 chain (B1) (Major)	R.YFDSFGDLSSASAIMGNAK.V	4	12832113
	Hemoglobin beta-2 chain (B2) (Minor)	R.YFDSFGDLSSASAIMGNPK.V	2	21595521
	Human Hemoglobin delta chain	R.LLVVYPWTQR.F	2	4504351
E	Carbonic anhydrase II	K.AVQQPDGLAVLGIFLK.V	1	4557395
	Cytosolic aspartate aminotransferase	K.IANDNSLNHEYLPILGLAEFR.S	11	6754034
	Peroxiredoxin 1 (HBP 23)	R.LVQAFQFTDK.H	6	16923958
	Heme-binding protein, p22 HBP	R.IPNQFQGSPPAPSDESVKIEER.E	1	4886904
	Sialic acid synthase	K.VLVTIEEDDTVMEESVESHS.K	5	16716467
	Malate dehydrogenase, cytoplasmic	K.ELTEEKETAFEFLSSA.-	2	15100179
	Nucleoside diphosphate kinase	R.TFIAIKPDGVQR.G	1	1703290
	Adenylate kinase 2	R.LEAYHTQTTPLVEYYR.K	2	8392883
	Alpha-hemoglobin	K.LRVDPVNFK.-	1	8481284
	Hemoglobin beta-1 chain (B1) (Major)	R.YFDSFGDLSSASAIMGNAK.V	5	12832113
	Hemoglobin beta-2 chain (B2) (Minor)	R.YFDSFGDLSSASAIMGNPK.V	1	21595521
	Human Hemoglobin delta chain	R.LLVVYPWTQR.F	2	4504351
F	Carbonic anhydrase II	K.AVQQPDGLAVLGIFLK.V	2	4557395
	Cytosolic aspartate aminotransferase	K.IANDNSLNHEYLPILGLAEFR.S	9	6754034
	Peroxiredoxin 1 (HBP 23)	R.LVQAFQFTDK.H	2	16923958
	Malate dehydrogenase, cytoplasmic	K.ELTEEKETAFEFLSSA.-	2	15100179
	Nucleoside diphosphate kinase	R.TFIAIKPDGVQR.G	2	1703290

Table 1 continued

Band	Protein name [a]	Peptide sequence [b]	No. of identified peptides	NCBI no.
	Alpha-hemoglobin	K.LRVDPVNFK.-	1	8481284
	Hemoglobin beta-1 chain (B1) (Major)	R.YFDSFGDLSSASAIMGNAK.V	3	12832113
	Hemoglobin beta-2 chain (B2) (Minor)	R.YFDSFGDLSSASAIMGNPK.V	1	21595521
	Human hemoglobin delta chain	R.LLVVYPWTQR.F	3	4504351
	Cytosolic aspartate aminotransferase	K.IANDNSLNHEYLPILGLAEFR.S	14	6754034
	Malate dehydrogenase, cytoplasmic	R.VLVTGAAGQIAYSLLYSIGN.G	7	15100179
G	**Peroxiredoxin 1 (HBP 23)**	R.QITINDLPVGR.S	5	16923958
	Peroxiredoxin 2 (Thioredoxin peroxidase 1)	K.SLSQNYGVLK.N	2	12846252
	Carbonic anhydrase II	K.AVQQPDGLAVLGIFLK.V	2	4557395
	Sialic acid synthase	K.VGSGDTNNFPYLEK.T	2	16716467
	Aldose reductase	K.TIGVSNFNPLQIER.I	1	3046247
	Nucleoside diphosphate kinase	R.TFIAIKPDGVQR.G	2	1703290
	Alpha-hemoglobin	K.LRVDPVNFK.-	1	8481284
	Hemoglobin beta-1 chain (B1) (Major)	R.YFDSFGDLSSASAIMGNAK.V	3	12832113
	Hemoglobin beta-2 chain (B2) (Minor)	R.YFDSFGDLSSASAIMGNPK.V	1	21595521
	Human hemoglobin delta chain	R.LLVVYPWTQR.F	1	4504351
	Cytosolic aspartate aminotransferase	K.IANDNSLNHEYLPILGLAEFR.S	16	6754034
H	Malate dehydrogenase, cytoplasmic	K.DLDVAVLVGSMPR.R	9	15100179
	Peroxiredoxin 1 (HBP 23)	R.QITINDLPVGR.S	5	16923958
	Peroxiredoxin 2 (Thioredoxin peroxidase 1)	K.SLSQNYGVLK.N	2	12846252
	Sialic acid synthase	K.GSDHSASLEPGELAELVR.S	2	16716467
	Polyubiquitin	K.TITXEVEPSDTIENVK.A	1	2627129
	Ubiquitin-conjugating enzyme E2N	R.LLAEPVPGIK.A	2	16758810
	Alpha-hemoglobin	K.LRVDPVNFK.-	1	8481284
	Hemoglobin beta-1 chain (B1) (Major)	R.YFDSFGDLSSASAIMGNAK.V	3	12832113
	Hemoglobin beta-2 chain (B2) (Minor)	R.YFDSFGDLSSASAIMGNPK.V	1	21595521
	Peroxiredoxin 1 (HBP 23)	R.QITINDLPVGR.S	7	16923958
I	Malate dehydrogenase, cytoplasmic	K.DLDVAVLVGSMPR.R	2	15100179
	Peroxiredoxin 2 (Thioredoxin peroxidase 1)	K.FVEGLPINDFSR.E	2	12846252
	Nucleoside diphosphate kinase	R.TFIAIKPDGVQR.G	2	1703290
	Alpha-2-macroglobulin receptor-associated protein precursor	K.IQEYNVLLDTLSR.A	1	1703290
	Alpha-hemoglobin	K.LRVDPVNFK.-	1	8481284
	Hemoglobin beta-1 chain (B1) (Major)	R.YFDSFGDLSSASAIMGNAK.V	3	12832113
	Hemoglobin beta-2 chain (B2) (Minor)	R.YFDSFGDLSSASAIMGNPK.V	1	21595521
J	**Peroxiredoxin 1 (HBP 23)**	R.QITINDLPVGR.S	9	16923958
	Malate dehydrogenase, cytoplasmic	K.FVEGLPINDFSR.E	1	15100179
	Peroxiredoxin 2 (Thioredoxin peroxidase 1)	K.FVEGLPINDFSR.E	2	12846252
	Nucleoside diphosphate kinase	R.TFIAIKPDGVQR.G	2	1703290
	Alpha-hemoglobin	K.LRVDPVNFK.-	1	8481284
	Hemoglobin beta-1 chain (B1) (Major)	R.YFDSFGDLSSASAIMGNAK.V	4	12832113
K	**Peroxiredoxin 1 (HBP 23)**	R.QITINDLPVGR.S	8	16923958
	Peroxiredoxin 2 (Thioredoxin peroxidase 1)	K.SLSQNYGVLK.N	2	12846252
	Nucleoside diphosphate kinase	K.FLQASEDLLK.E	1	20912830
	Hemoglobin beta-1 chain (B1) (Major)	R.YFDSFGDLSSASAIMGNAK.V	3	12832113
	Hemoglobin beta-2 chain (B2) (Minor)	R.YFDSFGDLSSASAIMGNPK.V	1	21595521
L	**Peroxiredoxin 1 (HBP 23)**	K.ATAVMPDGQFK.D	12	16923958
	Peroxiredoxin 2 (Thioredoxin peroxidase 1)	K.SLSQNYGVLK.N	2	12846252
	Malate dehydrogenase, cytoplasmic	K.FVEGLPINDFSR.E	1	15100179

Table 1 continued

Band	Protein name [a]	Peptide sequence [b]	No. of identified peptides	NCBI no.
	Complex IV			
	Hemoglobin beta-1 chain (B1) (Major)	R.YFDSFGDLSSASAIMGNAK.V	7	12832113
	Human hemoglobin delta chain	R.LLVVYPWTQR.F	1	4504351
	Peroxiredoxin 4 (Prx-IV)	R.QITLNDLPVGR.S	1	5453549
	Peroxiredoxin 2 (Thioredoxin peroxidase 1)	K.SLSQNYGVLK.N	3	12846252
M	Heat shock protein, 110 kDa	K.LEDTENWLYEDGEDQPK.Q	3	13277753
	Heat shock protein 2	R.ARFEELNADLFR.G	1	13435696
	Nascent polypeptide-associated complex alpha chain	SPASDTYIVFGEAK	1	20867687
	ATP synthase, beta polypeptide	K.VLDSGAPIKIPVGPETLGR.I	3	2623222
	Delta-aminolevulinic acid dehydratase	K.DEQGSAADSEDSPTIEAVR.L	10	3642647
	Protein disulfide isomerase	R.LITLEEEMTK.Y	1	6981324

a) Proteins known to contain heme or iron are in bold
b) Only one exemplary peptide sequence is presented for proteins with mulitiple identified peptides

Results B

The apical surface of polarized intestinal epithelial cells (the surface facing intestinal lumen) is characterized by structurally distinct cell protrusions referred as microvilli or brush border membranes (BBMs). BBMs are the sites where digested food comes into contact with the enterocyte layer. Cytoskeleton bundles interconnected with transmembrane protein complexes of BBM form a highly organized import–export membrane interface specialized for a variety of digestive and absorptive functions [231]. Identification and characterization of functional protein complexes in BBM are the crucial steps toward the conclusive view of the physiology of absorption, revealing the protein–protein interaction networks that determine the function of intestinal digestive and absorptive apparatus. The choice of proper solubilization and separation method is an essential factor in the identification of hydrophobic membrane protein complexes.

Intestinal brush border membranes are also of particular importance in maintaining Zn^{2+} homeostasis. Besides putative zinc carriers [232] they contain several zinc binding intermembrane enzymes involved in peptide digestion [233-235].

We decided to adopt BN PAGE to characterize the native protein complexes in murine intestinal BBM and to test the suitability of the method for the separation and characterization of non-covalent zinc binding protein complexes.

Enterocyte BBM purified by calcium precipitation have a rather uniform size and shape and are well suited for transport studies. Isolated vesicles are mostly oriented right side out as confirmed by sucrase activity assay and by electron microscopy.

BN-PAGE of isolated BBM resulted in visualization of 23 distinct bands (Fig.13a).

Protein composition of all identified bands was determined by LC-MS/MS. A total of 105 proteins were identified. Accounting for the occurrence of several proteins in more than one band, 55 individual proteins were identified, among them several peptidases, enzymes of carbohydrate metabolism, ion channels, membrane transporters, cytoskeletal proteins, chaperones, and regulatory enzymes (Fig.14). Radiograms revealed the presence of total zinc binding proteins were identified in 4 bands migrating in the upper part of the gel (bands 1-4) (Fig.13c).

Using co-immunoprecipitation we have shown that zinc binding enzyme aminopeptidase N interacts with another zinc containing enzyme aminopeptidase A and also with enzyme sucrase-isomaltase (Fig. 15). Another zinc binding enzyme *N*-acetylated-alpha-linked acidic dipeptidase was identified in protein complex represented by band 3. Bands 1–4 thus likely represent different zinc binding digestive protein supercomplexes in BBM. A summary of identified proteins is shown in Table 2.

Fig.13 Native electrophoretic separation of BBM

(a) Blue PAGE separation of isolated BBM on 4–20% gradient gel. To visualize the majority of migrating protein bands after electrophoretic separation, gels were additionally stained with Coomassie brilliant G (Sigma). (b) Immunoreactivity of aminopeptidase N on Western blot made from BBM lysate blue native electropherogram. (c) Radiogram of ^{65}Zn-labeled BBMs. Isolated BBMs were resuspended in 1 mL of PBS and incubated with two mCi of ^{65}ZnCl2 for 10 min at 37°C.

Proteomics 2007, 7, 121–129

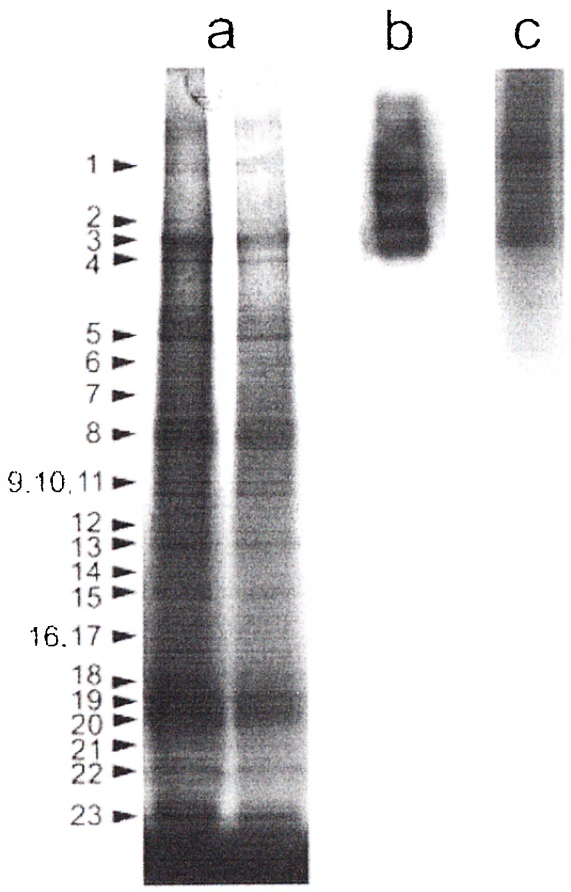

Fig.14 Functions of BBM proteins identified by LC-MS/MS.

A total of 55 individual proteins were identified in the BBM isolated by calcium precipitation.

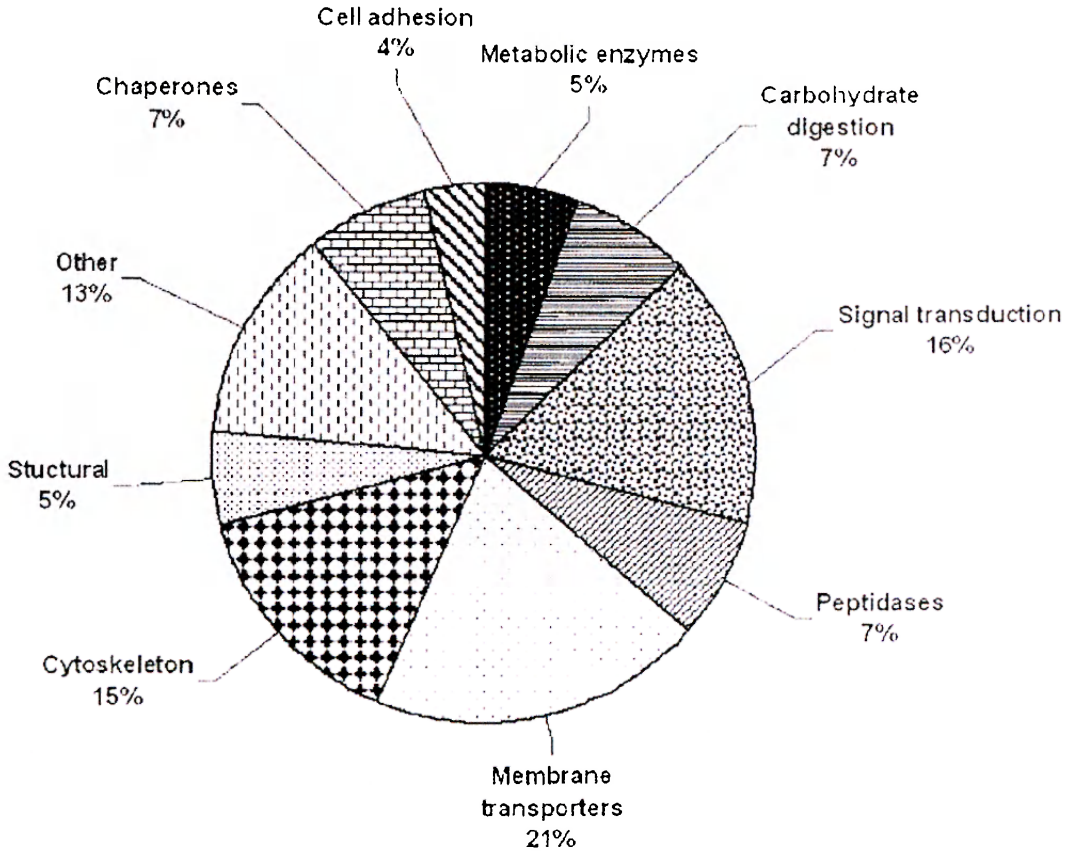

Fig.15 Co-immunoprecipitation of aminopeptidase N-associated proteins.

Anti-aminopeptidase N immunoprecipitate was prepared from BBM lysate as described in Materials and methods B, run on SDS gel and blotted to Hybond-P membrane. Separate lanes were cut from the membrane and probed with anti-sucrase isomaltase (lane a) anti-aminopeptidase A (lane b) antibodies. Immunoreactivity was visualized using peroxidase-labeled secondary antibodies and chemiluminiscence detection.

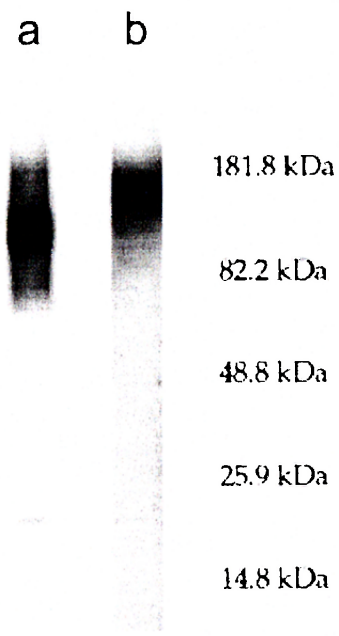

Table 2 Summary of proteins identified by LC-MS/MS

Band	Identified proteins	Gi	Peptide sequence	Peptides matched	Trans-membrane helixes
1	Fcgbp protein	7 513 694	VSQHGSDVVIETDFGLR	9	0
	Maltase-glucoamylase	28 523 399	QFLLGPAFLVSPVLEPNAR	3	1
	Sucrase-isomaltase	6 981 536	YTLLPFLYTLFYR	3	1
	Aminopeptidase N	13 529 377	TPDQIMELFDSITYSK	8	1
2	Fcgbp protein	7 513 694	VNGVLMALPVYLAGGR	9	0
	Aminopeptidase N	13 529 377	FSSEFELQQLEQFK	14	1
	Maltase-glucoamylase	28 523 399	WGGHWLGDNTAAWDQLGK	2	1
3	Fcgbp protein	7 513 694	VNGVLMALPVYLAGGR	17	0
	N-acetylated-alpha-linked acidic dipeptidase	13 929 070	HGVVGVLVYTDPGDINDGK	2	1
	Aminopeptidase N	13 529 377	TPDQIMELFDSITYSK	21	1
	Endopeptidase-2	6 678 862	ISEFEDVIGQR	2	1
	Na/K ATPase alpha	16 307 541	GVGIISEGNETVEDIAAR	6	8
	Aminopeptidase A	26 327 323	SSFIDDAFALAR	2	0
4	Fcgbp protein	7 513 694	VSQHGSDVVIETDFGLR	15	0
	Aminopeptidase N	13 529 377	QDTTSTIISIASNVAGHPLVWDFVR	15	1
	Na/K ATPase beta	54 130	GVGIISEGNETVEDIAAR	4	1
	Valosin-containing protein	26 326 751	K.NAPAIIFIDELDAIAPK.R	2	0
5	KSA preproantigen	13 542 838	ESPYDHQSLQTALQEAFTSR	3	2
	Na/K ATPase alpha	16 307 541	SPDFTNENPLETR	5	8
	Na/K ATPase beta	54 130	SYEAYVLNIIR	2	1
	Lactase-glycosylceramidase	126 428	EEYNNPLIYVTENGVSR	4	2
	Sodium-glucose cotransporter 1	6 681 727	K.MTKEEEEAMK.L	1	14
6	Na/K ATPase alpha	16 307 541	MSINAEDVVVGDLVEVK	9	8
	Na/K ATPase beta	54 130	SYEAYVLNIIR	2	1
	Actin-like protein 3	47 116 573	DITYFIQQLLR	3	1
	PEPT1	11 078 526	SSNLDFGSAYTYVIR	2	13
	KSA preproantigen	13 542 838	VNGEPLDLDPGQTLIYYVDEK	3	2
7	Na/K ATPase alpha	16 307 541	GVGIISEGNETVEDIAAR	12	8
	KSA preproantigen	49 457 512	TQNDVDIADVAYYFEK	2	2
	CD9	20 380 033	AMIVFQSEFK	2	4
	Actin-alpha	12 852 068	SYELPDGQVITIGNER	3	0
8, 9	Villin	26 388 975	MVDDGSGEVQVWR	23	0
	Microsomal triglyceride transfer protein	15 215 161	GLILLIDHSQDIQLQSGLK	26	0
	Alpha-actinin-4	26 346 759	TINEVENQILTR	10	0
	Protein disulfide-isomerase	38 197 382	HNQLPLVIEFTEQTAPK	11	1
10	Villin	26 388 975	IEDLELVPVESK	7	0
	Microsomal triglyceride transfer protein	15 215 161	YDVSFITDEVK	20	0
	Protein disulfide-isomerase	38 197 382	VLVGANFEEVAFDEK	9	1
	Sodium-dependent neutral amino acid transporter	45 822 265	RIPSLDELEVIEKE	2	12
11	Villin	26 388 975	ATSLNSNDVFILK	15	0
	KHK MOUSE Ketohexokinase	6 016 435	TIILYDTNLPDVSAK	1	0
	Actin like	8 850 209	KSYELPDGQVITIGNER	3	0
12	Villin	26 388 975	AAISDSVVEPAAK	9	0
	Actin like	8 850 209	KSYELPDGQVITIGNER	5	0
13	Actin-alpha	12 852 068	DSYVGDEAQSK	6	0
	HSP70	3 461 866	RIINEPTAAAIAYGLDKG	3	0

Table 2 continued

Band	Identified proteins	Gi	Peptide sequence	Peptides matched	Trans-membrane helixes
	Trafficking protein particle complex protein 2	51 477 744	YPIKHGIITNWDNMEK	2	1
	Ezrin	12 832 989	EVWYFGLQYVDNK	2	0
14	Annexin IV	1 703 319	SETSGSFEDALLAIVK	10	0
	Plastin-1 (I-plastin) (intestine-specific plastin)	85 986 577	MINLSEPDTIDER	1	0
	Actin-beta	40 225 338	DLYANTVLSGGTTMYPGIADR	1	0
15	Annexin IV	1 703 319	ENDDVVSEDLVQQDVQDLYEAGELK	6	0
	Protein disulfide-isomerase A3 precursor	26 353 794	DLLTAYYDVDYEK	2	1
	Cadherin 17	9 790 073	VPSDGLFLIGEYEGK	1	2
16	Actin-alpha	12 852 068	EITALAPSTMHK	4	0
	Carboxylesterase 2 precursor (CE-2)	26 329 245	LGVLGFFSTGDQHAK	3	1
	Laminin receptor	12 846 904	AIVAIENPADVSVISSR	2	0
	Guanine nucleotide binding protein G protein	13 384 618	SDPLLMGIPTSENPFK	2	0
	Serum albumin	26 341 396	LGEYGFQNAILVR	2	0
17	Calreticulin	6 680 836	GQTLVVQFTVK	2	0
	Carboxylesterase 6	19 354 488	MIPAVVDGEFLPK	6	1
	Actin-alpha	12 852 068	EITALAPSTMK	5	0
	Actin-gamma	809 561	VAPEEHPVLLTEAPLNPK	2	0
	Progesterone binding protein	2 801 793	FYGPEGPYGVFAGR	1	1
18	Actin-alpha	12 852 068	DSYVGDEAQSK	7	0
	Laminin receptor	12 846 904	SALSGHLETVILGLLK	4	0
	Actin-gamma	809 561	VAPEEHPVLLTEAPLNPK	2	0
	Protein disulfide-isomerase	38 197 382	HNQLPLVIEFTEQTAPK	8	1
	Membrane-associated progesterone binding component	2 801 793	FYGPEGPYGVFAGR	1	1
	Galectin 4	3 335 393	VAYNPFGPGQFFDLSIR	4	0
19	Actin-alpha	12 852 068	SYELPDGQVITIGNER	5	0
	Calreticulin	6 680 836	KPEDWDEEMDGEWEPPVIQNPEYK	3	0
	Actin-gamma	809 561	VAPEEHPVLLTEAPLNPK	2	0
	Protein disulfide-isomerase	38 197 382	HNQLPLVIEFTEQTAPK	6	1
	Annexin IV	26 328 509	GLGTDEDAIIGILAYR	5	0
	Annexin A13	12 841 399	ATFQAYQILIGK	3	0
20	Carboxylesterase 2	21 704 206	SHAPVYFYEFQHPPSYFK	12	1
	Guanine nucleotide-binding protein beta subunit 2	11 093 957	KGHNGWVTQIATTPQFPDMILSASRD	1	0
	Annexin IV	26 328 509	GLGTDEDAIIGILAYR	16	0
	Annexin A13	12 841 399	GMGTDEAAIIEVLSSR	2	0
	Calreticulin	6 680 836	IDNSQVESGSLEDDWDFLPPKK	5	0
	ribosomal protein S24	34 866 231	KDVNFEFPEFQL	2	0
	Membrane-associated progesterone binding component	2 801 793	FYGPEGPYGVFAGR	1	1
	Chloride intracellular channel protein 5	24 211 557	KGVVFNVTTVDLKR	1	0
	Actin-alpha	12 852 068	SYELPDGQVITIGNER	1	0
21	Cofillin	12 861 068	EILVGDVGQTVDDPYTTFVK	2	0
	Destrin	9 790 219	EILVGDVGATITDPFK	1	0
	Profillin	26 389 590	TFVSITPAEVGVLVGK	4	0
	Carboxylesterase 2	21 704 206	LGVLGFFSTGDQHAR	3	1
	Cyclophilin A	12 846 244	FEDENFILK	2	0

Table 2 continued

Band	Identified proteins	Gi	Peptide sequence	Peptides matched	Trans-membrane helixes
	Cell division control protein 42 homolog	26 342 014	KNVFDEAILAALEPPEPKK	1	0
	Galectin-2	20 381 452	RLGHSQLHYLSMGGLQISSFKL	3	0
	Anterior gradient protein 2 homolog precursor	27 662 826	RIVFVDPSLTVRA	1	1
	Sodium-hydrogen exchanger regulatory factor	5 732 682	RLLVVDPETDERL	1	0
	Ezrin	56 126	QPLTLSNELSQAR	1	0
	ATP-binding cassette subfamily G member 3	26 342 274	RLSNISGIMKP	1	5
	Annexin A13	12 841 399	GMGTDEAAIIEVLSSR	1	0
	Annexin IV	26 328 509	GLGTDEDAIIGILAYR	3	0
	Galectin 4	3 335 393	VAYNPFGPGQFFDLSIR	6	0
22	Annexin V	49 168 528	RETSGNLEQLLLAVVKS	9	0
	Galectin 2	20 381 452	ITITFQDKDFK	6	0
	Ubiquitin precursor	12 849 189	KTITLEVEPSDTIENVKA	3	0
23	Galectin 2	20 381 452	ITITFQDKDFK	3	0
	Gastrotropin	8 393 346	LVEISTIGDVTYER	2	0

The number of transmembrane helixes was predicted using SOSUI software application (http://sosui.proteome.bio.tuat.ac.jp/sosuiframe0.html) [24]. Proteins with predicted transmembrane domains are marked gray.
Full version of the Table 1 with sequences of all identified peptides and scores is available as online supporting material.

Discussion

Discussion A

In the experiments presented here, we investigated uptake of ^{59}Fe-labeled heme and its subsequent intracellular fate in MEL cells (line 707). We employed a novel 2-D technique enabling identification of native protein complexes. Ion exchange chromatography proved to be an efficient method for effective separation and enrichment of heme containing protein complexes in the presence of the detergent. However, no information on size is provided by this method and consequently, stoichiometry of the identified complexes cannot be determined. We did not utilize size exclusion chromatography which is often used for separation and sizing of soluble proteins or protein complexes because the presence of mixed detergent/protein/ lipid micelles in a total cell extract complicates both the separation and data interpretation [227]. Therefore we consider ion exchange chromatography to be the method of choice for the first dimension of the separation despite its minor drawbacks.

A total 13 protein complexes represented by bands A–M on autoradiographs (Fig. 2A) were analyzed and 33 individual proteins were identified (Table 1). The presence of several identical proteins in bands with similar electrophoretic mobility led us to the following hypothesis. We propose that all 13 detected bands represent different stages of dissociation and isoforms of four individual multi-protein heme containing complexes (complex I–IV) (Fig.16). Complexes I and II (represented by bands A-B and C-D respectively) undergo gradual loss of subunits caused by increasing salt concentration during the elution step of chromatography. The decreased molecular weight of the complex results in higher electrophoretic migration velocity and an obvious shift of band B relative to band A and D to C. We suggest bands E-H represent molecular variants or

isoforms of a third multi-protein system – complex III, which also partially dissociates due to the increased ionic strength during elution as represented by shifted bands I–L. Complex IV, represented by band M, migrates as a single band without any signs of salt induced dissociation.

Complex I

The invariable core of complex I (represented by bands A and B) is composed of a, b1 and b2 hemoglobin chains, and the antioxidant stress proteins peroxiredoxin I (Prx I) and peroxiredoxin 2 (Prx II). Band A also contains the hemoglobin d chain. The presence of peroxiredoxins have an apparent physiological connection to heme metabolism and hemoglobin synthesis. Peroxiredoxin I (Prx I) also known as HBP23 is a high affinity heme-binding protein with two heme-binding motifs [236] believed to be involved in cellular heme trafficking between mitochondria and hemoglobin [237]. In addition, peroxiredoxin I exhibits thiol-mediated peroxidase activity [238] which protects hemoglobin and other proteins and cellular structures against oxidative stress. Interestingly, mice with targeted disruption of the peroxiredoxin I gene demonstrate hemoglobin instability [239].

We suggest that the cysteine-rich peroxidase active side of Prx I acts as a direct scavenger for the reactive peroxide intermediates produced by continuous reactions of oxygen with iron atom in heme (either Prx I bound or external) [240]. Presence of Prx I in complex with hemoglobin and the presence of another member of peroxiredoxin family, Prx II in this protein complex, implies that both antioxidant proteins may cooperate, preserving the redox state and integrity of hemoglobin in cellular oxidation reactions [241]. The composition of bands A–B indicates that heme (either intracellular or taken up from the environment), destined for intact incorporation into hemoglobin, is bound by

cytosolic Prx I, which associates with Prx II and globin chain in the hemoglobin assembly and protection process. Protein complex I represents a "snapshot" of this process.

In addition to globins and peroxiredoxins, we identified several other components. The protein folding enzyme, peptidylprolyl isomerase, probably has an accelerating effect on the assembly of the hemoglobin. Integrin associated protein possibly anchors the whole complex to specific membrane sites. The physiological role of proteins identified in band A but not in band B, ubiquilin 1, G protein, beta subunit-like protein and aldolase A, is unclear, and requires further investigation.

Complex II

Identification of proteins present in bands C and D revealed a core protein complex composed of ATP synthase beta polypeptide, Prx I, Prx II and the iron storage protein, ferritin. Globin chains were not detectable in this complex. Stress-induced phosphoprotein 1 and Rho GDP-dissociation inhibitor 1 were identified only in band C. The physiological significance of such a protein conglomerate is not known, but the presence of ferritin suggests a possible role of this complex in a process of heme transport and degradation of heme by hemoxygenase I with subsequent iron storage in ferritin. The radioactive signal of this complex detected on radiograms could thus be attributed not only to heme in peroxiredoxins but also to iron liberated from heme and already stored inside the ferritin shell.

Complex III

Appearance of several identical proteins in bands E–H and I–L implies both the presence of four similar isoforms of one protein complex (bands E–H) and also a gradual salt-induced disassembly of these complexes (bands I– L). The original (non-

dissociated) four isoforms E–L of complex III differ only slightly in polypeptide composition. The invariant core of complex III comprises hemoglobin,

Prx I, Prx II, carbonic anhydrase, cytosolic malate dehydrogenase and nucleoside diphosphate kinase and cytosolic aspartate transaminase (for details see Table 1). From the presence of carbonic anhydrase II (CA) and its known association with hemoglobin [242], we assume that hemoglobin chains in complex III represent a completely assembled and functional hemoglobin tetramer associated with CA forming an active complex, in which heme serves as a proton transfer agent in oxygen exchange reactions catalysed by CA. CA, as well as aspartate transaminase, are dissociated from the complex by increased ionic strength in fraction 19 (Fig. 2) (CA is absent in bands I–L). Peroxiredoxins are similarly proposed to play a protective and heme transporting role as in complexes I and II. The fact that nucleoside diphosphate kinase, malate dehydrogenase and aspartate aminotransferase were identified in all four bands (E–H) testifies against the possibility of a random artifact. Nevertheless, the connection of these enzymes with heme metabolism is not known.

The abundant cytosolic heme-binding protein p22 (HBP 22), (identified only in band E) is thought to be a positive regulator of heme biosynthesis in erythroid cells [237] with no homology to any other known heme-binding protein. It could possibly play the role of a heme transporter or chaperone for heme incorporation into hemoglobin. Because of its high affinity for coproporphyrinogen it could also serve to ensure a flow of coproporphyrinogen to mitochondria [237]. However, further studies are needed to determine its particular function.

Complex IV

Complex IV (band M) represents a salt-resistant, chaperone rich protein complex. It consists of globin chains, Prx II, peroxiredoxin IV (Prx IV), nascent polypeptide-

associated complex (NAC) alpha chain, a protein folding enzyme, protein disulfide isomerase (PDI), accompanied by two other chaperones (heat-shock proteins), ATP synthase and delta aminolevulinic acid dehydratase (ALAD). We assume that complex IV represents another "snapshot" of the cellular heme metabolic machinery illustrating early stages of globin folding. NAC is known to transiently bind to ribosomes and to the nascent polypeptide chain as it emerges from the ribosome. NAC protects newly synthetized globin chains against proteolysis and improper interactions with cytosolic proteins [243, 244]. The absence of a potential heme carrier or donor such as Prx I or HBP 22 (Prx II and Prx IV are not known to bind or transport heme) in complex IV indicates that the heme molecule binds to *C*' terminus of a nascent globin chain early during its elongation and helps to moderate its proper folding as proposed previously [245]. The complex process of hemoglobin folding is mediated by molecular chaperones which are yet to be identified. However, the presence of two heat shock proteins (members of HSP70 family, see Table 1) in complex IV suggests a pivotal role for these chaperones in the folding process. Prx II along with another member of thioredoxin-like family, peroxiredoxin IV, probably exert shielding against oxidative damage [241]. The presence of the heme-synthesis enzyme ALAD seems to implicate a connection with heme production. However, the lesser known function of ALAD as a proteasome inhibitor [246] explains its presence in complex IV more conclusively, particularly in association with the fact that ATP synthase (also present in complex IV) is believed to stabilize the inhibitory function of ALAD on proteaseome by ATP production [247]. Identification of ALAD and ATP synthase in conjunction with hemoglobin, peroxiredoxines and chaperones in complex IV, leads us to the following hypothesis. ALAD functions as a proteasome inhibitor, preventing globin chains from proteolytic degradation in the process of hemoglobin assembly concertedly with NAC. This

alternate role of ALAD could explain the otherwise enigmatic, very high expression levels (relative to other heme synthesis enzymes) of the enzyme in differentiating heme and hemoglobin producing erythroid cells.

Fig.16 Hypothetical schemes of four identified heme-binding protein complexes.

(A) **Complex I**, Hb – hemoglobin; Prx I – peroxiredoxin I; Prx II – peroxiredoxin II; PPI – peptidylprolyl isomerase B; IAP – integtrin-associated protein; Int – integrin; ROS – reactive oxygen species. (B) **Complex II**, Ft – ferritin; Prx I – peroxiredoxin I; Prx II – peroxiredoxin II; Hox – heme-oxygenase; ATPs – ATP synthase; ROS – reactive oxygen species. (C) **Complex III**, Hb – hemoglobin; Prx I – peroxiredoxin I; Prx II – peroxiredoxin II; CA II – carbonic anhydrase II; NDK – nucleoside diphosphate kinase; MD – cytosolic malate dehydrogenase; AAT – aspartate amino transferase; ROS – reactive oxygen species. (D) **Complex IV**, NAC – nascent polypeptide-associated complex; Prx IV – peroxiredoxin IV; Prx II – peroxiredoxin II; HSP 2 – heat shock protein 2; HSP 110 – heat shock protein 110; ALAD – delta aminolevulinic acid dehydratase; ATPs – ATP synthase; PDI – protein disulfide isomerase.

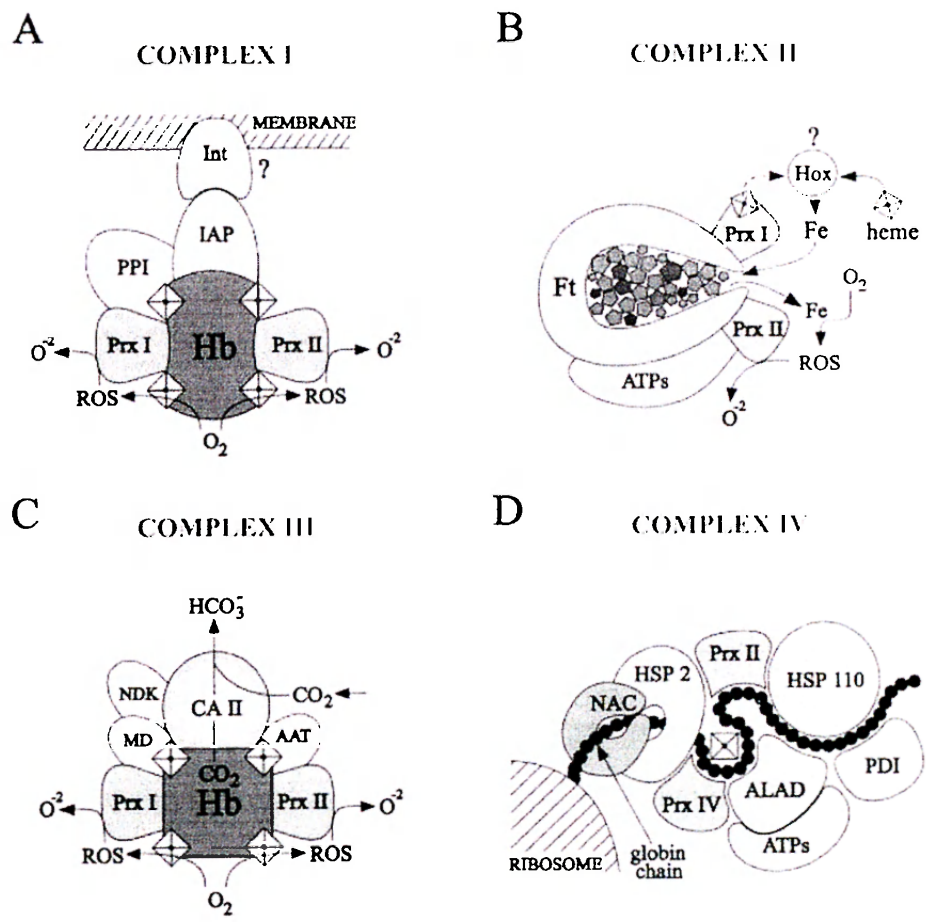

Discussion B

Integral membrane proteins represent 50% of all BBM proteins identified in our BN-PAGE experiment. Transmembrane proteins are among the most interesting molecules for biomedical research as some of the most important cellular functions are inherently tied to biological membranes. However, due to difficulties in the biochemical purification and structure/function analysis of membrane proteins, caused by their hydrophobic or amphophilic nature, membrane proteins are considered to be "the holy grail" of proteomics. Our results show that BN-PAGE is an effective tool for the study of membrane proteins in BBM.

We identified 27 proteins with one or more transmembrane domains as predicted by SOSUI software. Identified membrane proteins contained in an average three transmembrane helixes. Two proteins with the highest number of transmembrane helixes were sodium-glucose cotransporter 1 and peptide transporter PEPT1 with 14 and 13 transmembrane helixes, respectively.

Enzymes of peptide and carbohydrate metabolism were identified in four closely migrating bands in the upper part of the gradient gel. Band 1 and the wide triplet of bands 2–4 contained almost exclusively membrane proteins, particularly enzymes involved in digestion of saccharides (sucraseisomaltase, maltase-glucoamylase) and polypeptidases (aminopeptidase A, aminopeptidase N, endopeptidase-2 and *N*-acetylated-alpha-linked acidic dipeptidase). Majority of these proteins were previously reported to be present in brush border detergent insoluble microdomains (DIM) [248, 249]. Using co-immunoprecipitation we have verified that zinc binding enzyme aminopeptidase N interacts with at least two other digestive enzymes aminopeptidase A and sucrase-isomaltase (Fig.15). Bands 1–4 thus likely represent different

aminopeptidase N containing functional digestive protein supercomplexes in BBMs.

The undisputed advantage of BN-PAGE is that it preserves intact protein–protein complexes. To verify whether it preserves also protein–metal complexes, we employed radiolabeling of isolated BBM with ^{65}Zn. Zinc is an essential metal cofactor known to be present in several intestinal peptidases [250, 251]. Isolated BBMs were radiolabeled, solubilized, and separated by BN-PAGE as previously described in Materials and methods B. Analysis of radiograms revealed the presence of two major zinc binding bands. After matching of radiograms with scans of Coomassie brilliant stained gels, radioactive zinc was found in two wide and prominent bands that corresponded to band 1 and to the closely migrating triplet of bands 2–4 (Fig.13c). Indeed, zinc binding proteins were detected in these bands (aminopeptidase N in bands 1–4 and aminopeptidase A and *N*-acetylatad-alpha-linked acidic dipeptidase in band 3).

In bands 1–4, we also found a protein known as Fc fragment of IgG binding protein (Fcgbp). This molecule is a newly described immunoglobulin receptor, distinct from other known Fc gamma receptors. Interestingly, latest results by Mina-Osorio *et al.* and Riemann *et al.* [252, 253] demonstrate that other structurally distinct, but functionally related Fc gamma receptor (FcgammaR) associates with aforementioned aminopeptidase N on the cell membrane of monocytes.

The enzyme Na/K ATPase was found in bands 3–7 (Table 2). Na/K ATPase is known to be localized, predominantly, on enterocyte basolateral membrane [254]. Na/K ATPase detected in bands 3–7 could represent a small fraction of enzyme expressed on BBM, contamination of BBM by basolateral membrane or the possibility that in the course of BBM purification enterocyte tight junctions are destroyed by homogenization and basolateral Na/K ATPase leaks and diffuses also into the BBM domains [255].

Bands 5–21 contained membrane transporters, ion channels, and two surface antigen proteins potentially involved in cell growth signaling. Cell surface glycoprotein Trop-1 found in bands 5–7 is a single-pass type I membrane protein expressed in almost all normal tissue epithelia. This protein is also found on the surface of several tumors and is commonly used for targeted immunotherapy of carcinomas [256]. In band 6, Trop 1 was accompanied by multipass membrane protein tetraspanin-8. Tetraspanins are proteins with four highly conserved hydrophobic regions. Their potential roles are modulating cell adhesion, cell motility, and tumor metastasis [257].

Ion channels and transporters, identified in bands 5–7 included proton-coupled dipeptide cotransporter PEPT1, sodium-glucose cotransporter 1, and Na1/K1 ATPase alpha and beta subunits. PEPT1 is thought to constitute an exclusive route for the absorption of oligopeptides and peptidomimetic drugs in the small intestine [258]. Other transport molecules found in bands 8–21 include sodium-dependent neutral amino acid transporter, membrane-associated progesterone binding component, or trafficking protein particle complex protein 2.

Besides membrane BBM proteins, we also identified several cytoskeletal structural components and cytoskeleton-associated proteins (bands 8–21) such as a, b, g actins, villin, cofillin, destrin, and profillin. Proteins of endoplasmatic reticulum (calreticulin, protein disulfide isomerase) together with one ribosomal protein (RPS24) were the minor contaminants in bands 18–20.

Bands 21–23 contained BBM proteins of various functions involving intestinal calcium-dependent lipid binding molecules (annexins), clusters forming lectins involved in apical cargo (galectins) and the modulators of actin polymerization (cofilin, destrin, and profilin).

Conclusions

Conclusions on aim A: To investigate [^{59}Fe] heme uptake and its subsequent intracellular utilization in heme binding protein complexes by developing erythroid cells.

Newly identified heme binding complexes I–IV represent four different snapshots of hemoglobin metabolism and provide new insights into the process of hemoglobin synthesis.

Association of peroxiredoxins with hemoglobin in three of the four complexes analyzed suggests a stable and universal interaction. Peroxiredoxins may provide hemoglobin with protection against oxidative damage from the moment of its assembly, throughout its life span in the cell. In addition to an antioxidant function, peroxiredoxins could supply hemoglobin synthesis with heme or function as chaperones for heme incorporation into hemoglobin.

The presence of ALAD in a protein complex with ATP synthase and hemoglobin (complex IV) lends support to its contemplated proteasome inhibitory role.

Identification of the two heat-shock proteins belonging to HSP70 family suggests participation of these molecules in the folding of globin chains.

The presence of nascent polypeptide-associated complex in one functional complex with globin chains is consistent with its postulated role in cotranslational moderation of globin folding.

Our novel method of native 2-D separation offers a mild and non-denaturing separation of intact protein complexes. This method can be used in diverse arrangements with both low molecular and high molecular weight ligands,

radioactive or not. The method presented is fully compatible with mass spectrometric protein identification and may find broad applications in the study of various native protein complexes.

Conclusions on aim B: To investigate protein-protein interactions in purified brush border membranes (BBM) by blue native electrophoresis (BN PAGE) and to test the suitability of the method for the separation and characterization of BBM zinc binding protein complexes.

Our study is the first application of BN-PAGE technique for the native separation of intestinal BBM protein complexes.

In conclusion, BN-PAGE proved to be an effective tool for separation of membrane protein complexes contained in intestinal BBM. The BN-PAGE separation technique has the potential to be expanded from mitochondria to other membrane-bound compartments.

The presented technique maintains the protein complexes in native form, capable of binding metal cofactors, as shown by the presence of ^{65}Zn in newly identified metalloprotein complexes composed of several intestinal peptidases isolated from zinc-radiolabeled BBM.

BN-PAGE can notably help in the efforts of biochemistry and physiology to investigate the structure and function of novel membrane proteins and to accelerate the discovery of more effective drugs, targeted to new membrane receptor proteins which form the drug-targeted boundary between cells and their environment.

Summary

This thesis, The Biochemistry of Zinc and Iron - Proteomic Studies, consists of five sections. We were studying the biochemistry of two different metal elements - iron and zinc, therefore the thesis has two main aims (iron and zinc related) and each of the experimental sections are divided into two logical subsections A and B.

The first section – Introduction includes a general introduction reviewing the current knowledge about the biochemistry of iron and zinc and it also specifies the objectives of this study.

The first part of the Introduction is a review of iron biochemistry. It has following seven chapters: General properties of iron; Iron absorption, storage and toxicity in human; Iron transport and homeostasis; Iron regulatory proteins – IRP/IRE system; Mitochondrial iron metabolism; Liver and iron and Iron disorders.

In the second part of the Introduction, the biochemistry of zinc is reviewed in these eight chapters: Zinc – general properties; Zinc transporters; Zinc finger proteins; The role of zinc fingers in leukemogenesis; Functions of zinc in cellular signalling; Regulatory functions of zinc in cell proliferation; Role for Zinc in cell differentiation and apoptosis; Zinc - remarks and perspectives.

The third part of the Introduction introduces the specific objectives of this thesis. It gives a brief overview of proteomics in general, proteomics of metalloproteins and native separation methods. In the final part of the first section the factual aims of this thesis are specified.

The second section - Materials and metods summarizes the detailed experimental designs and protocols that were used in experiments in order to achieve our goals.

Materials and metods A part has following five chapters: [^{59}Fe] hemin synthesis, Cell culture and [^{59}Fe] hemin cell labeling, Flow protein liquid chromatography, Native electrophoresis and gel processing, Tryptic digestion and MS analysis.

Materials and metods B part has following six chapters: Cells and BBM preparation, Radiolabeling of BBM with ^{65}Zn, Blue native electrophoresis and native Western blotting, Immunoprecipitation and immunodetection, Proteolytic digestion and sample preparation, Mass spectrometric analysis.

The third section is comprised of our achieved results.

Part Results A presents the chromatogram of erythroid cellular lysates radiolabeled by [^{59}Fe] hemin that was separated on MONO Q anion-exchange column and the radiogram showing native electrophoretic separation of heme containing protein complexes in selected prepurified radioactive fractions. Also included are the representative examples of MS/MS spectra of tryptic peptides originating from carbonic anhydrase, alpha hemoglobin and heme-binding protein p22 HBP followed by Table 1, where all of the proteins identified by LC-MS/MS in this experiment are summarized.

Part Results B presents native electrophoretic separations of intestinal brush border membranes (BBM) which include Blue Native PAGE separation of protein complexes present in isolated BBM on 4–20% gradient gel, the immunoreactivity of aminopeptidase N on Western blot made from BBM lysate blue native electropherogram and radiogram of ^{65}Zn-labeled BBM.

The functions and relative percentage of 55 individual proteins from BBM identified by LC-MS/MS are presented in a circle/pie graph.

Co-immunoprecipitation of zinc binding protein aminopeptidase N and its associated proteins sucrase isomaltase and aminopeptidase A is showed on Western blots.

Finally the summary of proteins identified in BBM by LC-MS/MS is presented in Table 2.

In the **fourth section** our achieved results are disscused considering the previously published knowledge.

In the part A we discuss a total of 13 heme binding protein complexes represented by bands A–M on autoradiographs. Upon the composition and migration pattern of isolated complexes we propose that 13 detected bands represent different stages of dissociation and variable isoforms of four novel individual multi-protein heme containing complexes (Complex I–IV). The detailed composition and possible physiological functions of Complexes I-IV are examined and we suggest that Complexes I-IV represent four different snapshots of hemoglobin metabolism in the erythriod cells.

In the part B, the use of BN-PAGE as an effective tool for the study of native membrane proteins and metalloproteins in BBM is discussed. The functional properties and interactions of identified proteins are examined. We propose the presence of zinc binding protein complex composed of digestive enzymes aminopeptidase N, aminopeptidase A and sucrase isomaltase. Final conclusions from the results are made in the **fifth section** of the thesis.

Publications

Babusiak M, Man P, Petrak J, Vyoral D.
Native proteomic analysis of protein complexes in murine intestinal brush border membranes. *Proteomics*. 2007 Jan;7(1):121-9.
Impact factor: 6,088

Provaznikova D, Peslova G, Marinov I, Babusiak M, Vyoral D, Fuchs O.
The Increased Expression of SnoN and Undetectable Levels of Important Cell cycle Regulators, Proteins $p21^{Waf1/Cip1}$ and $p27^{Kip1}$ as Probable Causes of the Resistance of ML-2 Cells Proliferation to Transforming Growth Factor-βETA1.
New Research on Signal Transduction ISBN 1-60021-379-0
Editor: Bruce R. Yanson, © 2006 Nova Science Publishers, Inc.

Babusiak M, Man P, Sutak R, Petrak J, Vyoral D.
Identification of heme binding protein complexes in murine erythroleukemic cells: study by a novel two-dimensional native separation -- liquid chromatography and electrophoresis. *Proteomics*. 2005 Feb;5(2):340-50.
Impact factor: 6,088

Fuchs O, Babusiak M, Vyoral D, Petrak J.
Role of zinc in eukaryotic cells, zinc transporters and zinc-containing proteins. Review article. *Sb Lek*. 2003;104(2):157-70.

Vyoral D, Babusiak M, Fuchs O, Petrak J.
Native electrophoretic separation and femtomolar detection of ^{65}Zn-containing proteins by storage phosphorimaging. *J Biochem Biophys Methods*. 2003 Aug 29;57(2):177-82.
Impact factor: 1.201

Manuscripts in preparation

Ternes N, Sturm B, Babusiak M, Goldenberg H, Vyoral D, Scheiber-Mojdehkar B.
Cellular uptake and release of ferric-pyrophosphate by macrophages and liver parenchyma cells *in vitro*

Babusiak M, Babusiakova E, Richardson D, Halada P, Vyoral D.
Proteomic analysis of iron binding protein complexes in erythroid mitochondria.

Acknowledgements

Special thanks to Emilia and all of my family, my supervisor Daniel Vyoral, Róbert Šuťák, Jirka Petrák, good people of UHKT and magic city of Prague.

References

[1] Taylor PR, J Inorg Biochem, 2006 Apr; 100(4): 780-5.

[2] Voevodskaya N et al., Proc Natl Acad Sci U S A, 2006 Jun 27; 103(26):9850-4.

[3] Coates ML, J Mol Evol, 1975 Dec 29;6(4):285-307.

[4] Alayash AI, Cashon RE, Mol Med Today, 1995 Jun;1(3):122-7.

[5] Perutz MF, Trends Biochem Sci, 1989 Feb;14(2):42-4.

[6] Fago A et al., IUBMB Life, 2004 Nov-Dec;56(11-12):689-96.

[7] Mammen PP et al., J Histochem Cytochem, 2006 Aug 9; [Epub ahead of print]

[8] Wilkins RG, Harrington PC, Adv Inorg Biochem, 1983;5:51-85.

[9] Vanin S et al., J Mol Evol, 2006 Jan;62(1):32-41.

[10] http://en.wikipedia.org/wiki/Electron_transport_chain

[11] Ortiz de Montellano, Paul R. (ed.) (1995). Cytochrome P450: structure, mechanism, and biochemistry. Springer; 3rd edition (December 21, 2004).

[12] Lieberman RL, Rosenzweig AC et al., Crit Rev Biochem Mol Biol. 2004 May-Jun;39(3):147-64.

[13] Lardinois OM et al., Biochim Biophys Acta, 1996 Jul 18;1295(2):222-38.

[14] Shimizu N et al., Biochim Biophys Acta, 1989 Apr 6;995(2):133-7.

[15] http://en.wikipedia.org/wiki/Catalase

[16] Bartnikas TB, Gitlin JD, J Biol Chem, 2003 Aug 29;278(35):33602-8.

[17] Schmidt PJ et al., J Biol Chem, 2000 Oct 27;275(43):33771-6.

[18] Abreu IA et al., Phys Chem B Condens Matter Mater Surf Interfaces Biophys, 2005 Dec 29;109(51):24502-9.

[19] Dufernez F et al., Free Radic Biol Med, 2006 Jan 15;40(2):210-25.

[20] Hernick M, Fierke CA, Arch Biochem Biophys, 2005 Jan 1;433(1):71-84.

[21] Lindqvist Y et al., J Mol Biol, 1999 Aug 6;291(1):135-47.

[22] McCance RA, Widdowson EM, J Physiol, 1938 Oct 14;94(1):148-154.

[23] Sibille JC et al., Hepatology, 1988 Mar-Apr;8(2):296-301.

[24] Cook et al., Blood, 1986 Sep;68(3):726-31.

[25] Bothwell TH, Charlton RW, Prog Clin Biol Res, 1981;77:311-21.

[26] Muir A, Hopfer U, Am J Physiol, 1985 Mar;248(3 Pt 1):G376-9.

[27] Hubert N, Hentze MW, Proc Natl Acad Sci U S A, 2002 Sep 17;99(19):12345-50. Epub 2002 Sep 3.

[28] Arredondo M et al., FASEB J, 2001 May;15(7):1276-8.

[29] Frazer DM, Gut, 2003 Mar;52(3):340-6.

[30] Shayeghi M et al., Cell, 2005 Sep 9;122(5):789-801.

[31] Granick JL, Sassa S, J Biol Chem, 1978 Aug 10;253(15):5402-6.

[32] Malik Z et al., Exp Hematol, 1979 Apr;7(4):183-8.

[33] Kappas A et al., Pediatrics, 1993 Mar;91(3):537-9.

[34] Gutteridge JMC.et al., Biochem J, 1981 Oct 1;199(1):263-5.

[35] Bacon BR, Britton RS, Hepatology, 1990 Jan;11(1):127-37.

[36] Rank BH et al., J Clin Invest, 1985 May;75(5):1531-7.

[37] Corbett JD, Golan DE, J Clin Invest, 1993 Jan;91(1):208-17.

[38] Teti D et al., Cell Physiol Biochem, 2005;16(1-3):77-86.

[39] Giordani A et al., J Photochem Photobiol B, 2000 Jan;54(1):43-54.

[40] Brem F et al., J R Soc Interface, 2006 Jun 14; [Epub ahead of print]

[41] Ke Y, Ming Qian Z, Lancet Neurol, 2003 Apr;2(4):246-53.

[42] Qian ZM, Shen X, Trends Mol Med, 2001 Mar;7(3):103-8.

[43] Bonkovsky HL, Am J Med Sci, 1991 Jan;301(1):32-43.

[44] http://www.chemistry.wustl.edu/~edudev/LabTutorials/Ferritin/FerritinTutorial.html

[45] Chasteen ND, Harrison PM, J Struct Biol, 1999 Jun 30;126(3):182-94.

[46] Napier I, Blood, 2005 Mar 1;105(5):1867-74.

[47] Drysdale J et al., Blood Cells Mol Dis, 2002 Nov-Dec;29(3):376-83.

[48] Cazzola M et al., Blood, 2003 Mar 1;101(5):1996-2000.

[49] Nie G, Blood, 2005 Mar 1;105(5):2161-7.

[50] O'Connell M et al., Biochem J, 1986 Mar 15;234(3):727-31.

[51] Ozaki M et al., Biochem J, 1988 Mar 1;250(2):589-95.

[52] Chasteen ND, Harrison PM, J Struct Biol, 1999 Jun 30;126(3):182-94.

[53] Fleming MD et al., Nat Genet,1997 Aug;16(4):383-6.

[54] Gunshin H et al., Nature, 1997 Jul 31;388(6641):482-8.

[55] Hubert N, Hentze MW, Proc Natl Acad Sci U S A, 2002 Sep 17;99(19):12345-50.

[56] Lee PL et al., Blood Cells Mol Dis, 1998 Jun;24(2):199-215.

[57] Fleming RE, Proc Natl Acad Sci U S A, 1999 Mar 16;96(6):3143-8.

[58] Oates PS et al., Pflugers Arch, 2000 Jul;440(3):496-502.

[59] Yeh KY, Am J Physiol Gastrointest Liver Physiol. 2000 Nov;279(5):G1070-9.

[60] Raja KB etal., Biochim Biophys Acta, 1992 Jun 10;1135(2):141-6.

[61] Riedel HD et al., Biochem J, 1995 Aug 1;309 (Pt 3):745-8.

[62] Kobayashi K et al., J Biol Chem, 1998 Jun 26;273(26):16038-42.

[63] McKie AT et al., Science, 2001 Mar 2;291(5509):1755-9.

[64] Abboud S, Haile DJ, J Biol Chem, 2000 Jun 30;275(26):19906-12.

[65] McKie AT et al., Mol Cell, 2000 Feb;5(2):299-309.

[66] Aguirre P et al., BMC Neurosci, 2005 Jan 24;6(1):3.

[67] Devalia V et al., Blood, 2002 Jul 15;100(2):695-7.

[68] Jeong SY, David S, J Biol Chem, 2003 Jul 18;278(29):27144-8.

[69] Richardson DR, Ponka P, Biochim Biophys Acta, 1997 Mar 14;1331(1):1-40.

[70] Hentze MW et al.m, Cell, 2004 Apr 30;117(3):285-97.

[71] Kato J et al., Clin Chem, 2002 Jan;48(1):181-3.

[72] Harford JB, Klausner RD, Enzyme, 1990;44(1-4):28-41.

[73] Cheng Y et al., J Struct Biol, 2005 Dec;152(3):204-10.

[74] Robb A, Wessling-Resnick M, Blood, 2004 Dec 15;104(13):4294-9.

[75] Johnson MB, Enns CA, Blood, 2004 Dec 15;104(13):4287-93.

[76] Tomas Ganz, Blood, 15 December 2004, Vol. 104, No. 13, pp. 3839-3840.

[77] Cheng Y et al. Cell, 2004 Feb 20;116(4):565-76.

[78] Fleming MD, Andrews NC, J Lab Clin Med, 1998 Dec;132(6):464-8.

[79] Hentze MW et al., Cell, 2004 Apr 30;117(3):285-97.

[80] Harrison PM, Arosio P, Biochim Biophys Acta, 1996 Jul 31;1275(3):161-203.

[81] Hentze MW, Kuhn LC, Proc Natl Acad Sci U S A, 1996 Aug 6;93(16):8175-82.

[82] Muckenthaler M et al., Mol Cell, 1998 Sep;2(3):383-8.

[83] Rouault TA, Nat Chem Biol, 2006 Aug;2(8):406-14.

[84] Bianchi L et al., Nucleic Acids Res, 1999 Nov 1;27(21):4223-7.

[85] Ponka P, Blood, 1997 Jan 1;89(1):1-25.

[86] Muhlenhoff U, Lill R, Biochim Biophys Acta, 2000 Aug 15;1459(2-3):370-82.

[87] Richardson DR et al., Blood, 1996 Apr 15;87(8):3477-88.

[88] Muhlenhoff U et al., J Biol Chem, 2003 Oct 17;278(42):40612-20.

[89] Mitsuhashi N et al., J Biol Chem, 2000 Jun 9;275(23):17536-40.

[90] Shaw GC et al., Nature, 2006 Mar 2;440(7080):96-100.

[91] Breuer W et al., FEBS Lett, 1997 Feb 17;403(2):213-9.

[92] Lipinski P et al., Blood, 2000 May 1;95(9):2960-6.

[93] Vyoral D, Petrak, Biochim Biophys Acta, 1998 Jun 22;1403(2):179-88.

[94] Petrak JV, Vyoral D, J Inorg Biochem, 2001 Oct;86(4):669-75.

[95] Puccio H et al., Nat Genet, 2001 Feb;27(2):181-6.

[96] Miyazaki E et al., Gut, 2002 Mar;50(3):413-9.

[97] Palau F, Int J Mol Med. 2001 Jun;7(6):581-9.

[98] Cavadini P et al., Hum Mol Genet, 2002 Feb 1;11(3):217-27.

[99] Rotig A et al., Nat Genet, 1997 Oct;17(2):215-7.

[100] Irazusta V et al., J Biol Chem, 2006 May 5;281(18):12227-32.

[101] Zhang Y et al., J Biol Chem, 2006 Aug 11;281(32):22493-502.

[102] Huynen MA et al., Hum Mol Genet. 2001 Oct 1;10(21):2463-8.

[103] Gerber J et al., EMBO Rep. 2003 Sep;4(9):906-11.

[104] Ramazzotti A et al., FEBS Lett. 2004 Jan 16;557(1-3):215-20.

[105] Lili R et al., Biol Chem, 1999 Oct;380(10):1157-66.

[106] Gardner PR et al., Proc Natl Acad Sci U S A, 1994 Dec 6;91(25):12248-52.

[107] Beinert H et al., Chem Rev, 1996 Nov 7;96(7):2335-2374.

[108] Vasquez-Vivar J, J Biol Chem, 2000 May 12;275(19):14064-9.

[109] Ross KL, Eisenstein RS, J Nutr, 2002 Apr;132(4):643-51.

[110] Schalinske KL et al., J Biol Chem, 1998 Feb 6;273(6):3740-6.

[111] Irazusta V et al., J Biol Chem, 2006 May 5;281(18):12227-32.

[112] Aspinwall R et al., Proc Nati Acad Sci U S A, 1997 Jan 7;94(1):109-14.

[113] Kikuchi G et al., J Biol Chem. 1958 Nov;233(5):1214-9.

[114] Krishnamurthy PC et al., Nature, 2006 Oct 5;443(7111):586-9.

[115] Zhang AS et al., Blood, 2005 Jan 1;105(1):368-75.

[116] Cox TC et al., EMBO J, 1991 Jul;10(7):1891-902.

[117] Vyoral D, Petrak J, Int J Biochem Cell Biol. 2005 Sep;37(9):1768-73.

[118] Bonkovsky HL, Am J Med Sci, 1991 Jan;301(1):32-43.

[119] Lesbordes-Brion JC et al., Blood, 2006 Aug 15;108(4):1402-5. Epub 2006 Mar 30.

[120] Lou DQ et al., Blood, 2004 Apr 1;103(7):2816-21. Epub 2003 Nov 6.

[121] Knutson MD et al., Proc Natl Acad Sci U S A, 2005 Feb 1;102(5):1324-8.

[122] Atanasiu V et al., Eur J Haematol, 2006 Oct 17.

[123] Lee P et al., Proc Nati Acad Sci U S A, 2004 Jun 22;101(25):9263-5.

[124] Delaby C et al., Blood, 2005 Dec 1;106(12):3979-84. Epub 2005 Aug 4.

[125] Nemeth E et al., Blood, 2006 Jan 1;107(1):328-33. Epub 2005 Sep 1.

[126] Nicolas G et al., J Clin Invest, 2002 Oct;110(7):1037-44.

[127] Roy CN, Andrews NC, Curr Opin Hematol, 2005 Mar;12(2):107-11.

[128] Aggett PJ, Harries JT, Arch.Dis.Child, 1979 Dec;54(12):909-17.

[129] Vallee BL, Auld DS, Biochemistry, 1990 Jun 19;29(24):5647-59.

[130] Coleman JE, Annu Rev Biochem, 1992;61:897-946.

[131] Barceloux DG, J Toxicol Clin Toxicol, 1999;37(2):279-92.

[132] Coyle P, Philcox Jcet al., Cell Mol Life Sci, 2002 Apr;59(4):627-47.

[133] Ramadurai J, Shapiro C et al., Am J Hematol, 1993 Feb;42(2):227-8.

[134] Alcindor T, Bridges KR, Br J Haematol, 2002 Mar;116(4):733-43.

[135] Williams DM, Loukopoulos D et al., Blood, 1976 Jul;48(1):77-85.

[136] Mukhopadhyay CK, Attieh ZK et al., *Science*, 1998 Jan 30;279(5351):714-7.

[137] Har-El R, Chevion M, *Free Radic Res Commun*, 1991;12-13 Pt 2:509-15.

[138] Scott BJ, Bradwell AR, *Clin Chem*, 1983 Apr;29(4):629-33.

[139] Pinna K, Woodhouse LR, *J Nutr*, 2001 Sep;131(9):2288-94.

[140] Rink L, Gabriel P, *Proc Nutr Soc*, 2000 Nov;59(4):541-52.

[141] Evans GW, *Proc Soc Exp Biol Med*, 1976 Apr;151(4):775-8.

[142] Charlwood PA, *Biochim Biophys Acta*, 1979 Dec 14;581(2):260-5.

[143] Masuoka J, Saltman P, *J Biol Chem*, 1994 Oct 14;269(41):25557-61.

[144] Eide DJ, *Annu Rev Nutr*, 1998;18:441-69.

[145] Grotz N, Fox T et al., *Proc Natl Acad Sci U S A*, 1998 Jun 9;95(12):7220-4.

[146] Gaither LA, Eide DJ, J Biol Chem. 2000 Feb 25;275(8):5560-4.

[147] Grider A, Mouat MF, *J Nutr*, 1998 Aug;128(8):1311-4.

[148] Gaither LA, Eide DJ, J Biol Chem. 2001 Jun 22;276(25):22258-64.

[149] Costello LC, Liu Y et al., *J Biol Chem*, 1999 Jun 18;274(25):17499-504.

[150] Lioumi M, Ferguson CA et al., *Genomics*, 1999 Dec 1;62(2):272-80.

[151] Reyes JG, *Am J Physiol*, 1996 Feb;270(2 Pt 1):C401-10.

[152] Fuchs O, *Biol.listy* ,1999, 64, p.241-252 (in czech, abstract in english)

[153] Gunshin H, Mackenzie B et al., *Nature*, 1997 Jul 31;388(6641):482-8.

[154] Sacher A, Cohen A et al., *J Exp Biol*, 2001 Mar;204(Pt 6):1053-61.

[155] Palmiter RD, Findley SD, *EMBO J*, 1995 Feb 15;14(4):639-49.

[156] Huang L, Gitschier J., *Nat Genet*, 1997 Nov;17(3):292-7.

[157] Palmiter RD, Cole TB et al., *EMBO J*, 1996 Apr 15;15(8):1784-91.

[158] Palmiter RD, Cole TB et al., *Proc Natl Acad Sci U S A*, 1996 Dec 10;93:14934-9.

[159] Liuzzi JP, Blanchard RK et al., *J Nutr*, 2001 Jan;131(1):46-52.

[160] Michalczyk AA, Allen J, *Biochem J*, 2002 May 15;364(Pt 1):105-13.

[161] Kambe T, Narita H et al., *J Biol Chem*, 2002 May 24;277(21):19049-55.

[162] McMahon RJ, Cousins RJ, *Proc Natl Acad Sci U S A*, 1998 Apr 28;95(9):4841-6.

[163] Wenzel HJ, Cole TB et al., *Proc Natl Acad Sci U S A*, 1997 Nov 11;94:12676-81.

[164] McMahon RJ, Cousins RJ, *J Nutr*, 1998 Apr;128(4):667-70.

[165] Miller J, McLachlan AD et al., *EMBO J*, 1985 Jun;4(6):1609-14.

[166] Wolfe SA, Nekludova L et al., *Annu Rev Biophys Biomol Struct*, 2000;29:183-212.

[167] Choo Y, Klug A, *Nucleic Acids Res*, 1993 Jul 25;21(15):3341-6.

[168] Bieker JJ, *Curr Opin Hematol*, 1998 Mar;5(2):145-50.

[169] Turner J, Crossley M, *Trends Biochem Sci*, 1999 Jun;24(6):236-40.

[170] Bittel DC, Smirnova IV et al., *J Biol Chem*, 2000 Nov 24;275(47):37194-201.

[171] Sun L, Liu A et al., *EMBO J*, 1996 Oct 1;15(19):5358-69.

[172] Morgan B, Sun L et al., *EMBO J*, 1997 Apr 15;16(8):2004-13.

[173] Tang XB, Liu DP et al., *Cell Mol Life Sci*, 2001 Dec;58(14):2008-17.

[174] Fox AH, Liew C et al., *EMBO J*, 1999 May 17;18(10):2812-22.

[175] Kowalski K, Czolij R et al., *J Biomol NMR*, 1999 Mar;13(3):249-62.

[176] Nichols KE, Crispino JD et al., *Nat Genet*, 2000 Mar;24(3):266-70.

[177] Freson K, Devriendt K et al., *Blood*, 2001 Jul 1;98(1):85-92.

[178] Lu JR, McKinsey TA et al., *Mol Cell Biol*, 1999 Jun;19(6):4495-502.

[179] Crans HN, Sakamoto KM, *Leukemia*, 2001 Mar;15(3):313-31.

[180] Scandura JM, Boccuni P et al., *Oncogene*, 2002 May 13;21(21):3422-44.

[181] Ruggero D, Wang ZG et al., *Bioessays*, 2000 Sep;22(9):827-35.

[182] Miller WH Jr, Waxman S, *Oncogene*, 2002 May 13;21(21):3496-506.

[183] Xi ZF, Russell M et al., Leukemia. 1997 Feb;11(2):212-20.

[184] Jolkowska J, Witt M, *Leukemia Res*, 2000, 24, p. 553-58.

[185] Izutsu K, Kurokawa M et al., *Oncogene*, 2002 Apr 18;21(17):2695-703.

[186] Downing JR, *Br J Haematol*, 1999 Aug;106(2):296-308.

[187] Licht JD, *Oncogene*, 2001 Sep 10;20(40):5660-79.

[188] Hildebrand D, Tiefenbach J et al., *J Biol Chem*, 2001 Mar 30;276(13):9889-95.

[189] Costoya JA, Pandolfi PP, *Curr Opin Hematol*, 2001 Jul;8(4):212-7.

[190] McNulty TJ, Taylor CW, *Biochem J*, 1999 May 1;339 (Pt 3):555-61.

[191] Francis SH, Colbran JL et al., *J Biol Chem*, 1994 Sep 9;269(36):22477-80.

[192] Lefebvre D, Boney CM, *FEBS Lett*, 1999 Apr 23;449(2-3):284-8.

[193] Samet JM, Graves LM et al., *Am J Physiol*, 1998 Sep;275(3 Pt 1):L551-8.

[194] Samet JM, Silbajoris R et al., *Am J Respir Cell Mol Biol*, 1999 Sep;21(3):357-64.

[195] Csermely P, Szamel M et al., *J Biol Chem*, 1988 May 15;263(14):6487-90.

[196] Chesters J.K.: Biochemistry of zinc in cell division and tissue growth, in : C.F. Mills (Ed.), Zinc in Human Biology, Springer, London, 1989, p. 109-118.

[197] Baker GW, Duncan JR, J Natl Cancer Inst, 1983 Feb;70(2):333-6.

[198] Urrutia R, *Int J Pancreatol*, 1997 Aug;22(1):1-14.

[199] Tsujikawa K, Imai T et al., *FEBS Lett*, 1991 Jun 3;283(2):239-42.

[200] Petrie L, Chesters JK et al., *Biochem J*, 1991 May 15;276 (Pt 1):109-11.

[201] Schmidt C, Beyersmann D, *Arch Biochem Biophys*, 1999 Apr 1;364(1):91-8.

[202] Apostolova MD, Ivanova IA et al., *Toxicol Appl Pharmacol*, 1999;159(3):175-84.

[203] Record IR, Jannes M et al., *Biol Trace Elem Res*, 1996 Summer;53(1-3):19-25.

[204] Sunderman FW Jr, *Ann Clin Lab Sci*, 1995 Mar-Apr;25(2):134-42.

[205] King LE, Osati-Ashtiani F et al., *J Nutr*, 2002 May;132(5):974-9.,

[206] Verhaegh GW, Parat MO et al., *Mol Carcinog*, 1998 Mar;21(3):205-14.

[207] Blanchard RK, Moore JB et al., *Proc Natl Acad Sci U S A*, 2001;98(24):13507-13.

[208] Blanchard RK, Cousins RJ, *Am J Physiol*, 1997 May;272(5 Pt 1):G972-8.

[209] Cui L, Blanchard RK et al., *J Nutr*, 2000 Nov;130(11):2726-32.

[210] Nagaoka M, Sugiura Y, *J Inorg Biochem*, 2000 Nov;82(1-4):57-63.

[211] Beerli RR, Schopfer U et al., *J Biol Chem*, 2000 Oct 20;275(42):32617-27.

[212] Sera T, Uranga C, *Biochemistry*, 2002 Jun 4;41(22):7074-81.

[213] Choo Y, Sanchez-Garcia I et al., *Nature*, 1994 Dec 15;372(6507):642-5.

[214] McNamara AR, Ford KG, *Nucleic Acids Res*, 2000 Dec 15;28(24):4865-72.

[215] Hebestreit, HF, *Curr Opin Pharmacol*, 2001 Oct;1(5):513-20.

[216] Beeckmans S, *Methods*, 1999 Oct;19(2):278-305.

[217] Burgess RR, Thompson NE, *Curr Opin Biotechnol,* 2002, Aug;13(4):304-8.

[218] Kellogg DR, Moazed D, *Methods Enzymol*, 2002;351:172-83.

[219] Heiss K, Junkes C et al., *Proteomics*, 2005 Sep;5(14):3614-22

[220] Vyoral D, Petrak J et al., *Biol Trace Elem Res*, 1998 Mar;61(3):263-75.

[221] Suchan P, Vyoral D et al., *Microbiology*, 2003 Jul;149(Pt 7):1911-21.

[222] Vyoral D, Babusiak M et al., J Biochem Biophys Methods, 2003;57(2):177-82.

[223] Marks PA, Rifkind RA, Annu Rev Biochem, 1978;47:419-48.

[224] Braccia A, Villani M et al., J Biol Chem, 2003 May 2;278(18):15679-84.

[225] Tabb DL, McDonald WH et al., *J Proteome Res*, 2002 Jan-Feb;1(1):21-6.

[226] Kessler M, Acuto O et al., *Biochim Biophys Acta*, 1978 Jan 4;506(1):136-54.

[227] von Jagow, G., Schägger, H. (Eds.), A Practical Guide to Membrane Protein Purification, Academic Press, New York, 1994, pp. 86–103.

[228] Sambrook, J., Fritsch, E. F., Maniatis, T., Nolan, C. H. (Eds.), Molecular Cloning a Laboratory Manual, Cold Spring Harbor Laboratory Press, New York 1989, pp. 18.55–18.56.

[229] Mitaku S, Ono M et al., *Biophys Chem*, 1999 Dec 13;82(2-3):165-71.

[230] Vyoral D, Petrak J, Anal Biochem. 1998 Jun 15;260(1):103-6.

[231] Hofer D, Jons T et al., *Ann N Y Acad Sci*, 1998 Nov 17;859:75-84.

[232] Tacnet F, Lauthier F et al., J Physiol. 1993 Jun;465:57-72.

[233] Hirose J, Iwamoto H et al., *Biochemistry*, 2001 Oct 2;40(39):11860-5.

[234] Hirose J, Kamigakiuchi H et al., *Arch Biochem Biophys*, 2004 Nov 1;431(1):1-8.

[235] Vanderheyden PM, Demaegdt H et al., *Fundam Clin Pharmacol*, 2006 Dec;20(6):613-9.

[236] Hirotsu S, Abe Y et al., *Proc Natl Acad Sci U S A*, 1999 Oct 26;96(22):12333-8.

[237] Taketani S, Adachi Y et al., *J Biol Chem*, 1998 Nov 20;273(47):31388-94.

[238] Hofmann B, Hecht HJ et al., *Biol Chem*, 2002 Mar-Apr;383(3-4):347-64.

[239] Neumann CA, Krause DS et al., *Nature*, 2003 Jul 31;424(6948):561-5.

[240] Bunn HF, Poyton RO, *Physiol Rev*, 1996 Jul;76(3):839-85.

[241] Nagababu E, Rifkind JM, *Biochem Biophys Res Commun*. 2000;273(3):839-45.

[242] Silverman DN, Tu C, *J Biol Chem*, 1978 Apr 25;253(8):2563-7.

[243] Rospert S, Dubaquie Y et al., *Cell Mol Life Sci*, 2002 Oct;59(10):1632-9.

[244] Wiedmann B, Sakai H et al., *Nature*, 1994 Aug 11;370(6489):434-40.

[245] Komar AA, Kommer A et al., *J Biol Chem*, 1997 Apr 18;272(16):10646-51.

[246] Guo GG, Gu M et al., *J Biol Chem*, 1994 Apr 29;269(17):12399-402.

[247] Driscoll J, Frydman J et al., *Proc Natl Acad Sci U S A*, 1992 Jun 1;89(11):4986-90.

[248] Danielsen EM, *Biochemistry*, 1995 Feb 7;34(5):1596-605.

[249] Nguyen HT, Amine AB et al., *Biochem Biophys Res Commun*, 2006 Mar 31;342(1):236-44.

[250] Albiston AL, Ye S et al., *Protein Pept Lett*, 2004 Oct;11(5):491-500.

[251] Erdos EG, Skidgel RA, *FASEB J*, 1989 Feb;3(2):145-51.

[252] Mina-Osorio P, Ortega E, J. Leukoc. Biol, 2005;77, 1008–1017.

[253] Riemann D, Tcherkes A et al., *Biochem Biophys Res Commun*, 2005, 331, 1408-1412.

[254] Tosco M, Orsenigo MN, *Mech Ageing Dev*, 1990 Dec;56(3):265-74.

[255] Albers TM, Lomakina I, *Lab Invest*, 1995 Jul;73(1):139-48.

[256] McLaughlin PM, Kroesen BJ et al., *Cancer Immunol Immunother*, 1999 Sep;48(6):303-11.

[257] Maecker HT, Todd SC et al., *FASEB J*, 1997 May;11(6):428-42.

[258] Adibi SA, *Am J Physiol Gastrointest Liver Physiol*, 2003 Nov;285(5):G779-88.

Corrections of the THESIS by Mgr. Marek Babušiak

- The Biochemistry of Zinc and Iron –

Proteomic Studies

Page 5 Line 23 "ubichinione" <-> "ubiquinone"

Page 8 Line 1 "H2O2" <-> "H_2O_2"

Page 9 Line 16 "no-heme" <-> "non-heme"

Page 14 Line 7 "plays" <-> "play"

Page 27 Line 21 "haemochromatosis" <-> "hemochromatosis"

Page 34 Line 1 "relativelz" <-> "relatively"

Page 34 Line 1 "yinc" <-> "zinc"

Page 34 Line 2 "affinitz" <-> "affinity"

Page 36 Line 10 "fortransporting" <-> "for transporting"

Page 36 Line 22 "upto" <-> "up to"

Page 43 Line 5 "cental" <-> "central"

Page 43 Line 7 "Regulatogy" <-> "Regulatory"

Page 44 Line 20 "pf" <-> "of"

Page 45 Line 14 "rfflux" <-> "efflux"

Page 51 Line 4 "FeCl3"<-> "$FeCl_3$"

Page 51 Line 8 "mL"<-> "µL"

Page 51 Line 11 "mg"<-> "µg"

Page 51 Line 16 "mL"<-> "µL"

Page 51 Line 19 “acetic acid:- methanol” <-> “acetic acid:methanol“

Page 52 Line 3 “5%CO2 “<-> “5% CO_2“

Page 52 Line 6 “d“<-> “days“

Page 52 Line 9 “16108” <-> “$1x10^8$”

Page 52 Line 7, Line 11, Line 17 “6*g*” <-> “*g*”

Page 54 Line 9 “mL” <-> “µL”

Page 55 Line 13 “g” <-> “*g*”

Page 55 Line 21, Line 22 “6*g*” <-> “*g*”

Page 56 Line 10, 11, 14 “mL” <-> “µL”

Page 57 Line 15, Line 24 “600 mL” <-> “600 µL”, “100 mL” <-> “100 µL”

Page 58 Line 7 “mL” <-> “µL”

Page 58 Line 8 “mL” <-> “µL”

Page 58 Line 13 “mL” <-> “µL”

Page 59 Line 23 “mL” <-> “µL”

Page 60 Line 9 “1507C” <-> “150°C”

22.8.2007, Tampere

Mgr. Marek Babušiak